Implementation of Smart Charging Algorithm with V2G Services Considering its Effect on Battery Degradation

Kumar Yash

Technische Universiteit Delft

http://www.cleanfuture.co.in/2020/03/16/v2g-1-terrawatt-worth-ev-storage/

TU Delft

Implementation of smart charging algorithm with V2G services considering its effects on battery degradation

by

Kumar Yash

to obtain the degree of Master of Science
at the Delft University of Technology,
to be defended publicly on Thursday May 27, 2021 at 10:00.

Student number:	4801520	
Daily Supervisor:	Prof. dr. ir. G.R. Chandra Mouli.,	TU Delft
Advisor:	Ir. Y. Yu,	TU Delft
Thesis committee:	Prof. dr. ir. Pavol Bauer,	TU Delft
	Prof. dr. ir. Patrizio Manganiello,	TU Delft
	Prof. dr. ir. G.R. Chandra Mouli.,	TU Delft

Abstract

Electric vehicles (EVs) are going to take over the conventional cars industry like a wave in the foreseeable future. The exponential increase in sales of EVs is seen and market study has predicted that EV sales will increase by 15%–20% of total new vehicle sales by the year 2035. Despite being superior to fuel-driven vehicles, the increase in the number of EVs will have its challenges. For example, EVs are heavy uncontrolled charging loads that can lead to power surges in the grid which would then lessen the grid reliability. It is important to address the important question on *how to maintain EV charging and use it in such a way that it will not pose a threat to the grid rather become its helping hand?*

The focus of this thesis will be to answer the aforementioned question. The main objective of the thesis is to minimize the cost of energy for charging EVs by developing and implementing a smart charging algorithm with V2G services considering the effects of battery degradation. The said objective is achieved by first formulating a mathematical model for the minimization optimization problem. Several assumptions were made to mimic real-life situations. Then an algorithm is developed and case studies on four sensitivity parameter are done. The parameters selected are the cost of penalty, cost of PV generation, cost of selling energy, and grid import power limitations. The case study is done to verify the sanity of the code and it has been observed that the algorithm developed prioritizes PV utilization, minimizes the overall cost of the node as well as EV charging cost.

The algorithm incorporates the V2G application of EVs to support renewable (here, PV) sources. It has been observed that EVs that perform V2G generate financial benefit by exporting power to the grid and reduce the grid involvement by charging other EVs through V2G. V2G has adverse effects on the battery lifetime. Frequent charging and discharging can degrade the battery much quicker. The thesis tackles this problem by incorporating a battery degradation model in the developed algorithm for V2G.

Two degradation model are used and compared to check the effectiveness and control while performing V2G. The first model is a simplified one and calculates the cost of battery degradation using energy exported from the battery. The second models the degradation considering one of the stress factors of cyclic aging which is C-rate. The newly developed model is observed to be more effective as the model is dependent on charging and discharging current rates. The EVs are seen charging just to their requested energy demand with relatively less power as compared to when the simplified degradation model is implemented. The V2G functionality is also observed to be reduced and utilized to reduce the grid involvement and reducing the overall cost of energy.

Finally, the algorithm is compared with the uncontrolled charging algorithm. The developed smart charging algorithm is observed to reduce the charging cost of EVs significantly when the PV generation is sufficient. The smart charging algorithm utilizes the PV generation in supplying the energy demands of the local loads and EVs. This reduces the involvement of the grid. The grid is only observed to be involved when the cost of buying energy from the grid is lower to reduce any possible penalty for unfinished scenarios or when the PV generation is insufficient.

Keywords: smart charging, V2G, battery degradation

Acknowledgement

I started my master thesis in May 2020, and after an eventful journey of 12 months, I have finally arrived at defending my thesis to obtain a Master's in Electrical Engineering degree from TU Delft. The journey of completing my thesis and curriculum to obtain the degree has seen several ups and downs. My family and friends showed their continuous support, encouragement and motivated me to cross every hurdle I faced. They constantly reminded me that the journey is not as exciting and amazing at the end if we do not cross these hurdles.

During my thesis, I tried to gain the knowledge and deeper understanding of the concept, infrastructure and implementation of smart charging of electric vehicles and accomplished it. I would like to express my sincere appreciation to those who supported me throughout the journey. I have had the chance to be guided by one of the most critical and insightful supervisors Dr. ir. Gautham Ram Chandra Mouli and Ir. Yunhe Yu who have guided me throughout the project and was always available for questions and provided constructive feedback. They showed continued enthusiasm whenever I showed my progress and was a great source of motivation. They were very critical and never failed to amaze me with their incredibly insightful feedback and suggestions during our weekly and monthly meetings. Despite supervising so many MSc students, they were always up-to-date on my progress and showed great expertise on the topic. I would also like to express my appreciation for the staff of DCES. I would also like to thank Prof. dr. Pavol Bauer, Prof. dr. ir. Patrizio Manganiello and Dr. ir. Gautham Ram Chandra Mouli for taking time out of their busy schedule to be part of my graduate committee. I look forward to your evaluation.

Finally, I can not thank enough to my parents and my brother who are always there for me whenever I thought that the situation or the work is getting difficult. They were always a constant source of motivation and smile. They are always uplifting me and supported me with everything they got to push me an inch forward to perfection.

Thank you all for your love and support!

.

Delft, May 2021

Contents

List of Figures

List of Tables

Nomencletures

1. EV : Electric Vehicle
2. BEV : Battery Electric Vehicle
3. PHEV : Plug-in Hybrid Electric Vehicle
4. V2X : Vehicle to Everything
5. V2G : Vehicle to Grid
6. V2B : Vehicle to Building
7. V2V : Vehicle to Vehicle
8. PV : Photovoltaics
9. EoL : End of Life
10. SoH : State of Health
11. SOC : State of Charge
12. MILP : Mixed Integer Linear Programming
13. HEV : Hybrid Electric Vehicle
14. AC : Alternating Current
15. DC : Direct Current
16. IEC : International Electrotechnical Commission
17. CCS : Combined Charging System
18. CharIN : Charging Interface Initiative
19. CHAdeMO : CHArge de MOve
20. LP : Linear Programming
21. EVSE : Electric Vehicle Supply Equipment
22. EMS : Energy Management System
23. V2H : Vehicle to Home
24. DSO : Distribution system operator
25. ISO : Independent System Operator
26. CSO : Charging System Operator
27. MIP : Mixed Integer Programming
28. RES : Renewable Energy Sources
29. BMS : Battery Management System
30. SEI : Solid Electrolyte Interface

31. C-rate : Charging or discharging current rate of the battery
32. DOD : Depth of Discharge
33. LCOE : Levelized Cost of Energy
34. HT or LB : Highlight or Label (to emphasize on the duration of the difference between plot)

1

Introduction

Electric vehicles (EVs) are going to take over the conventional cars industry like a wave in the foreseeable future. The research on improving performance and charging schemes are currently attracting lots of attention. Meanwhile, various countries are providing various incentives for people to buy more and more electric vehicles. Norway is providing incentives like no purchase tax, reduction in ownership tax and so on. Whereas countries like the Netherlands are planning to introduce a complete take over of EVs on the combustion engine vehicles by the year 2035. Great incentives by the government, comparatively low prices for the EVs is encouraging customers to incline towards EVs which can be seen in the trend shown in figure 1.1

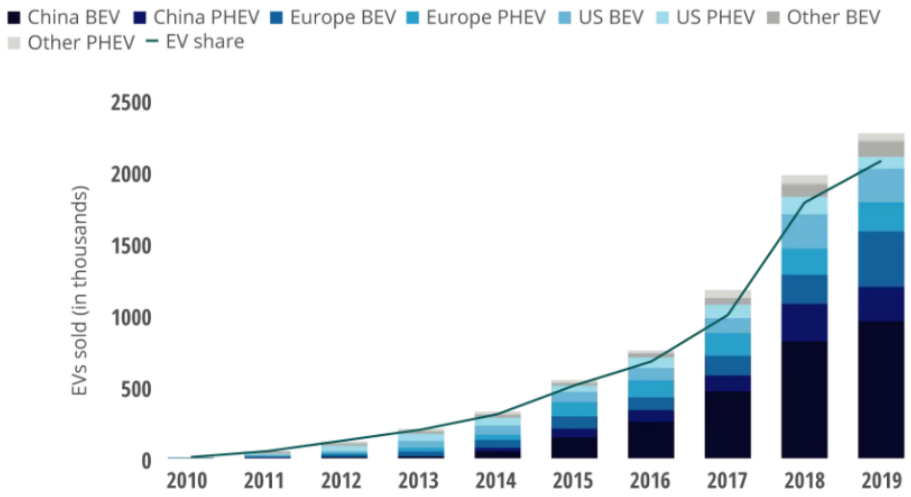

Figure 1.1: Trend to show increase in EV sales across globe [1]

It can be seen from figure 1.1 that the Battery Electric Vehicles (BEV) and Plug-in Hybrid Electric Vehicles (PHEV) sales are increasing exponentially over the years. Despite being superior to fuel-driven vehicles, the increase in the number of EVs will have its challenges. For example, EVs are heavy uncontrolled charging loads which can lead to power surges in the grid which would then lessen the grid reliability. Therefore, it is important to address *how to maintain EV charging and use it in such a way that it will not pose a threat to the grid rather become its helping hand?* The answer to that lies in using the EVs as a source of power by participating in a vehicle to everything (V2X) services. V2X services refer to the use of EVs (either BEV or PHEV) to distribute the power to either Vehicle to Grid (V2G), Vehicle to Building (V2B), Vehicle to Vehicle (V2V) and so on. One of the applications for V2G is to minimize grid congestion, however, an uncontrolled and frequent charge and discharge of the vehicle can have a significant effect on the battery life cycle as well as increase the charging cost for the user. The next question which arises is *how to reduce the cost of energy paid by the user while participating in V2G services and schedule the charging and discharging process to minimize the losses?*

1.1. Research Objective

The main objective of the thesis is **to minimize the cost of energy for charging of EVs by developing and implementing smart charging algorithm with V2G services considering the effects of battery degradation.** A smart charging algorithm will provide controlled, scheduled and optimized charging scheme. The algorithm will incorporate bi-directional power flow which would enable EVs in performing V2G services when the Photovoltaics (PV) is not able to meet the charging demand of the vehicles or the local load (where the energy demand of the building are always first priority than charging of EV) or when the selling the electricity to the grid is leading to great profits (given the energy available in the battery of EV and parking time is sufficient). Services like V2G can have significant effects on battery End of Life (EOL) and State of Health (SOH), which can be negated significantly by including a battery degradation model to monitor the capacity loss due to charging and discharging of the batteries and calculating cost of battery degradation losses when performing V2G, thereby limiting the bidirectional function of the EVs.

To achieve the set objectives several sub-objectives are set which are as follows:

- Develop a mathematical model for V2G with proper constraints to include in smart charging algorithm.
- Verification of the sanity of the algorithm by conducting sensitivity parameter analysis.
- A trade-off between various battery degradation model to calculate the cost of battery degradation will be performed. The selection will be based on its flexibility to be included in the Mixed Integer Linear Programming (MILP) optimization.

1.2. Research Question

To obtain the aforementioned objective a set of research question will be formulated that will act as a guidelines and will be answered during the course of this thesis. The research questions pertaining to the objective are as follows:

1. How to formulate an optimal and cost-effective smart charging algorithm for EVs charging when EVs can participate in V2G?
   (a) How do the mathematical model and developed algorithm mimic the physical world?
   (b) How is the battery degradation is taken into consideration?
   (c) What are the factors or parameters that affect the behaviour of the algorithm?
2. How do V2G services of the smart charging algorithm be used to prevent faster battery degradation?How is the degradation model developed and how effective it is as compared to a simplified model?
3. How effective and optimal the developed smart charging algorithm is as compared to uncontrolled charging?

1.3. Research approach

To answer the research question and achieve the set objective goals it is important to make a scheduled workflow. The first task is to understand the previously developed algorithm and try to implement the bidirectional power flow which would aid in implementing the V2G functionality of the algorithm. The sanity of the algorithm is checked to ensure that the algorithm developed is doing what was expected. The test includes the following steps:

- Verifying the power balance at any time t
- Verifying that cars are charged to the requested energy demand (if the penalty of not fulfilling the charging demand is very high)
- Verify that the scheduling of the charging of EV is in such a way that it should utilize the PV power the most. The node only uses grid power supply in case PV is not able to meet the demand of the EV or the EV is leaving soon

- Proving the hypothesis that the EV will perform V2G when the PV fails to supply the demand of the local load or charging demand, or to obtain some profit by sending the energy back to the grid, or to support the grid to meet the local load or charging demand

After successful implementation and verification of the bidirectional power flow algorithm a series of sensitivity analysis cases studies will be performed on the parameters, like changing the cost of penalty, cost of PV generation, cost of selling energy, and so on, which changes the behaviour of the algorithm.

The last part of the thesis is to include a more efficient battery degradation model in the developed algorithm for V2G. The battery degradation model will be used to calculate the cost of battery degradation losses that the user will have to bear if user participates in V2G services. The cost of battery degradation will also be a limiting factor for the power exported from the battery. To verify the working of battery degradation model an analysis of battery energy during V2G with simplified battery degradation model and with new battery degradation model will be done to check how it affects the charge and discharge cycles. Figure 1.2 shows the workflow for this thesis.

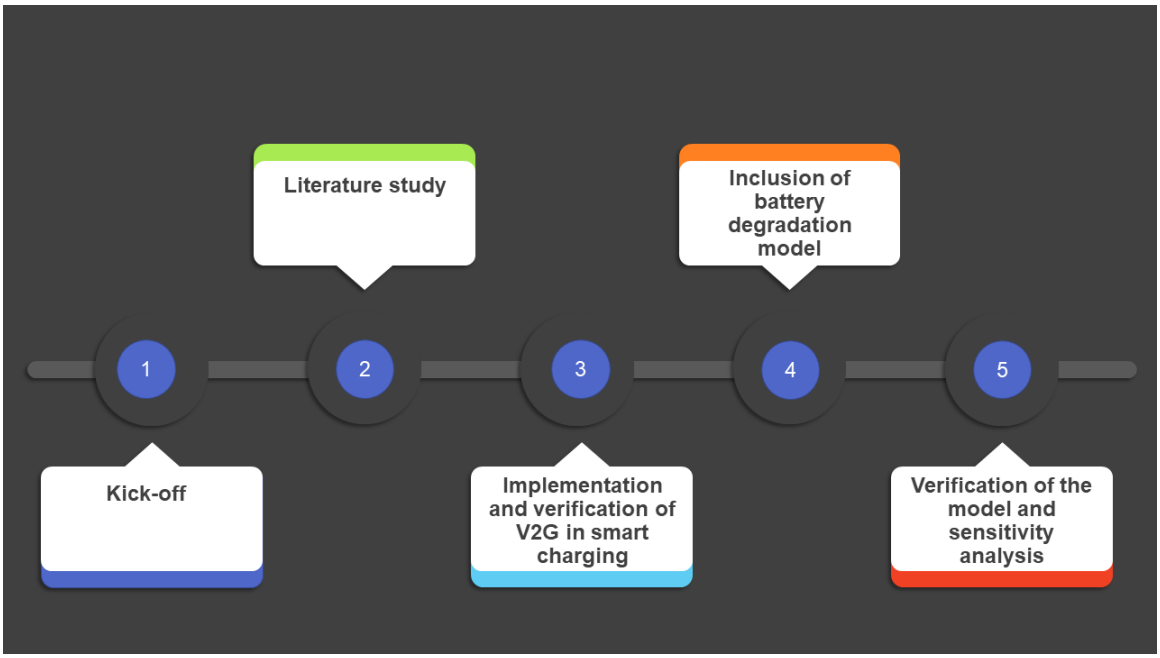

Figure 1.2: Workflow

1.4. Report outline

The content of this report is as follows:

- **Chapter 2** introduces various literature present on the topic, selection criteria for mathematical model or optimization strategy.
- **Chapter 3** explains the mathematical model followed by algorithm explanation.
- **Chapter 4** shows various case studies performed using the algorithm and analysis of the simulations performed.
- **Chapter 5** explains the effect of stress factor C-rate on battery aging and a comparative analysis with simplified model is made. Chapter 5 also include a comparative analysis of the smart charging with V2G and battery degradation model with uncontrolled charging.
- **Chapter 6** will conclude the report followed by future recommendations.

2

Literature study

This chapter aims at summarizing the literature study done for this thesis. A thorough literature study has been done to provide the state of the art research and advancement in the field. The structure of this chapter will be as follows: Section 2.1 deals with the introduction of Electric vehicles (EV), charging strategies of EV, smart charging algorithm. Section 2.2 introduces the V2X services, and V2G which is the main focus in this thesis. The section also provides various V2G optimization techniques implemented and current research. Section 2.3 provide an overview of the battery degradation process. A detailed study is done for various degradation model to select a degradation model for this thesis.

2.1. Introduction to Electric vehicles

In this section, an introduction to the EV, its charging strategy and challenges in charging of EV is explained. Section 2.1.1 explains how the trend of EV progressed through ages, section 2.1.2 explains the charging strategy of EV and section 2.1.3 explains the challenges associated with charging an EV.

2.1.1. Trend of electric vehicles

Electric vehicles (EVs) are defined as a vehicle which is based on electric propulsion which uses onboard battery storage system as a power source [2]. After the first introduction of EVs in the early 19th century, the EVs were not popular until 1873 because of the limitations of charging rechargeable batteries. In 1873, Robert Davidson built the first electric car to be working on the road which was powered by the disposable iron/zinc batteries which incurred an increased cost [3]. Since then, there has been continuous ups and downs advancement of research of EV keeping it always on and off the market until the early 1990s.

During the 1990s concern about the environment emerged and the potential of hybrid or electric vehicles seemed more alluring which resulted in forming new regulations and incentives for the EV user [4]. This paved the path for an exponential increase in the use of EVs as people across the globe which can also be seen in Figure 1.1. Looking at the exponential increase in sales of EVs and market study it is predicted that EV sales will increase by 15%–20% of total new vehicle sales by the year 2035 [5]. In 2014, a study showed that the EV sales saw a sharp increase by 80% (total sale 320,000) [6] and by 2016 it has surpassed the 2 million mark [7]. It is expected that the number will continue to increase even further and will exceed the mark of 7 million in the "medium-term"[8]. These studies opened up the window of opportunity for the EV and companies like Chevrolet, Nissan and so in starting their own EV production [9].

2.1.2. Charging strategy of electric vehicles

As the number of EV is increasing at a rapid rate and expected to cross 7 million mark, it is necessary to look at how charging an EV works, what are the charging strategy and any latest advancement in the research? At the moment there are three types of electric vehicles in the market: Hybrid Electric Vehicles (HEV), Plug-in Hybrid Electric Vehicles (PHEV) and Battery Electric Vehicle (BEV). Table 2.1 shows the electric vehicle categories along with their current charging strategy [10].

Vehicle Category	Utilizes Conventional Engine	Manner in which to charge battery
HEV	Yes	Onboard (internal)
PHEV	Yes	Onboard internal and/or external loading
BEV	No	External loading

Table 2.1: EV categories and charging strategy [10]

Among the three types of electric vehicles, the main focus for this thesis will be on the BEV. The main power source of the BEV can be rechargeable battery packs, a capacitor or a flywheel [11]. Charging a battery of an EV is easy and as electricity is everywhere the EV can be charged almost anywhere. However, the major problem with EV charging is that a single time charge might not be sufficient for the trip, and it is uncertain how quickly a vehicle will be charged [12]. An EV can have the option to charge either using an AC or DC charging [13]. In AC charging, the EV is charged using AC power coming from the grid which is then converted to DC power to charge the battery [12]. This can be done using three types of AC charging system which is worldwide accepted. The type of AC charging system are as follows[12],[14-15]:

1. Type 1: Also known as Yazaki, Type 1 is a single-phase charger mostly famous in the USA.
2. Type 2: Type 2 is a single phased charger used in Europe, it can either be a three-phase or a single phase.
3. Type 3: Popular in EV plug alliance, Type 3 is a single or three-phase charger.

Different types of charger account for different port configuration, power input and output limitations, protocol for transferring data (if any). To standardize the charging type International Electrotechnical Commission (IEC) set up a standard which is IEC 62196 which deals with aspects mentioned earlier [12].

Nowadays, it is convenient to use the AC power to charge the car, however, an inclination towards the DC charging systems have already begun its implementation and standardization. In DC charging, the battery can be charged using an off-board charging converter which delivers power to the battery of the EV. An off-board charging system eliminated the need for on-board chargers and the charger can go to a higher power level as compared to AC charging [12],[15]. The most important type of DC chargers available are as follows[12]:

1. Combined Charging System (CCS), developed by Charging Interface Initiative (CharIN) in the year 2011 by European and US car manufacturers. The CCS version of the charger can provide a charging rate of 350kW, accepts both Type 1 and Type 2 AC plus and is suitable for both European and US-style.
2. Another type of charger, developed by Japan in 2009 as a fast charger, is “CHArge de MOve” or CHAdeMO.

As it has been already mentioned earlier that current charging process majorly involves AC charging. However, an inclination towards the DC charging system has been seen. DC chargers mentioned above are beneficial for another reason as it can support both AC and DC charging. Moreover, DC flexibility to connect to renewable energy resources provide another advantage. Given the recent increased popularity in the use of Photovoltaics it can become one of the major sources in providing the energy charging the EV. Drastic reduction in the PV costs in recent years and a sustainable outlook provide concrete evidence on why using PV to charge the EV and also use to supply the load demand is beneficial. Advancement in the DC charger mentioned above, CCS and CHAdeMO type of chargers are more likely to be used for charging [15].

Apart from high charging power rating, compact size of the EV due to off-board chargers, flexibility to use PV, the other benefit of the DC charging is that the charger can be made bidirectional. A bidirectional charger is beneficial in implementing vehicle to everything or V2X [16]. A V2X is a service which enables EV to discharge to supply power to the grid (V2G), to another vehicle (V2V), to home (V2H) and so on (a detailed study is explained in section 2.2). Using service like V2X, the EV can be used for the following purposes[15-17]:

- To support the grid or renewable energy source when the load demands are higher compared to the supply
- As a storage system for the renewable energy source
- Ancillary services like peak shaving, demand response, frequency regulation and so on.

2.1.3. Smart charging

A rapid increase in the sales of EV and the advancement in the PV research makes it easier to use PV to charge the EV which will also imply higher penetration of both the technologies [18]. However, there are still some challenges that need to be overcome. The most common challenge in using PV as a source to charge the EV is that PV generation is very uncertain. As the increase in the number of EV in the market increase, it will get more and more difficult to charge the EV with just a PV source thereby it will rely on the grid. Relying on the grid will imply that there might be a situation when the grid will experience higher peak load demand due to higher EV penetration [12].

A study in the USA has shown that grid can bear the 25% penetration of EV at a low charging level, however, if the penetration increases that will have an adverse effect on the grid. It has been observed in the study that the transformer experience a decrease in the lifespan by a magnitude of two order when it goes 50% of the nominal capacity [19]. A method to overcome the issue and reduce the stress on the grid, with charging using PV, a storage system for PV can be used. It will be used to supply the EV energy request when the PV power is not sufficient or changes due to unprecedented weather. However, a storage system will increase the cost of the system and will not be optimal in size as mentioned in [20]. Services like V2X can enable the EV to help the grid with the ancillary services, however, it can also have an adverse effect on the battery. V2X services lead the EV to frequent charging and discharging cycles which will deteriorate the battery making it more prone to cyclic aging battery degradation [21] (a detailed study of battery degradation is done in section 2.3).

Another method to improve the utilization of PV and reducing the stress on the grid is developing a smart charging algorithm. A smart charging algorithm is a method in which the EV is charged with varying power throughout parking. The schedule of charging is determined with the help of PV generation forecast, and are scheduled to charge when the generation is sufficient [22]. In [22],[23] it has been shown that the use of smart charging provides maximum utilization of PV generation and include grid when the generation is not sufficient. A generation dependent scheduling of the charging is proved to be beneficial in not reducing the stress on PV or grid but also economical as seen in [24]. Apart from economical and sustainable benefit, adding V2X services along with smart charging has also proved to be beneficial. Addition of V2X along with smart charging can be used to schedule the charging and discharging of the EV effectively to reduce the peak demand. Apart from scheduling the charging and discharging, smart charging can also keep a check on the battery degradation, and provide a threshold on the frequency of charge and discharge cycle of the EV [25].

Various works have been done earlier to make smart charging more optimized and modelling the optimization problems including different applications. In [26], a Linear Programming (LP) approach to the optimization problem is used. The study focusses on reducing the cost of energy for the EV. The study followed the current trend of DC charging and used PV generating units and real-time tariffs and forecasting to formulate the optimization problem. The reduction of 6% is observed for the cost. Whereas in the study [27], a Mixed Integer Linear Programming approach is used (MILP). The optimization problem in the study [27] is a cost minimization problem for EV charging. Parameters like PV generation, EV data, and energy prices are used for the problem. A reduction of 10-171% in cost is seen using this optimization method. In [28], the optimization problem not only deals with minimizing the cost of energy for the EV user but also include ancillary service like frequency regulation using a stochastic problem. An average reduction of 7.2% is observed in the study. The gap in the aforementioned studies is that they did not include various applications altogether and provided results based on a fixed application with a very low reduction percentage of the cost. The main contribution of this thesis is derived from [15], where a MILP objective problem is formulated which includes EV scheduling, V2G services and other applications. The objective of the problem in [15] is a cost minimization MILP which showed a significant reduction of the range of 32% to 651% in the cost of energy for the EV user is seen.

2.2. Vehicle to Grid: Advancement and challenges

The purpose of this literature study is to provide a detailed review of the Vehicle to Grid. The study is divided into three sections where: section 2.2.1 provides the introduction to V2X. In section 2.2.2 Vehicle to Grid is introduced, section 2.2.3 provide an overview of the current studies on optimization techniques with V2G, challenges with V2G and focus of the thesis.

2.2.1. Introduction to Vehicle to Everything

Electric vehicles spend a large amount of time parked when they are stationed at home, workplace or parking station. A study in [29] shows that an EV can be at parking for an average of 12 hours at home or up to 7-9 hours at a workplace [22]. During the interval, the EV can get charged to the requested energy input by the user. The recent advancement in the field of charging strategy and chargers, the EV can be charged to its requested energy within 1.5 hours (depending upon the requested energy and power supply from the charger) [29]. For an EV parked for the duration of say 8 hours and it gets charged to the requested energy within 1.5 hours will give EV a standby time of 6.5 hours. As mentioned earlier higher EV penetration can affect the grid. To minimize the stress on the grid and to utilize the standby time of the electric vehicles, V2X application is introduced [16].

Vehicle to everything or V2X is an application which enables the EV, connected to Electric Vehicle Supply Equipment (EVSE), to discharge energy of the battery to support the outside system [29]. The energy discharged from the EV can be utilized in various applications. The first application is Vehicle to Home or V2H where the outside system is the home. V2H is said to be less complex as it does not involve a large number of EVs at the parking or does not require an infrastructure for the energy management system (EMS). As the EV stand parked for an average of around 12 hours, the V2H services can use the EV as a backup power source in case of a power outage or as a load management system, if the house is a micro-grid. The load management system will allow the home to use the renewable power generation as much as possible to minimize grid dependency [30]. V2H is different from Vehicle to Building, where the external system is a commercial or industrial building. In V2B the EV is used rather differently, the EV is used to reduce the peak of the building load which will reduce the tariff due to demand charges [31]. Another application of V2X is Vehicle to grid or V2G where the external entity is the grid. Section 2.2.2 provides a detailed study of V2G, it is also one of the main focus of the thesis.

2.2.2. Vehicle to Grid

Vehicle to Grid or V2G refers to an application of V2X where the external system is the grid. In V2G, the EV is used as an energy source to provide grid management services. The grid management services are monitored by entities which are called electrical system operators such as Distribution system operators (DSOs) or Independent System Operators' (ISOs). These operators regulate the power market and allow V2G for various situations. When enabled, V2G can perform numerous grid support applications such as spinning reserve, peak shaving, time-shifting and other ancillary services [29]. Ancillary services are defined as additional support services that are being provided to the grid to maintain its reliability, improve efficiency and making it more sustainable [32]. Few of the applications that V2G support are defined as follows:

1. Spinning reserve: Spinning reserve is defined as "unloaded generation that is rotating in synchronism with a utility-grid" by [33]. The V2G application provides an input to the grid via spinning reserve using the energy of the EV. This application of the V2G provides benefits to the grid as it initiates failure recovery, decrease the backup generation and compensate for any outages [34].

2. Peak shaving: Peak shaving is defined as reducing the amount of energy purchased from the grid during the peak hours of the energy demand. Making the EV go bidirectional to perform V2G enable it to support the load demand of the node. Through V2G application peak shaving application can be performed by using the energy of the EV to reduce the peak demand [34].

3. Time-shifting: In this application of V2G, the EV are used as a storage system for the renewable generation. The stored energy in the EV (EV which are parked for longer duration 5-10 hours) can be used to supply the demand during the off-peak generation of the renewable power source [35].

The technological advancement of the V2G is still in progress. Researches and studies are being conducted to make the application more optimal and include most of the application along with smart charging operation. Various studies have modelled the V2G application in the smart charging algorithm which provides ancillary services. The development of the mathematical model, optimization technique and findings are explained in the following section.

2.2.3. Optimization techniques for Vehicle to Grid

V2G application along with smart charging algorithm is being mathematical modelled to determine the most optimal solution for either minimization or maximization objective. The objective problem can include cost optimization for EV and renewable energy source, operational cost minimization for other stakeholders like the DSO, ISO, charging cost optimization for EV users and so on [34]. The mathematical model of the objective function can be different depending upon the objective, optimization techniques or application. The optimization techniques which are commonly used are as follows [34]:

1. Classical technique: Classical technique is used when the objective function is "continuous and differentiable". The most commonly used classical model include Linear Programming (LP), Mixed-Integer Programming (MIP), Non-Linear Programming and so on.

2. Meta-heuristic optimization technique: This technique uses a more practical approach in finding the optimal solution for the objective. The most commonly used techniques are Genetic Algorithm, Swarm optimization and so on.

3. Hybrid technique: This technique uses two or more optimization technique to generate a more combined iterative solution.

Various studies have been done using the aforementioned technique to generate a more efficient and cost-effective model for the given objective function. In [34], various types of objective function has been modelled to utilize the V2G and optimize the Cost, efficiency, renewable energy use and emission and so on. This thesis focuses on cost minimization, therefore the studies related to cost optimization will be taken into account. The study in [36] was done to use V2G services in charging the EV which will ease the stress from the increasing load. The optimization was two-step optimization where the first step was to minimize the cost of charging and the second was to maximize the profit for an islanded microgrid. The discharging cost and the power is multiplied over the length of the horizon. The model in [36] was developed based on a classical approach. In [37], a MILP approach is used to minimize the operational cost and a V2G application is used to provide the peak shaving services. The model minimizes the total operational cost for supplying energy to EV and generate controlled and scheduled charging. Studies have been done to minimize the EV charging cost. In [38], a classical optimization model is made to minimize the EV charging cost as well as determine how charging of EV affect congestion in the distribution network.

In [39] a stochastic programming approach is used to determine optimal charging schedule for the EV and maximize the V2G performance while generating benefits for the grid operators. The study in [40] a minimization objective problem is formulated based on classical technique. The objective in [40] is to minimize the cost of the EV charging cost by scheduling the charging and discharging at the interval when the energy tariffs are beneficial. In [41], a MILP approach is used to minimize the operational cost and V2G application is used to provide the peak shaving services. Other studies [42-44] is based on a classical approach to increase the utilization of renewable energy sources by generating an optimal charging strategy for EV and using EV as a storage system for RES.

The studies mentioned above provide a very optimal solution for smart charging and V2G application. Although, the V2G services provide great beneficial services to grid and other parties it involves various challenges. The few challenges corresponding to V2G are [34]:

- To provide V2G applications charger should have a bidirectional converter. The current station might not have a suitable infrastructure for the V2G and could involve huge investments

- Getting the support of the EV user, the grid operators and policymaker is difficult.

- V2G enables EV undergoes frequent charging and discharging process which accelerates the battery degradation

The aforementioned studies provide a smart and optimal charging and discharging strategy for the EV. The energy source can involve RES or the grid or using RES along with the grid. One of the major gap in the research in the studies mentioned above is that they do not consider the effect of battery degradation in V2G model. In this thesis, V2G is mathematically modelled along with smart charging algorithm which uses a MILP optimization technique. The objective of the optimization process is to minimize the cost of energy

by the user and provide ancillary services using V2G. A detailed study on battery degradation model is done in Section 2.3 and a model is selected. Including the battery degradation model along with smart charging algorithm will restrict the V2G application. A restriction in V2G application will provide the user with an optimal cost of energy along with benefits from the V2G while keeping the degradation loss to a minimum.

2.3. Battery degradation: Mechanisms and Modelling

Implementing a smart charging algorithm can provide benefits to the EV users as well as to the other stakeholders by scheduling charging of EVs when the cost is minimal. Apart from the scheduling of EV charging, the algorithm can also feature V2X services that will enable EVs to act as a source. EVs acting as a source provide services to the grid, to the building and so on. The focus of the thesis is on the V2G services of the EVs. However, it has been seen that V2G involves EV undergoing frequent charging and discharging process. The increased frequency leads to much faster battery degradation [34]. Being said that, it is important to understand the mechanism of battery degradation, factors affecting the battery degradation and modelling the battery in such a way that the algorithm will account for the cost of battery degradation that the user must bear if participating in V2G. The algorithm when implemented with battery degradation will try to minimize the loss. The question that rises here to *what extent V2G application of the EV battery will affect battery capacity over its lifetime?*. To answer this question, in this section, the literature is focused on the basics of battery degradation, various mechanisms, various degradation model and finally the model that will be a reference for this thesis.

2.3.1. Battery degradation mechanisms

A battery cell comprises of three important components: two electrodes (anode and cathode) and an electrolyte. A series of oxidation and reduction in the electrodes provide the basic mechanism of the battery to convert chemical energy to electrical energy. A collection of various cells connected construct a battery pack which is controlled by the Battery Management System or BMS [45]. One of the most commonly used batteries used in electric vehicles is Li-ion batteries [45]. Battery manufacturers test the battery cells under certain conditions and provide the lifetime of the battery if operated at certain conditions. The lifetime of the battery here implies the period that the battery will be able to provide electrical energy. Charging or discharging the battery frequently reduces the lifetime of the battery due to the formation of a Solid Electrolyte Interface or SEI [46-47]. An SEI is a passive layer that is formed at anode responsible for the degradation of the battery. The formation of the SEI layer significantly affects the total capacity of the battery which thereby affects the State of Health of the battery. The State of Health is important in determining the lifetime of the battery and the End of Life or EoL of the battery [46]. If the SoH of the battery reaches 0% it means the battery has served its purpose and now have reached its EOL. Typically, the EoL of a battery in automotive application is said to be reached when the battery capacity drops below 80% [48]. The State of Health is associated with the capacity reduction or Capacity fade or the increase in internal impedance which is also referred to as Power fade. Capacity and power fade are the two degradation mechanism that occurs due to the increased growth rate of SEI [49].

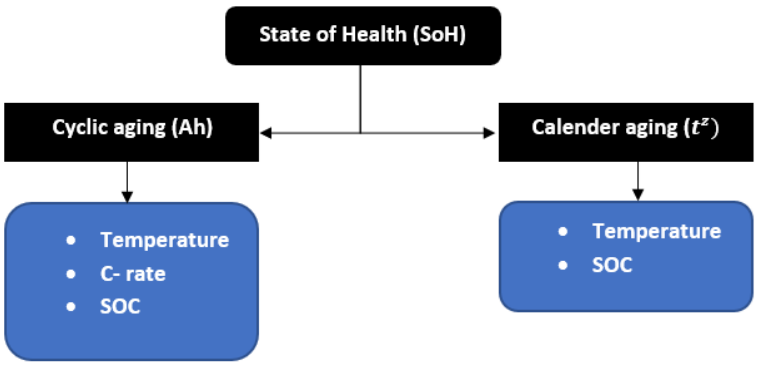

Figure 2.1: Aging mechanism and its stress factors [45]

The capacity and power fade degradation mechanism results in two aging characteristics in the battery namely Calendar and Cyclic aging. The aging of the battery depends upon various factors which are also called stress factors [45]. Calendar aging is one of the degradation that happens to the battery when the battery is at rest. The stress factor that aggravates the Calendar aging of the batteries is temperature and State of Charge (SOC). The SOC and temperature dependence of the aging is formulated with the help of the Arrhenius equation. The studies in [50],[51] has shown the dependence of Calendar aging concerning time. The dependence is formulated as t^z where t is the time and z is 0.5. Other aging characteristics of the batteries are Cyclic aging. Cyclic aging is the aging mechanism that occurs due to the usage of the battery. The stress factors associated with Cyclic aging are SOC, temperature, charge current (C-rate), Depth of Discharge (DOD) and so on [45-51]. The studies in [52],[53] have also shown other stress factor that determines the cyclic aging which is the number of cycles (N), the energy throughput (Ah) or remaining energy that can be extracted from the battery. Figure 2.1 [45] shows the aging mechanism and its stress factors where the black box represents the concept and blue represents the stress factors.

2.3.2. Battery degradation model

This thesis prioritizes the modelling of battery degradation because of cyclic aging. Calendar aging for an EV battery is out of scope for this thesis. Various researchers have modelled the degradation of battery to determine the cost of battery degradation and try to minimize the frequency of charging and discharging during V2G services [42]. The study on cyclic aging focus on the capacity fade of the Li-ion battery in electric vehicles have been done in [45]. The paper modelled the throughput, C-rate temperature and SOC stress factors using empirical methods. The battery was tested under the condition and an experiment was conducted. The experiment helped in concluding a few important behaviour analysis. The capacity fading was observed to be very low for low average SOC. The C-rate does not influence the battery capacity at room temperatures and the increase in temperature due to ohmic loss was observed to be increasing the capacity fade. The Arrhenius equation was used to model the temperature influence.

In the study [54], a semi-empirical life model for the capacity loss [%] is used which includes both Calendar and cyclic aging. The value of time (t) in Calendar aging was taken as the square root of days and calculated using the assumptions based on 10% DOD. The cyclic aging model used is seen to have a linear relationship with the throughput (Ah) but an exponential relationship with temperature and C-rate. The model was successful in correlating the effects of temperature and C-rates in determining capacity loss. Moreover, the “decoupling” of Calendar and cyclic aging provided a more perceptive and deeper understanding of the two mechanisms.

In [55], a semi-empirical model is used for LiFePO4 graphite battery aging which incorporates real-life data to mimic the physical simulation. The model is used for hybrid electric vehicles and a multi-objective optimization problem is formulated. The objective of the problem is to minimize battery aging and fuel consumption. The study showed a linear relationship between battery SOC and capacity loss [%] whereas exponential relation with C-rate and the throughput (Ah) was modelled as the square root. The model was designed for a Li-ion cell and the curve fitting tool is used to determine the relationship between modelled and experimented data. The model was tested under various condition and the following was concluded. The paper determines the “inter-dependency” between battery aging and its management using the method of severity factor map in controlling the capacity loss.

In [56], the author has used an empirical model to determine the cyclic aging and calendar aging based on capacity fade and resistance increase in Li-ion batteries. The study on calendar aging is done by first keeping SOC at 50% and varying the temperature from 308-323K, and then varying SOC from 0-100% at 323K. The cyclic aging study is done based on average SOC at 308K. The accuracy of the result from the empirical method was observed to be 0.998 for capacity fade and 0.986 for resistance increase. Even though the results are promising the study has some gaps like the author checked the SOC dependence for very low DOD, the temperature effect on cyclic aging is not observed and the lifetime of the battery determined is observed to be very low.

In [57], the author developed an empirical model to account for Li-ion degradation due to EV charging. The study is done for cyclic aging and both capacity and power fade is taken into account. The model calculates the cost of battery degradation by determining the maximum cost due to stress factor like temperature, SOC and DOD for both fading. The temperature for calendar aging is varied from 283K to 328K and is kept constant at 293K for cyclic aging. The accuracy of the model in determining the degradation is observed to be 93% and 96% for DOD 0.6 and 0.3 for 3800 cycles. The model developed showed no interrelation between other conditions and no decoupling of stress factor is seen.

The study in [58] is done to determine the cycle life for graphite-LiFePO4 cells. Using the empirical model, the author determines the capacity loss due to cyclic aging as a power law factor of throughput and showed an Arrhenius relationship for temperature. The cells were cycled at various temperatures, DOD, C-rate. The study shows that at low discharge rates, the DOD is not important in determining the capacity loss. It is to be noted that the power law for throughput is claimed to be due to the SEI interface. In another study, the empirical model was developed to assess the impact of V2G on battery lifetime [59]. The model was based on capacity fade due to cyclic and calendar aging. Calendar aging is calculated due to the effect of temperature with the Arrhenius equation and power law for a time. The capacity fade due to cyclic aging is dependent on the current and power law function throughput. The model is simulated SIMCAL SIMSTOCK and different factors like C-rates, charging strategies and V2G on battery lifetime is observed. The study concludes for a better battery lifetime, if the EVs are performing V2G, a controlled and limited V2G is essential.

This thesis will focus on the work in [54], where a linear relationship between throughput and capacity loss is modelled. The thesis will incorporate two degradation model: first, a simplified one, where the cost of battery degradation will be calculated based on energy throughput. The second model will incorporate C-rate stress factor. In [54], the C-rate shows an exponential relationship with capacity loss, therefore to adapt it to the existing MILP algorithm the linearization is done. Further explanation on linearization and implementation of the model is explained in Chapter 5.

3

Implementation

This section of the report deals with the modelling and implementing the optimization problem to minimize the cost of energy used by the user. It also incorporates V2G function to the smart charging algorithm and its implementation using Python and an optimization solver - Gurobi. The section is divided into three parts: the first part contains necessary assumptions made, the second part is mathematical model necessary for the optimization process, the third part describes the software used and finally explaining how the algorithm works to minimize the cost of energy used.

3.1. Assumptions

Assumptions play an important role in creating a mathematical model and implementing it as a simulation so it mimics the real-world scenarios. During this thesis, several parameters or cases are assumed and several other input parameters like local load profiles, EV data are derived from NEDU [60], ElaadNL [61] respectively. These assumptions hold for all the base case and are listed as follows:

1. All loads and charging stations are kept at 3 phase and node voltage and maximum phase current are 230 V and 25 A respectively. Even though changing the voltage and current changes the grid power limitations, it hardly had any significant effect on the results. Keeping all the loads and charging stations at 3 phase is done to avoid any grid imbalances.

2. Local loads always have the priority in using PV power and the charging stations use the PV power when the PV generation is sufficient.

3. Grid import and export power (here, Grid import = phase*node voltage* maximum phase current and Grid export = $\frac{Gridimportpower}{3}$) limitations and PV parameters such as scaling factor of PV (taken as 1, ideal condition), the efficiency of the inverter at PV (taken as 0.95) [62] is kept constant. For the grid power limitations, an agreement between the DSO and the node is made beforehand agreeing of the import and export power parameters [63]

4. The cost of buying electricity is taken from a data set containing Day-ahead market prices. The cost of selling is taken as 70% of the cost of buying [64]. The predetermined market prices are essential in this thesis because the optimization algorithm must know the prices of buying and selling the energy for proper scheduling of charging and discharging of EVs present at the charging station.

5. Data set containing local load data is used in this thesis to provide various local load profiles, for a year, for different locations.

6. The efficiency of the power converter and maximum power limitations for charger and EV are the same and kept constant.

7. It is assumed that all the forecast PV power and PV power follows the same trend before and after the optimization horizon. It is assumed that the value of PV power used is decided by MPPT and will be

curtailed according to the local load demand and maximum grid export power. During the optimization, algorithm decides on how much PV power it can use from the generation. After the demand are met, any excess power can be exported to the grid for financial benefits.

8. EV fleet dataset is used based on locations such as Public, semi-public or household locations to provide the optimization algorithm with EV data such as arrival time, energy demand and so on. However, the algorithm only retrieves the information for the duration of the optimization and use the data only after the EV is connected to the charging station.

9. Cost of battery degradation when the battery degradation model is taken as 0.112 euro/kWh. The reason for the assumption is explained in section 3.2.3

10. The value of data resolution of the input parameters and timestep for the optimization process is taken as one minute.

11. The cost of PV generation for 25 kW PV panels (c_PV) is 0.0 euro/kWh. The value is selected based on the assumption that all the cost leading to LCOE is being paid off

12. The cost of penalty for this thesis is taken as 50 times maximum cost of buying energy for the day. The value is selected based on the study in [15]. The value will remain same for all case studies except when sensitivity analysis of the cost of penalty is done.

3.2. Mathematical model of the optimization process

This section explains the mathematical framework that is needed for the optimization problem. The section contains a list of optimization parameters, input parameter, objective function and constraints which affect the outcome of the results and helps in simulating physically possible scenarios. A layout of the energy management system is shown in figure 3.1. The layout and the optimization algorithm is based on the project of *OSCD* [65]. It is to be noted that the optimization process is for a single node with power supply from the grid and PV. The node layout is for a local load (a public building) where total number of charging stations available are 4.

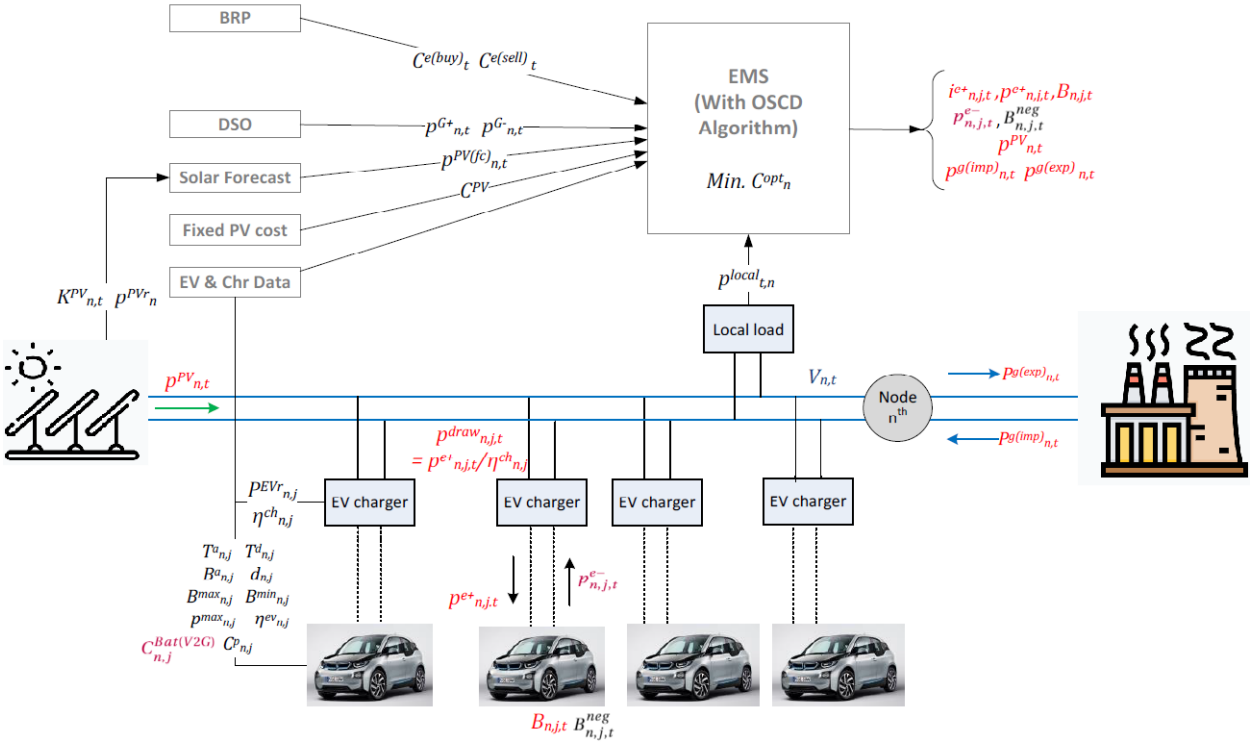

Figure 3.1: Layout of the energy management system [65]

3.2.1. Optimization Parameters: Decision variables

Solving an optimization problem requires assigning a set of quantities or variables, which are needed to be solved to reach the objective of the problem. The optimization problem is said to be solved when all the variables are assigned their best possible values, the variables are called decision variables. Defining the variables and understanding their correlation is a must take step in solving the problem. The variables in this thesis are classified as positive parameters in table 3.1 and negative parameters in table 3.2 as described below.

Positive parameters:	
$p_{n,t}^{PV}$	Power generated by the renewable energy source at the car park at time t,nth node (kW)
$p_{n,t}^{g(imp)}$	Power imported from the grid to node n park at time t, respectively (kW)
$p_{n,t}^{g(exp)}$	Power exported to grid by node n at time t, respectively (kW)
$B_{n,j,t}$	Battery energy at jth charger EV battery which connected to the nth node at time t (kWh)
$p_{n,j,t}^{e+}$	Charging power at jth charger EV which connected to the nth node at time t (kW)
$i_{n,j,t}^{e+}$	Charging current at jth charger EV which connected to the nth node at time t (kW)
$S_{n,j,t}$	SOC value of the battery of EV at jth charger at node n at time t

Table 3.1: Positive variables

Negative parameters:	
$p_{n,j,t}^{e-}$	Discharging power at jth charger which is connected to the nth node at time t (kW)
$B_{n,j,t}^{neg}$	Energy exported from jth charger EV battery which connected to the nth node at time t (kWh)
$i_{n,j,t}^{e-}$	Discharging current at jth charger EV which connected to the nth node at time t (kW)

Table 3.2: Negative variables

3.2.2. Optimization Parameters: Input Parameters

Reducing the complexity of the optimization problem is done by assuming few input parameters and using a data set for values like the cost of buying and selling the electricity, grid limitations, user input EV parameters and so on. In the table below, various input parameters are shown along with the source of the input like the user, EV collected data, from Charging system operator (CSO), Distribution system operators (DSO), Balance responsible parties (BRP) and Electric Vehicle Supply Equipment (EVSE).

Input parameter	Description	Source
$B^{a}_{n,j}$	Arrival Energy of the battery at the jth charger EV (kWh)	EV
$d_{n,j}$	Charging energy demand at jth charger EV(kWh)	User
$C^{p}_{n,j}$	Penalty for not meeting energy demand by departure time at jth charger EV (/kWh)	CSO
T	Time duration of optimization horizon	CSO
ΔT	Time step (data resolution) (min)	CSO
C^{PV}	Cost of obtaining PV energy (/kWh)	CSO/User
$C^{e(buy)}_{t}$	Market clearing price for buying electricity from the grid respectively (/kWh)	BRP
$C^{e(sell)}_{t}$	Market clearing price for selling electricity to the grid respectively (/kWh)	BRP
$C^{Bat(V2G)}_{n,j}$	Losses the User has to bear for the battery degradation when participating in V2G for nth node and at jth charger	CSO
T^{a}_{j}	Arrival time at jth charger EV (h)	User
$\eta^{ev}_{n,j}$	Efficiency of bi-directional converter at the EV connected to jth charger at node n	EVSE
$\eta^{ch}_{n,j}$	Efficiency of bi-directional converter present at the jth charger at node n	EVSE
T^{d}_{j}	Departure time of EV (h)	User
$B^{min}_{n,j}$	Minimum possible energy in the battery at jth charger EV, respectively (kWh)	EV
$B^{max}_{n,j}$	Maximum possible energy in the battery at jth charger, respectively (kWh)	EV
$p^{max}_{n,j}$	Maximum charging power of the EV at jth charger at node n	EV
$p^{EVr}_{n,j}$	Rated power of the jth EV charger connected to the EV (kW)	EVSE/CSO
$p^{inv}_{n,j}$	Inverter maximum power limits at the jth charger	EVSE/CSO
p^{diff}	Difference between supply power and power demand	CSO/User
$p^{G+}_{n,t}$	Distribution network (Grid) capacity for feeding power to node (kW)	
$p^{G-}_{n,t}$	Distribution network (Grid) capacity for drawing power from node (kW)	

Table 3.3: Input variables description and its source

3.2.3. Objective function

The objective function in an optimization problem indicates how decision variables along with a coefficient contribute to minimizing or maximizing a problem. The objective function below comprises of the various function of energy (decision variables) and their cost to find the minimum cost of energy used by the user. Furthermore, a list of sub-functions is described to explain the relationship between the decision variables.

$$Min.C^{opt}_{n} = \sum_{j=1}^{J}(B^{a}_{n,j} + d_{n,j} - B_{n,j,T^{d}_{j}}) * C^{p}_{n,j} + \Delta T \sum_{t=1}^{T} p^{PV}_{n,t} * C^{PV} + \Delta T \sum_{t=1}^{T} p^{g(imp)}_{n,t} * C^{e(buy)}_{t} - p^{g(exp)}_{n,t} * C^{e(sell)}_{t} - \sum_{j=1}^{J} \Delta T \sum_{t=1}^{T} p^{e-}_{n,j,t} * C^{Bat(V2G)}_{n,j} \quad (3.1)$$

The Equation 3.1 describing cost minimization objective function consists of four parts.

1. The first part defines the cost of penalty $C^{p}_{n,j}$ that is to be provided to the user if the demand $d_{n,j}$ is not fulfilled. When the user connects to the charging station the EMS stores the EV arrival battery energy and asks for the energy demand from the user during the duration of parking $T^{d}_{n,j} - T^{a}_{n,j}$.

2. The PV power supply is not necessarily always free of cost to charge the EV. The cost C^{PV} is introduced which defines the LCOE if the PV is installed by the third party.

3. The cost of buying and selling energy from the grid based on the settlement point prices $C^{e(buy)}_{t}, C^{e(sell)}_{t}$. The market dynamics always ensure that the $C^{e(buy)}_{t} \geq C^{e(sell)}_{t}$ [15]

4. The loss in the form of cost of battery degradation that the user has to bear if the user decides to participate in V2G activity. The cost of battery degradation, that the users has to bear, is given by $C_{n,j}^{Bat(V2G)}$. The battery degradation model used in this equation is a simplified version which can also be interpreted as the cost of selling energy from the battery. After the algorithm is implemented the degradation model will be changed to a more effective model which will consider the factors affecting the cyclic aging. In this equation the cost of battery degradation when the simplified battery degradation model is taken as 0.112 euro/kWh. This is calculated by using the following equation 3.2 [66] where, $C_{n,j}^{Bat(V2G)}$ is the cost of battery degradation, c_{new} is the cost of a new battery (taken as 175 euro/kWh), L is the is the life cycle, which is 2000 cycles for DOD (depth of discharge) at 80%, η is the round-trip efficiency which is 0.97, and nominal battery capacity $E_{nominal}$ depends upon the user input data.

$$C_{n,j}^{Bat(V2G)} = \frac{c_{new} * E_{nominal}}{L * \eta * E_{nominal} * DOD} \tag{3.2}$$

Note: The variables in the equation 3.1 are $B_{n,j,T_j^d}, p_{n,t}^{PV}, p_{n,t}^{g(imp)}, p_{n,t}^{g(exp)}, p_{n,j,t}^{e-}$ rest are the input parameters

$$B_{n,j,t} = B_{n,j}^{a} + \Delta T \sum_{T_j^a}^{t} (\frac{p_{n,j,t}^{e-}}{\eta_{n,j}^{ev}}) + \Delta T \sum_{T_j^a}^{t} (p_{n,j,t}^{e+} * \eta_{n,j}^{ev}) \quad \forall n, j, t \in [T_{n,j}^{a}, T_{n,j}^{d}] \tag{3.3}$$

$$B_{n,j,t}^{neg} = \Delta T \sum_{t=1}^{T} (\frac{p_{n,j,t}^{e-}}{\eta_{n,j}^{ev}}) \quad \forall n, j, t \in [T_{n,j}^{a}, T_{n,j}^{d}] \tag{3.4}$$

$$B_{n,j,T_{n,j}^{d}} = B_{n,j}^{a} + \Delta T \sum_{t}^{T_j^d} (\frac{p_{n,j,t}^{e-}}{\eta_{n,j}^{ev}}) + \Delta T \sum_{t}^{T_j^d} (p_{n,j,t}^{e+} * \eta_{n,j}^{ev}) \quad \forall n, j, t \in [T_{n,j}^{a}, T_{n,j}^{d}] \tag{3.5}$$

$$i_{n,j,t}^{e+} = \frac{p_{n,j,t}^{e+}}{3 * V_{n,t}} \quad \forall n, j, t \in [T_{n,j}^{a}, T_{n,j}^{d}] \tag{3.6}$$

$$S_{n,j,t} = \frac{B_{n,j,t} - B_{n,j}^{min}}{(B_{n,j}^{max} - B_{n,j}^{min})} \quad \forall n, j, t \in [T_{n,j}^{a}, T_{n,j}^{d}] \tag{3.7}$$

The equations 3.3-3.7 explains how the different parameters and variable are defined and how they are related to each other. Equation 3.3 describes the limit that is being put on the battery energy and estimate the value at any time t after the arrival. It consists of three parts: the arrival battery energy, the energy imported to the EV during charging and the energy exported from the EV during V2G. The energy exported from the EV is also described by $B_{n,j,t}^{neg}$ is described in equation 3.4. The departure energy of the EV is described by equation $B_{n,j,T_{n,j}^{d}}$. Equation 3.6 defines the charging current and equation 3.7 is used to calculate the state of the charge of the battery. It is to be noted that since a battery can't charge and discharge at the same time, the value of $p_{n,j,t}^{e+}$ can only be true if $p_{n,j,t}^{e-}$ is false or vice versa for any t in $[T_{n,j}^{a}, T_{n,j}^{d}]$.

3.2.4. Acceptance criteria

Acceptance criteria are the minimum requirements that is to be fulfilled by an EV when it arrives at a node n and is connected to the charger. Connecting to the charger enables EMS which asks user to connect to a charger depending upon the two criteria mentioned in equation 3.8 and 3.9. Equation 3.8 is the first criteria which takes the energy demand and parking time for all the EVs and checks if it is within the power limit of the charger. The second criteria mentioned by equation 3.9 is to check that the arrival energy content of the vehicle must be above the minimum limit as set by the user.

$$\frac{d_{n,j}}{T_{n,j}^{d} - T_{n,j}^{a}} \leq Min.\{p_{n,j}^{EVr}, p_{n,j}^{max}\} \quad \forall n, j \tag{3.8}$$

$$B_{n,j}^{min} \leq B_{n,j}^{a} \quad \forall n, j \tag{3.9}$$

3.2.5. Constraints

Constraints or boundary conditions are restrictions that are put on decision variables to limit their maximum and minimum value. The constraints in this thesis are based on the physical limitations of the charger, EV or the grid; for example, the import and export power from the grid is limited by the DSO. The equations below help the solver to closely mimic the real-world situation and generate the best possible solution for the objective.

$$p^{e+}_{n,j,t} \leq Min.\{p^{EVr}_{n,j}, p^{max}_{n,j}\} \quad \forall n,j,t \in [T^a_{n,j}, T^d_{n,j}] \tag{3.10}$$

$$0 \geq p^{e-}_{n,j,t} \geq -Min.\{p^{EVr}_{n,j}, p^{max}_{n,j}\}, \quad \forall n,j,t \in [T^a_{n,j}, T^d_{n,j}] \tag{3.11}$$

The EMS at node n controls the charging and discharging power of each EV at time t. The charging power $p^{e+}_{n,j,t}$, and the discharging power $p^{e-}_{n,j,t}$ is limited by the power limits of the the charger and EV.

When EV is connected

$$B_{n,j,t} \leq B^{max}_{n,j} \quad \forall n,j,t \in [T^a_{n,j}, T^d_{n,j}] \tag{3.12}$$

$$B_{n,j,t} \geq B^{min}_{n,j} \quad \forall n,j,t \in [T^a_{n,j}, T^d_{n,j}] \tag{3.13}$$

The EMS restricts the capacity of the battery to be within the limits $B^{min}_{n,j} and B^{max}_{n,j}$ as set by the EV manufacturers and/or user. The battery capacity is controlled to not exceed the maximum battery capacity $B^{max}_{n,j}$ as shown in equation 3.12.

When EV is not connected

$$i^{e+}_{n,j,t}, p^{e+}_{n,j,t}, i^{e-}_{n,j,t}, p^{e-}_{n,j,t}, B_{n,j,t} == 0 \quad \forall n,j,t \leq T^a_{n,j} and t \geq T^d_{n,j}] \tag{3.14}$$

Equation 3.14 describes the condition when the EV is not connected to the charger for t before arrival time and t after the departure time.

$$(i^{e+}_{n,j,t} == 0) or (i^{e+}_{n,j,t} \geq 6) \quad \forall n,j,t \in [T^a_{n,j}, T^d_{n,j}] \tag{3.15}$$

$$i^{e+}_{n,j,t} = i^{e+}_{n,j,t} + \Delta i^{e+} \tag{3.16}$$

$$-25 \leq i^{e-}_{n,j,t} \leq 0 \tag{3.17}$$

For each EV charger, if the charging process is on then the minimum charging current is 6A which implies that the minimum charging power is 4.14kW. The current value increments in integer steps of Δi^{e+} as 1A. Whereas the discharging current is subjected the inverter limitations and is not bounded like charging current. The bound is shown in the equation 3.17.

$$\sum_{j=1}^{J} (\frac{p^{e+}_{n,j,t}}{\eta^{ch}_{n,j}}) + \sum_{j=1}^{J} p^{e-}_{n,j,t} * \eta^{ch}_{n,j} + p^{local}_{n,t} - p^{PV}_{n,t} = p^{diff} = p^{g(imp)}_{n,t} - p^{g(exp)}_{n,t} \tag{3.18}$$

$$p^{g(imp)}_{n,t} \leq p^{G+}_{n,t} \quad \forall n,j,t \in [T^a_{n,j}, T^d_{n,j}] \tag{3.19}$$

$$p^{g(exp)}_{n,t} \leq p^{G-}_{n,t} \quad \forall n,j,t \in [T^a_{n,j}, T^d_{n,j}] \tag{3.20}$$

The AC grid is used for power exchanges between the EV, PV, the local loads and the grid. The intra-car park power exchanges between different EV chargers and PV are related to the power exchanged with the external grid is given by equation 3.18. Both $p^{g(imp)}_{n,t}$ and $p^{g(exp)}_{n,t}$, the grid import and export power, is not allowed to be imported or exported at the same time because the node and the grid is connected via a single transmission line which makes it physically impossible to export and import power at the same time. It is

also to be noted that market dynamics ensures $C_t^{e(buy)} \geq C_t^{e(sell)}$ at all times [15]. The $p_{n,j,t}^{e+}$ and $p_{n,j,t}^{e-}$ will not have finite values (here implies that if $p_{n,j,t}^{e+}$ is greater than 0 then $p_{n,j,t}^{e-}$ will be equal to zero or if $p_{n,j,t}^{e-}$ is less than 0 then $p_{n,j,t}^{e+}$ will be equal to zero) at any given time t because of the physical limitations of a battery to not charge and discharge at the same time.

Finally, $p_{n,t}^{g(imp)}$ and $p_{n,t}^{g(exp)}$ should be within the distribution network capacity as shown by equation (3.19) and (3.20) . The values of $p_{n,t}^{G+}$ and $p_{n,t}^{G-}$ are used as a thermal proxy for all potential limitations in the distribution network including voltage limits, line limits and transformer capacity. The values can come from the distribution system operator (DSO), ISO based on loading and voltage in the network and an agreement between the DSO and the seller is made beforehand agreeing of the import and export power parameters.

3.3. Programming language and solver

Realizing the aforementioned mathematical equations and study various scenarios to understand the working of smart charging along with V2G function, an environment is created. *Python* programming language is used to write the scripts for the mathematical model. Different set of scripts are created to perform the following tasks:

- Importing real-world data set like the cost of buying and selling electricity, load profile and so on
- Collect the user input EV parameters like arrival time, departure time, energy demand
- Store optimization parameters
- Set the optimization duration and time resolution of the input data
- Set up a controller to trigger the optimization process and saving the result
- Create an optimization model

As mentioned earlier, the mathematical model aims to minimize the cost of energy used by the user. To achieve the goal, an optimization solver *Gurobi* is used to solve the optimization problem. The optimization problem is identified as Mixed Integer Linear Programming (MILP) and Gurobi is one of the fastest and powerful mathematical tools to solve MILP problems. Vast information on using the solver available on the internet, less solving time for MILP, its simple integration with Python by just accessing the library gurobipy and availability of a free license for the students make it the appropriate choice for the thesis.

3.4. Algorithm

This section of the report explains how the mathematical model is implemented to create a smart charging algorithm with V2G function. To understand the working of the algorithm a flowchart is shown in the figure below. It can be seen from figure 3.2 that the algorithm mainly involves in three processes: the first process: Set time, adjusts the input parameters according to the duration and time resolution of the optimization process, the second process: controller, which is the MILP controller and checks for triggers to start the optimization process which is the third process of the algorithm.

3.4.1. Process 1: Set time

Set time part of the code takes duration, start time and time step and discritize according the timestep and duration of the optimization process. The algorithm uses the pre-generated EV fleet data as an input which contains EV arrival, departure, the energy demand, SOC and so on for the year. When implemented in the real world this data is provided by the user or EV when the EV arrives at the charger and gets connected to the EMS. As the algorithm uses predefined dataset, the code retrieves the EV data for the duration of the optimization. Set time function also generates an uncontrolled charging profile for the EVs to make a trade-off between the controlled and uncontrolled charging.

Uncontrolled and average charging profile

Uncontrolled charging profile or immediate charging is a process by which when an EV arrives at the charging station and connects to the charger, the charger immediately start charging the car the the nominal maximum power rating. The power supplied is almost constant for the duration of charging and the charging stops when the battery is charged to the demanded energy.

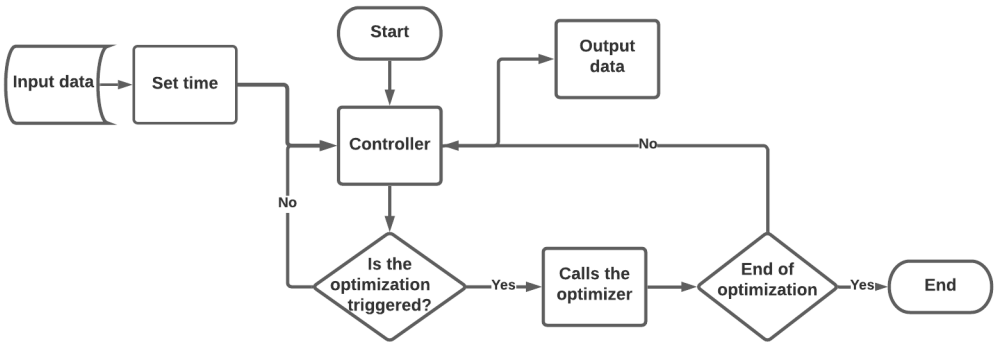

Figure 3.2: Schematic of smart charging algorithm

3.4.2. Process 2: Controller

The set time process is followed by the controller part of the algorithm. The main function of this process is to check for triggers and operate as a controller. Figure 3.3 shows the controller algorithm flowchart. The algorithm performs the following sets of steps before it calls the optimizer for the optimization process.

After the set time function, the algorithm starts the controller function. The controller initializes all the node and EV parameters. All the EV related parameters are set to a null value or default value at the start. The controller starts the loop for the duration at 1-minute timestep. At every timestep the algorithm checks for the new EV arrival. If the EV does not arrive at any of the chargers the parameters are kept the same. However, if an EV arrives at the charger, the user connects the EV to the charger and EMS takes the EV input. The EMS checks the EV connectivity criteria as mentioned in section 3.1.4. If the EV clears the criteria, the EV parameters are overwritten by the new EV parameter. An ordinal number is assigned to the EV for the given charger to keep a count of EV arriving at that particular charger.

After the parameters of EV are overwritten, the controller checks for any existing EV at other chargers. If an EV is already present at other chargers, the controller splits the parameter as old and new EV. The new split EV parameters such as SOC, arrival time, arrival battery capacity and energy request is changed to the value a timestep before a new EV arrives. Other parameters are kept the same. The algorithm then uses the receding horizon to determine the optimization horizon, the number of steps for the horizon, time sequence of the horizon. After determining the optimization parameters, the controller calls the optimizer and record the output parameter.

Receding horizon

The algorithm uses receding horizon control to increase the flexibility to trigger and reset the parameters by using events or at a certain interval. Events like the arrival of a new car, change in the energy demand, departure of the car or the use of the reset cycle at a reasonable frequency can be used to trigger the optimization process. However, the trigger for this thesis is selected as the arrival time of the EV at the charger. The algorithm updates the input parameters at the start of a new optimization sequence and schedule the charging for the available EVs for their parking duration.

Let us assume a node n, with the number of chargers J=4, is considered for the optimization algorithm. Figure 3.4 charging profile for a charger with X-axis as the time of parking and Y-axis as the presence of EV at the charger. The figure depicts four chargers namely j = 1 to j = 4, where a block represents the EV parking duration. At t1, charger 2 detects the arrival of the new EV. The user connects the EV to the charger and the EMS stores the EV data such as the arrival time, the energy of the battery, the departure time and so on. The algorithm checks for the connectivity criteria as mentioned in section 4.1.4 for the EV and if the EV clears the connectivity criteria the algorithm triggers the next process where the controller checks the duration of the parking and checks the presence of other EV at other chargers. If an EV is present at a charger, it updates the value of EV parameters and determines the optimization horizon based on the last departure time of the EV at charger j. In case of a charger (as in j = 4) is empty or a car leaves, the controller resets the value to default or null value. After all the parameters are set, a new optimization process starts with $t_{start} = t1$, and after a few sequences of computation, a schedule for each EV at charger j is determined such that the cost of energy

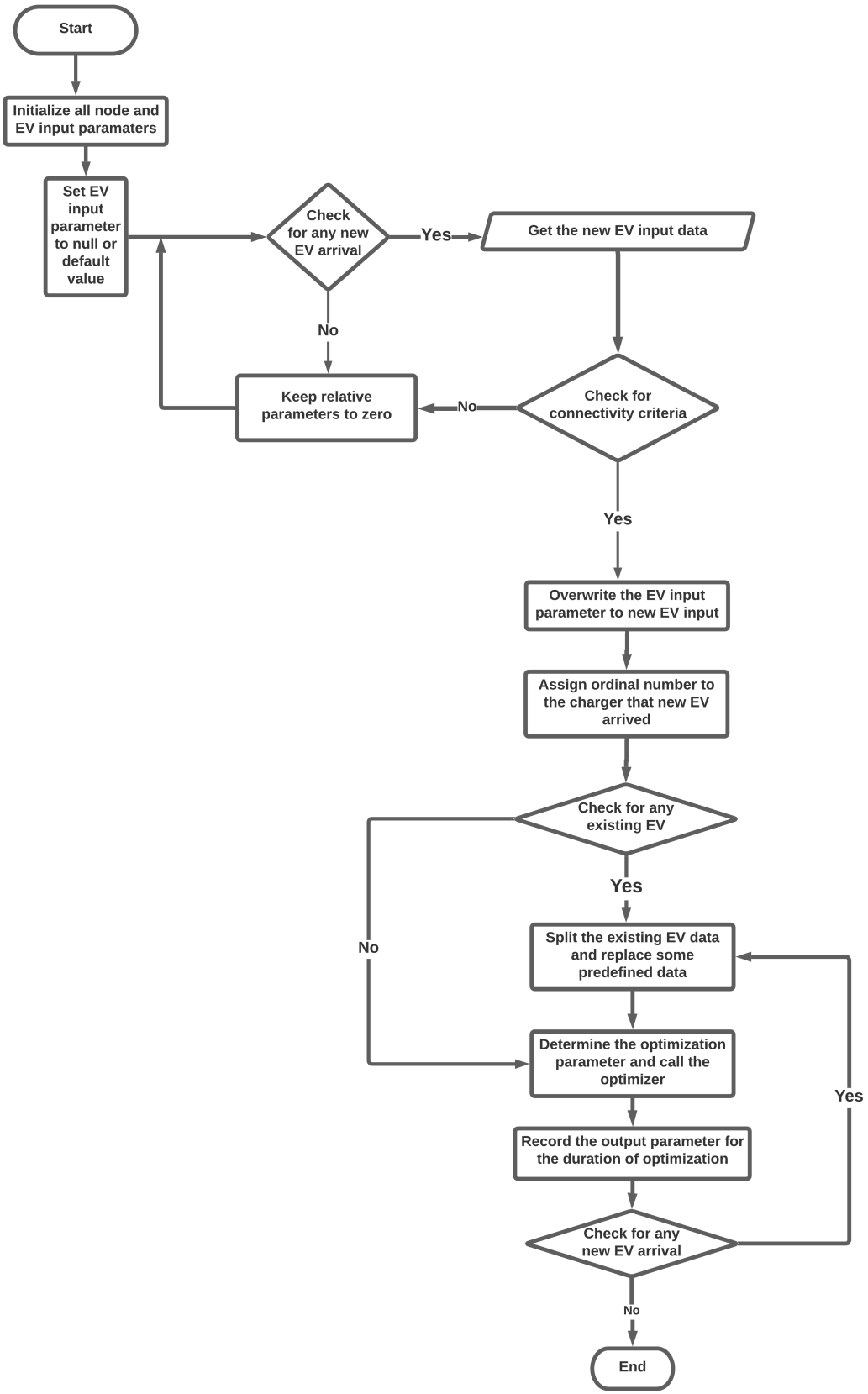

Figure 3.3: Controller algorithm flowchart

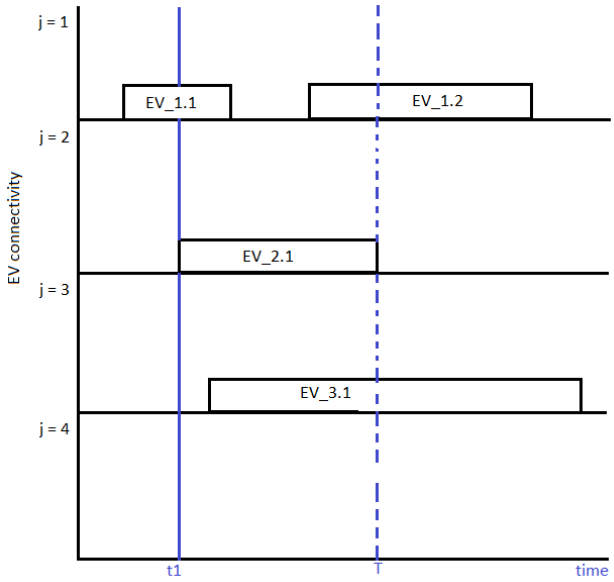

Figure 3.4: Receding horizon explanation and horizon determination

is minimum and the parameters are updated. It is to be noted that the algorithm stops optimization after EV_3.1 leaves, the optimization won't be triggered unless there is a new EV after the departure of EV_3.1.

3.4.3. Process 3: Optimizer

The optimizer part of the algorithm convert the mathematical model mentioned in Section 3.1 into *Python* script. The optimizer algorithm imports library for *Gurobi* solver called *gurobipy* as *Python* interface provides a lot more options for translating the mathematical model to an optimization model. The script creates a model using Model() object which includes other commonly used methods like Model.addVars, Model.update(), Model.addConstrs(), Model.setObjective(). After creating the model, the script add the decision variables and input parameters using Model.addVars. Binary switches like to prevent the grid import and export at the same time or charging and discharging of EVs are included which is switched on and off according to the condition mentioned in section 3.1.5. After setting the objective function according to section 3.1.3 constraints and boundaries are added to limit the behavior of the variables. Model.Params.timeLimit is used to set the timeout for the optimization process and after the controller calls the optimizer as mentioned in section 3.3.2 the optimizer performs the optimization process and data are extracted using Model.getVars() and stored for plot and analysis.

3.5. Summary

In this chapter, a mathematical model and algorithm for the cost minimization objective function were developed and explained. For the algorithm to mimic the real-world situations several assumptions were made. the mathematical model developed is a MILP optimization problem that minimizes the cost of energy for the user. Several constraints and sub-functions are defined based on the assumption made in section 3.1 and to realize the mathematical model more practically. The mathematical model comprises four parts namely: cost of penalty for unfinished charging, cost of energy from PV, cost of buying or selling energy from and to the grid, and finally cost of battery degradation. It is to be noted that the degradation model used in this chapter and for the case study in chapter 4 is a simplified one and can be implied as to the cost of energy from the battery. After the model is developed, *Python* programming is used to develop the algorithm. The algorithm contains three important functions namely: Set time, controller and optimizer. As the algorithm developed is an optimization problem, *Gurobi* is used to solve the problem. The algorithm uses the receding horizon principle to determine the optimization horizon for the algorithm. The algorithm developed is tested and several case study is performed for the parameter that affects the behaviour of the algorithm and is explained in Chapter 4.

4

Case studies

After the successful implementation of the algorithm, it is necessary to check how the behaviour of the algorithm will change by varying certain parameter? This section deals with the case study for various sensitivity parameter. To perform the sensitivity analysis of the algorithm various parameter are selected, varied and results are analysed. The parameters selected for sensitivity analysis are the cost penalty, cost of PV generation, cost of selling energy and grid import power. A simplified battery degradation model is used for this chapter and after the inclusion of a more effective battery degradation model in the algorithm, the algorithm behaviour change is analyzed for the case with new battery degradation in the next chapter. The duration of the process is selected for 4 days which includes two weekdays and two weekends. Assuming the parameter value as 4 days provides the range of weekdays and weekend days where the behaviour of the local load profile changes.

	Batt_size (kWh)	**t_arr(DD-MM-YYYY hh:mm)**	**t_park (min)**	**t_dep(DD-MM-YYYY hh:mm)**	**E_event (kWh)**
Charger 1	**50**	**07-09-2018 08:28**	**140**	**07-09-2018 10:48**	**4.1**
Charger 4	**50**	**07-09-2018 10:19**	**5**	**07-09-2018 10:24**	**1.4**
Charger 3	**50**	**07-09-2018 11:52**	**15**	**07-09-2018 12:07**	**0.5**
Charger 4	**50**	**07-09-2018 17:28**	**88**	**07-09-2018 18:56**	**8**
Charger 1	**50**	**08-09-2018 10:00**	**471**	**08-09-2018 17:51**	**5.2**
Charger 3	**100**	**08-09-2018 11:13**	**808**	**09-09-2018 00:41**	**13.6**
Charger 4	**50**	**08-09-2018 11:38**	**82**	**08-09-2018 13:00**	**5.7**
Charger 2	**100**	**08-09-2018 16:20**	**219**	**08-09-2018 19:59**	**2.2**
Charger 1	**50**	**09-09-2018 08:20**	**383**	**09-09-2018 14:43**	**5.2**
Charger 4	**50**	**09-09-2018 13:02**	**576**	**09-09-2018 22:38**	**3**
Charger 3	**100**	**09-09-2018 14:51**	**178**	**09-09-2018 17:49**	**8.3**
Charger 2	**50**	**09-09-2018 17:19**	**107**	**09-09-2018 19:06**	**8.3**
Charger 1	**50**	**10-09-2018 09:10**	**52**	**10-09-2018 10:02**	**0.1**
Charger 2	**50**	**10-09-2018 10:17**	**323**	**10-09-2018 15:40**	**2.3**
Charger 3	**100**	**10-09-2018 14:21**	**148**	**10-09-2018 16:49**	**5**
Charger 1	**50**	**10-09-2018 16:54**	**44**	**10-09-2018 17:38**	**0.4**
Charger 4	**100**	**10-09-2018 18:37**	**121**	**10-09-2018 20:38**	**10.9**

Table 4.1: EV input parameter for the duration

4.1. Analysis for cost of penalty (c_p)

Introducing V2G along with a smart charging algorithm involves EVs undergoing frequent cycles of charging and discharging. Due to which EVs arriving at the charger can experience a reduction in the battery energy and might depart the charging station without its energy demand fulfilled. Unfulfilled energy demand can cause an antipathy among the EV user and decline the involvement of EV for V2G. To prevent the decline of the involvement of EV for V2G, a parameter is introduced in the algorithm. The parameter introduced is the cost of the penalty. Introducing the cost of penalty in the algorithm will increase the overall cost of the node, and therefore the algorithm will try to minimize it by charging the EV to requested energy. The study in [15] suggests that the value of the cost of the penalty for not charging the EV to their requested energy can be as high as 25 times the maximum cost of buying energy. In this case study, the cost of penalty (c_p) sensitivity is analysed. The change in the behaviour of the algorithm is observed by keeping a c_p value to 0 euro/kWh to 25 times the maximum cost of buying energy. Values larger than 25 times the maximum cost of buying energy is also used to check how tighter the value should be to ensure that the EV demands are always fulfilled.

Table 4.1 shows the EV parameter data for the duration arriving at each charger. The EV arrival at a charger is shown by the first column. During a day, multiple EV can arrive at the charger; for example on 07/09/2018 two EV arrive and connect to charger 4. Therefore, repeated value of charger number shows multiple EV charging events. The table also consists of arrival time, battery size, parking duration, departure time and energy request.

4.1.1. Methodology

To prevent the misuse of the penalty factor, an analysis is performed for the c_p by assuming a few parameters as constant and by using the following steps:

1. A set of parameters are kept constant which might affect the outcome of the optimization process. The parameters which are kept constant during the whole analysis are described below:
    - Cost of selling energy or c_e_sell value is taken as 0.7*c_e_buy
    - All the assumptions mentioned in section 3.1 hold in this analysis as well.
2. After the parameters are defined, the cost of penalty or c_p is varied from 0 euro/kWh to 50* maximum cost of buying energy in steps of 25.
3. An increase in the c_p value is done to make the algorithm more restrict to charge the EV at their requested demand.
4. An analysis is then performed for the range of values, separately, to check how the behaviour of the algorithm changes.
5. A summary for each case explained and a final comparative analysis is done.

4.1.2. Analysis

To analyse the results clearly, one of the day from the duration is selected which is 10-09-2018 whose EV input data can be seen from Table 1. The EV input data provide an idea of how the EV are arriving, leaving and what are the energy demands during the parking time. For the various value of c_p, an analysis of node power profile, charging and discharging of EV and overall power and cost distribution is done. Figure 4.1 shows the cost of energy and cost of penalty change value for the duration.

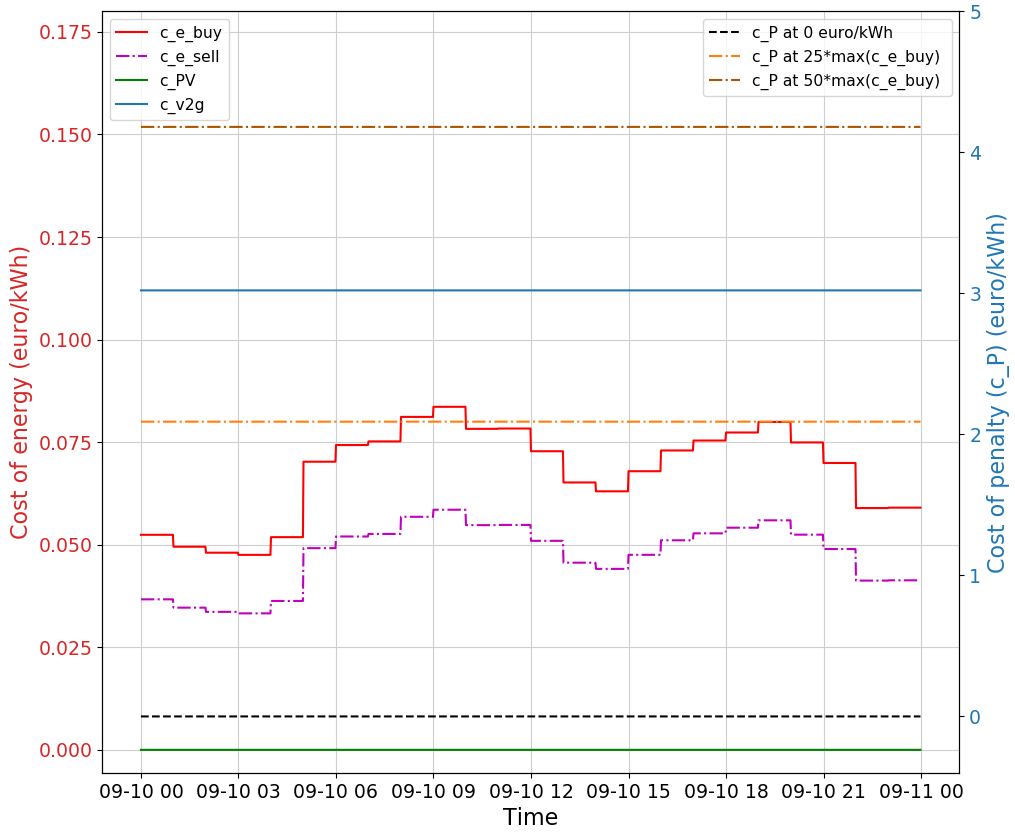

Figure 4.1: Cost of energy and cost of penalty vs time

At c_p = 0 euro/kWh

As mentioned earlier that the cost of penalty for not charging the EV is varied from 0 euro/kWh to kWh to 50* maximum cost of buying energy in steps of 25. The maximum cost of buying for the date 10-09-2018 is 0.08362 euro/kWh. In this section, the focus will be on the value of c_p at 0 euro/kWh. A value of 0 euro/kWh implies that the EVs arriving at the charging station can charge or discharge to any SOC value (without necessarily being charged till the requested SOC at departure) without any penalty involved. As there is no penalty involved, it can be assumed that the algorithm will try to charge or discharge EV to minimize the overall cost of energy for the node. The EVs will participate in V2G to maximize the export power for a higher profit. The grid will involve only to supply the local load demand when the PV generation is insufficient. For the analysis, a node power profile, SOC for EV at various chargers and other necessary plots are plotted and explained.

Figure 4.2 shows the node power profile for the date at c_p 0 euro/kWh. From the figure, it can be seen that the grid power is imported when there is less or no generation of PV. The grid power import is used to supply the local load energy demand, as it has been assumed earlier that the local load demand must always be fulfilled. During the period when the PV generation is sufficient, the local load energy demands are met using PV power. The PV power is curtailed to a value sufficient enough to meet the energy demand of local load, or exporting power to the grid at maximum export capacity which is 5.75 kW. The EVs arriving at the charger is not bounded by penalty anymore, so the EVs are observed to discharge to support PV in maximizing the export power to generate more profit. The EVs are observed performing V2G when the PV power is not enough to meet the energy demand or to match the maximum export power as seen by label 'LB: a' in the figure. . Performing V2G application or PV power export at maximum export value provide EV and node with financial benefits which reduce the cost of energy.

It has been seen from figure 4.2, that the grid involvement is present when the PV generation is insufficient or zero. The EVs arriving at the chargers during this interval are not charged to their requested energy demand. Being said that, it is necessary to see how much the EVs are discharged or the energy of the EV at the

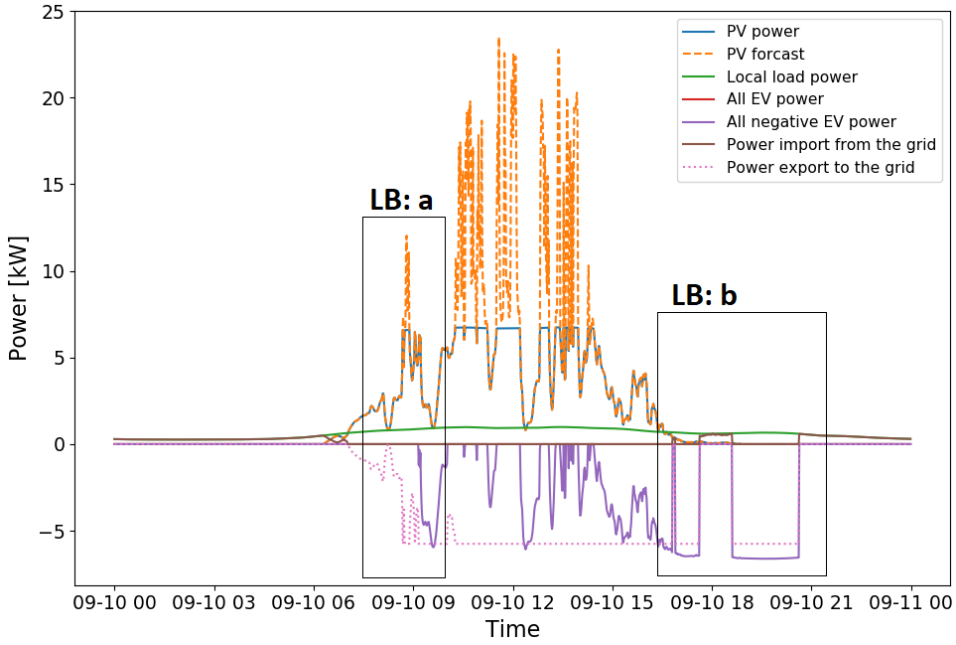

Figure 4.2: Node power profile for c_p = 0 euro/kWh

end of departure. Table 4.2 shows the charger number that the EV arrives at, the arrival SOC, the requested SOC and the departure SOC for c_p at 0 euro/kWh. According to equation 3.12 and 3.13 mentioned in section 3.1.5, the EVs can have energy anywhere in between the maximum battery capacity to minimum battery capacity. It can be seen from the table that the EV leave the charging station with SOC less than the arrival SOC. As there is no penalty involved for charging the EVs, the EVs are not scheduled to charge. The EVs rather perform V2G to maximize the export power or support PV when necessary or reduce the grid involvement. In order to prevent the situation when the EV is not scheduled to charge rather discharge below arrival SOC, a higher value of c_P can be used. The analysis for a higher value of c_P is explained below.

	SOC_arr	**SOC_requested**	**SOC_departure**
Charger 1	**0.4896**	**0.4916**	**0.4265**
Charger 2	**0.4461**	**0.4921**	**0.2511**
Charger 3	**0.3683**	**0.4183**	**0.3141**
Charger 1	**0.4646**	**0.4726**	**0.3698**
Charger 4	**0.4090**	**0.5180**	**0.2732**

Table 4.2: SOC value for various EV at c_P = 0 euro/kWh

At c_p = 25*max(c_e_buy) euro/kWh

As the cost of penalty or c_p is increased, the algorithm becomes more strict in charging the EV to the requested SOC before departure. Figure 4.3 shows the node power profile for c_p at 25 times maximum c_e_buy. The red lines in figure 4.3 are EV charging power at that interval of time. The presence of red lines in the power plot implies that the algorithm charges the EV to the requested SOC. As contrary to the situation in Figure 4.2, for the c_p at 25 times maximum c_e_buy the algorithm tries to charge the EV as much as possible.

There are three distinguishable difference in the behaviour of the algorithm can be observed when the c_p value is increased from 0 euro/kWh to 25*max(c_e_buy). The first difference that can be observed during the duration when the first EV arrives at charger 1 at 09:10. The label 'LB:a' in figure 4.2 and 'LB:c' in figure 4.3 represents power profile for the duration of the EV parking time. It can be seen that in 'LB: a' the EV discharges to perform V2G to support PV in maximizing the export as well as supply the local load demand. It is not the case in 'LB:c', the reason for the behaviour is that as the cost of the penalty is finite the algorithm

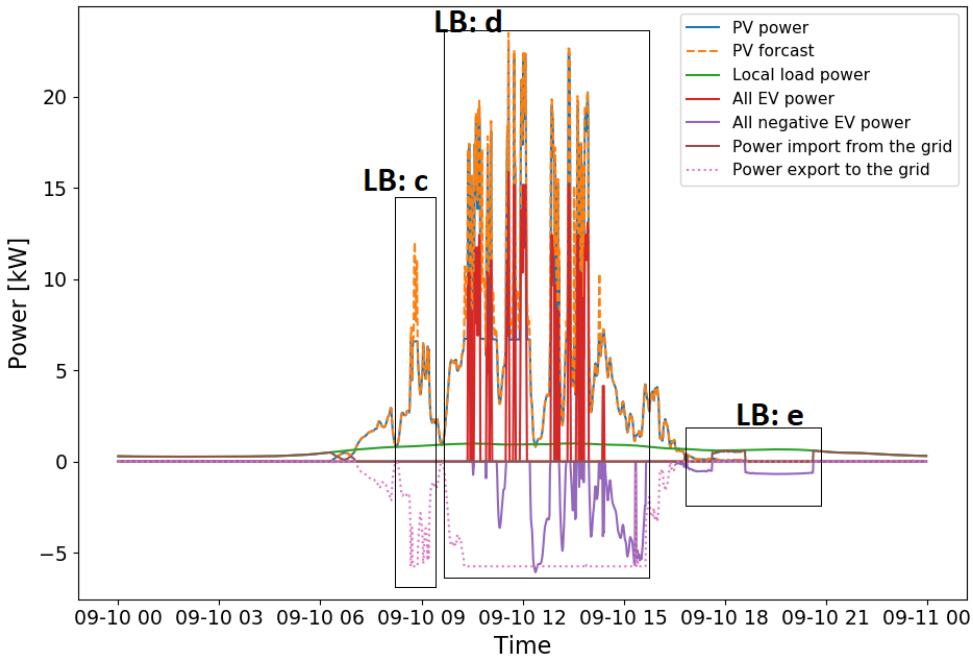

Figure 4.3: Node power profile for c_p = 25* max(c_e_buy) euro/kWh

tries to reduce the penalty cost that is to be paid by the CSO. A V2G operation without charging the EV will lead to a reduction in SOC below the arrival SOC. Thus, an increased cost of the penalty would be paid by the CSO.

The second difference can be observed by the label 'LB:d' in figure 4.3. When the EV arrives during the higher PV generation, the EVs are charged using PV power. The PV still tries to maximize its profit by exporting power at the maximum limit, and any difference is compensated by the V2G application of EV. V2G function of the EV is also observed to be helping in charging other EV and supporting PV in meeting the load demand. The final difference can be observed during the interval of label 'LB: e'. During this interval, two EVs arrive at the charger, namely charger 1 and charger 4. The PV generation is decreasing and is insufficient to charge the EV and supply the local load demand, the grid is involved to support PV to supply any energy demand. As seen from the figure 4.1 that the cost of buying energy is increasing during the interval from 16:00 till 21:00. As the algorithm is designed to minimize the overall cost and benefit the node and EV user; using EVs for V2G to supply the energy demand will reduce the overall cost and compensate for the increased grid involvement. Moreover, as the EV are not charged to their requested energy demand, the EV user will benefit from the finite penalty cost from the CSO.

	t_arr(DD-MM-YYYY hh:mm)	**B_arr (kWh)**	**Energy requested (kWh)**	**Energy at departure (kWh)**	**Penalty cost (euro)**
Charger 1	**10-09-2018 09:10**	**24.481**	**0.1**	**24.48**	**0.21**
Charger 2	**10-09-2018 10:17**	**22.305**	**2.3**	**24.647**	**0**
Charger 3	**10-09-2018 14:21**	**36.833**	**5**	**37.008**	**10.08**
Charger 1	**10-09-2018 16:54**	**23.234**	**0.4**	**22.87**	**1.59**
Charger 4	**10-09-2018 18:37**	**40.909**	**10.9**	**39.545**	**25.63**

Table 4.3: Cost of penalty for c_p = 25* max(c_e_buy)

To determine the penalty cost, it is necessary to check if the EVs are charged to their requested SOC. The SOC at the departure, when multiplied by the battery capacity, gives the energy of the battery at departure. In figure 4.4, SOC for various EV is plotted against time. It can be seen that not all the EVs are charged to their requested SOC which implies that there is a possible penalty for unfinished charging scenario. As the cost of the penalty is calculated by calculating the remaining energy multiplied by c_p, if the remaining energy is x kWh, the penalty cost is x*25*0.08362 euro (where 0.08362 euro/kWh is the maximum cost of buying energy

for the day). Table 4.3 shows the penalty cost for the EV arriving at the charger.

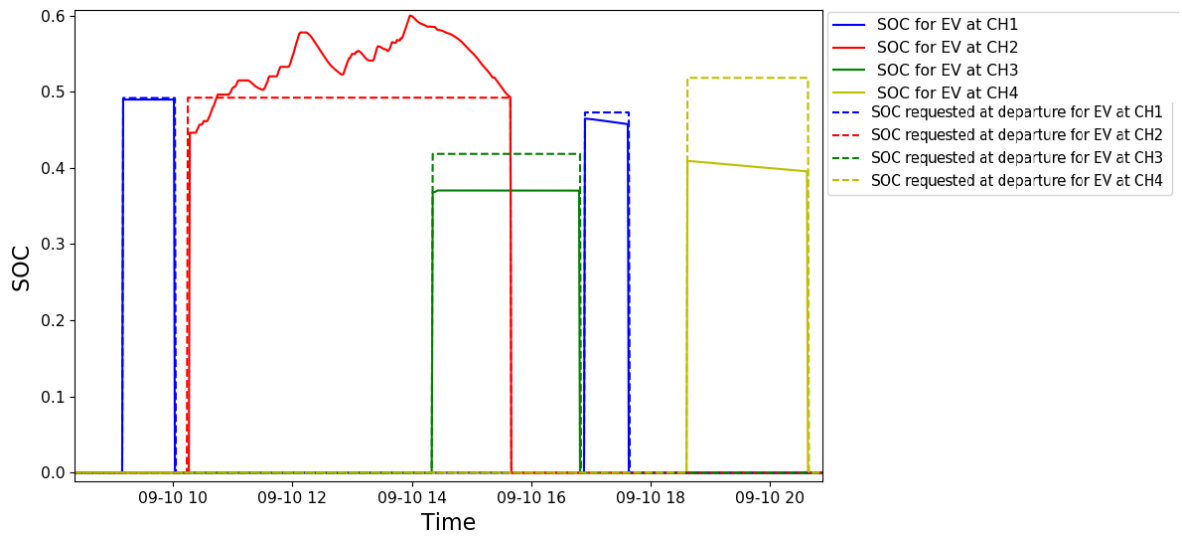

Figure 4.4: SOC vs time for c_p = 25* max(c_e_buy) euro/kWh

At c_p = 50*max(c_e_buy) euro/kWh

As it has been observed earlier that at 25*max(c_e_buy) there are some EVs that are still not charged to their requested energy at departure. The consequences of this are seen on the CSO as they have to pay the penalty for not supplying the demand. The reduced grid involvement to charge the EV is related to the fact that the algorithm tries to benefit the node as much as possible. To improve the situation, a method is suggested where the cost of penalty value is increased to make the algorithm more strict in supplying the energy demand of the EVs. The value of c_p is increased to 50 times the maximum c_e_buy value, which is 4.18 euro/kWh for the date 10-09-2018. The node power profile for the case is plotted and a comparative analysis is performed with other values of c_p. The EV SOC graph is plotted to check if the EVs request is fulfilled and a penalty cost analysis is done.

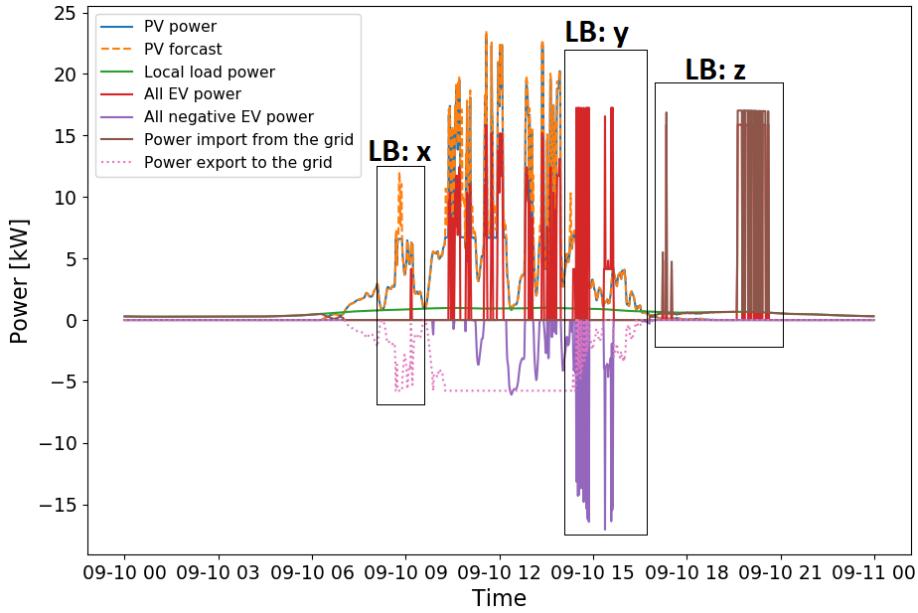

Figure 4.5: Node power profile for c_p = 50* max(c_e_buy) euro/kWh

Figure 4.5 shows a node power profile for the c_p value of 4.18 euro/kWh for the date 10-09-2018. As mentioned earlier, the value of c_p is increased to make the algorithm more strict in charging the EV to the requested energy demand. Three distinguishable feature has been observed as compared to other c_p values. The label (LB) x,y,z in figure 4.5 shows the change in the behaviour of the algorithm when c_p values changes to 50*max(c_e_buy) or 4.18 euro/kWh. In the 'LB:x', the EV arriving at charger 1 is being charged which is not the case for c_p 0.0 and 25*max(c_e_buy) euro/kWh. In 'LB: y', the concentration of EV charging power is increased as compared to that of figure 4.3. The reason for this is as the cost of the penalty is increased the grid involvement is observed to have increased. More grid involvement in seen to support the PV to charge EV or meet local load demand to reduce the penalty cost to be paid by the CSO. It is to be noted that during the interval of 'LB: y' EV at charger 2 provide V2G support PV in charging the EV which is present at charger 3. Another difference is highlighted by 'LB: z', where the grid involvement is seen more prominently. The EV arriving in that interval does not get charged at all in the case when c_p was 0 euro/kWh and when c_p was 25*max(c_e_buy) euro/kWh. However, now when the c_p value is increased, the algorithm becomes more strict and tries to negate the penalty possibility by importing grid power to charge the EV.

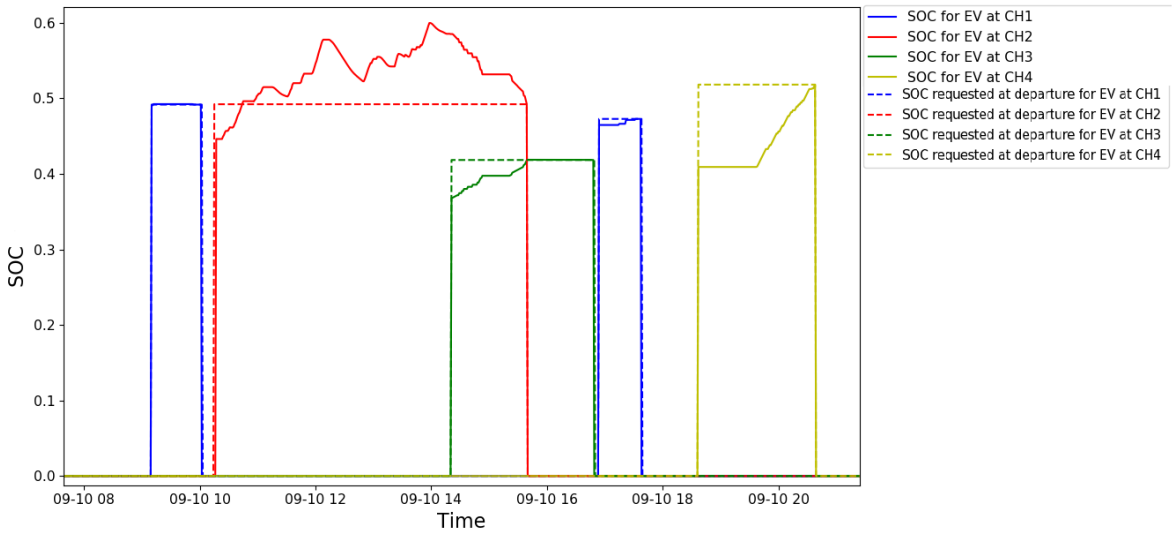

Figure 4.6: SOC vs time for c_p = 50* max(c_e_buy) euro/kWh

To determine the penalty cost, it is necessary to check if the EVs are charged to their requested SOC. The SOC at the departure, when multiplied by the battery capacity, gives the energy of the battery at departure. In figure 4.6, SOC for various EV is plotted against time. It can be seen that all the EVs are charged to their requested SOC, so the remaining energy is 0 kWh. As the cost of the penalty is calculated by calculating the remaining energy multiplied by c_p, if the remaining energy is 0 kWh, the penalty cost is 0 euro. Table 4.4 shows the penalty cost for the EV arriving at the charger.

	t_arr(DD-MM-YYYY hh:mm)	**B_arr (kWh)**	**Energy requested (kWh)**	**Energy at departure (kWh)**	**Penalty cost (euro)**
Charger 1	**10-09-2018 09:10**	**24.481**	**0.1**	**24.581**	**0**
Charger 2	**10-09-2018 10:17**	**22.305**	**2.3**	**24.62**	**0**
Charger 3	**10-09-2018 14:21**	**36.833**	**5**	**41.83**	**0**
Charger 1	**10-09-2018 16:54**	**23.234**	**0.4**	**23.635**	**0**
Charger 4	**10-09-2018 18:37**	**40.909**	**10.9**	**51.85**	**0**

Table 4.4: Cost of penalty for c_p = 50* max(c_e_buy)

Concluding this analysis, it can be said that the cost of penalty plays an important role in determining the EV charging or discharging schedule. The schedule is dependent on PV generation and the cost of buying energy from the grid. At 0 euro/kWh c_p value, the EVs leave the charging station without being charged. When increasing the value of c_p to 25*max(c_e_buy), the algorithm tries to charge the EV, using PV, as much

as possible. As the algorithm tries to decrease the overall cost of energy for the node, the EVs arriving during off-peak hours does not charge using the grid power import. The consequence is that the CSO has to pay a significant amount of penalty to the EV user. To remove the possibility of penalty, the algorithm is made more strict by increasing the value of c_p to 50*max(c_e_buy). Upon increasing the value of c_p, the algorithm is making sure that the EVs are charged to their requested energy at the end of departure. This will negate the possibility of the penalty, and EV users will be satisfied as they can depart with their demand fulfilled. Finally, it can be said that the value of c_p higher or equal to 50*max(c_e_buy) can result in similar behaviour.

4.2. Analysis for cost of PV generation (c_PV)

The advancement in the research in Photovoltaics is increasing at an exponential rate to increase its efficiency and reduce the cost of PV generation. In this thesis, the use of PV source is prioritized and is done by including the PV source in the optimization process at 0.0 euro/kWh assuming all the cost leading to LCOE is paid off. As the optimization problem is cost minimization, it is necessary to check how the behaviour of the algorithm will change for the case where the aforementioned assumptions are not valid. The analysis is done for a range of c_PV where the value varies from zero cost of energy (c_PV = 0 euro/kWh) to the value of c_PV at 0.03 euro/kWh and 0.07 euro/kWh. The values are selected based on the study in [67]. The value of c_PV higher than the maximum value of c_e_buy (0.175 euro/kWh) for the year is selected (0.2 euro/kWh). The value is selected to see how the algorithm will change the behaviour of grid import and EV scheduling at higher c_PV. Changing the value of c_PV will change the behaviour of the PV profile which will also be assumed to affect parameters such as grid import and export power. Figure 4.7 below shows a cost comparison which is useful for understanding the analysis.

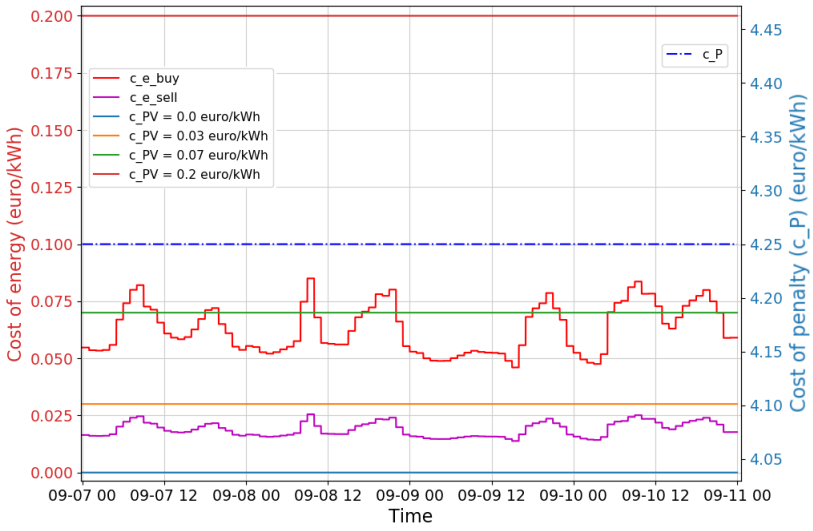

Figure 4.7: Cost vs time for various value of c_PV

4.2.1. Methodology

The analysis of the cost of PV generation is performed by assuming a few parameters as constant and by using the following steps:

1. A set of parameters are kept constant which might affect the outcome of the optimization process. The parameters which are kept constant during the whole analysis are described below:
   - Cost of selling energy or c_e_sell value is taken as 0.7*c_e_buy
   - All the assumptions mentioned in section 3.1 hold in this analysis as well.
2. After the parameter is kept constant, the value of c_PV is varied from 0 euro/kWh, 0.03 euro/kWh, 0.07 euro/kWh to 0.2 euro/kWh for 25 kW PV.
3. At every increase in the value of c_PV, the node power profile is checked and the values are recorded.

4. A comparative study between the c_PV and parameters such as grid power import and export, charging and V2G energy and so on is done to analyse the change in the behaviour due to change in c_PV.

5. Finally, various plot to show the behaviour change is plotted and the observation is explained.

4.2.2. Analysis

As mentioned earlier the PV generation is a prioritized power source in this thesis and its power is dependent upon the correlation among c_PV, c_e_sell, c_e_buy, load demand (local load and EV charging). The value of c_PV is varied from 0 euro/kWh, which would make the PV power the main source, until 0.2 euro/kWh which is very large as compared to the value of c_e_buy (0.175 euro/kWh) which would restrict the use of PV power.

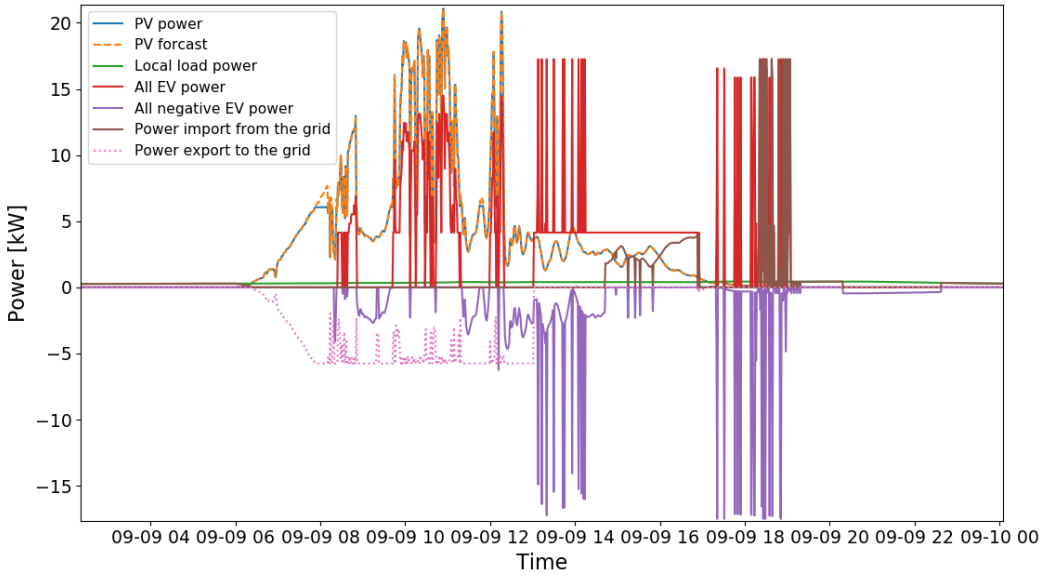

Figure 4.8: Node power profile for c_PV = 0.0 euro/kWh date: 09/09/2018

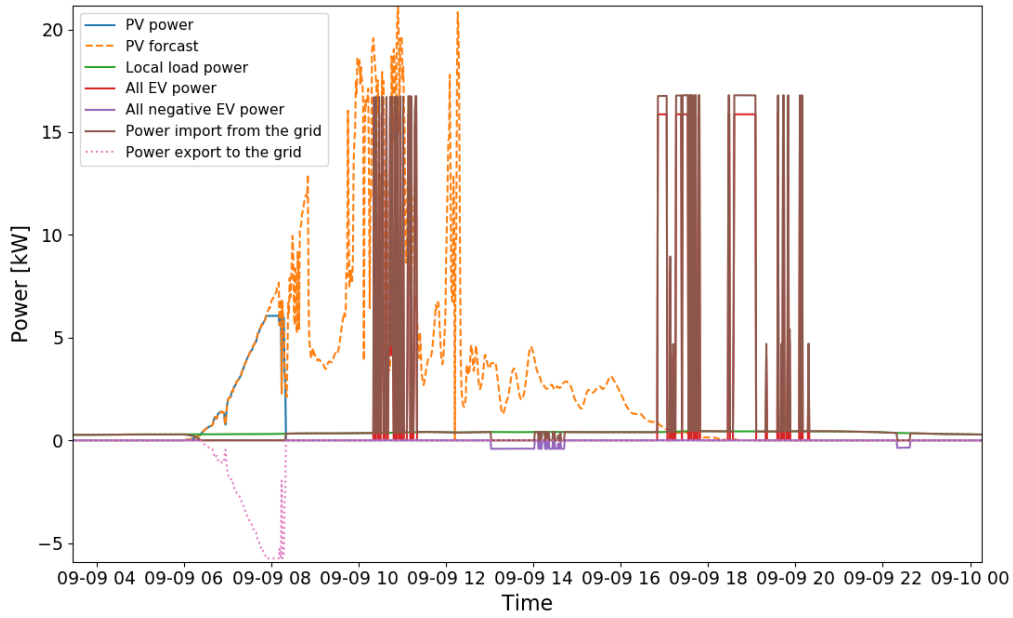

Figure 4.9: Node power profile for c_PV = 0.2 euro/kWh date: 09/09/2018

After the simulation, the power profile is zoomed in to date: 09/09/2018 for a better analysis. Figure 4.8 and 4.9 shows the node power plot for the two extreme value of c_PV. The difference between the two cases

can be explained by looking at each plot lines. Firstly, the plot lines for PV forecast (orange dotted lines) and PV power (blue lines) used (blue) will be compared. From figure 4.8 it can be seen that the utilized PV power follows the same trend as forecast power. The PV power provides the demand of local load and EV charging demand and export the remaining power to the grid which can be seen by the export power plot lines (dotted pink) in negative power axis. Whereas, in figure 4.9 the PV is generating power which is not utilized by the algorithm instead the algorithm prefers the grid import power to supply any energy demand (shown by brown plot lines). The reason for the behaviour change is observed when the c_PV value is 0.0 euro/kWh; using PV energy will not contribute to overall cost of energy. The excess PV power can be exported to the grid and any grid involvement can be compensated by generating at 0.0 euro/kWh and selling at a much higher value. This is not the case when c_PV is increased to 0.2 euro/kWh where the algorithm realizes that using PV power will incur a higher cost for the node and any demand can be fulfilled using the grid as the main source. It is to be noted that in figure 4.9 an export power is seen around 06:00 - 09:00. It is because of the limitation of the algorithm to only optimize the charging process of the EV in the duration of its optimization horizon. The optimization horizon is adjusted according to the arrival and departure time of the EV as explained in section 3.4.2.

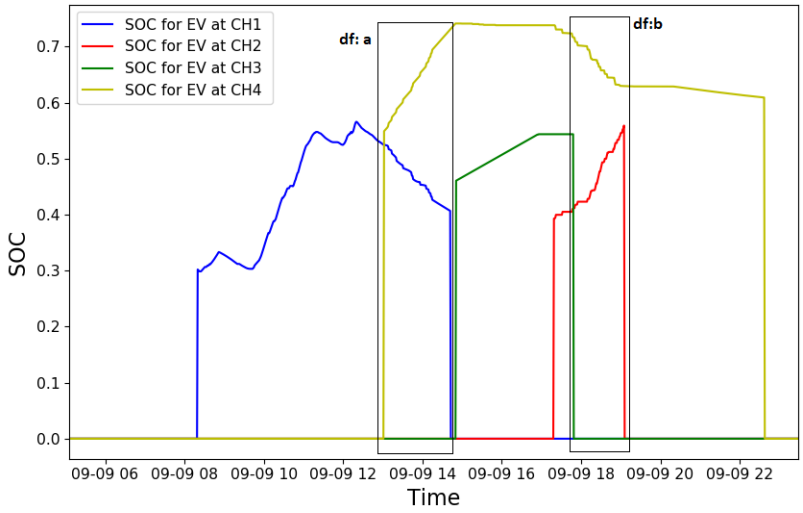

Figure 4.10: SOC vs time plot for date: 09.09.2018

It can be seen that in Figure 4.8 around 14:00 and around 18:00 the EV is charged using V2G energy. The reason for this can be explained using SOC vs time plot which is shown in figure 4.10. The first instance at 14:00, the highlight box 'df: a', EV at charger 1 performs V2G (represented by the decrease in SOC) to charge the EV at charger 4 (represented by the increase in SOC). During the second instance, the highlight box 'df: b', EV at charger 4 perform V2G (represented by the decrease in SOC) to charge the EV at at charger 2 (represented by the increase in SOC).

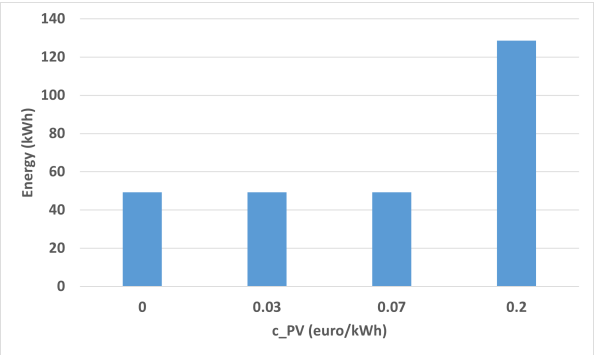

Figure 4.11: Grid import energy for the duration of the simulation for various c_PV

It can be said that an increase in the value of c_PV will increase grid involvement. Figure 4.11 shows a bar

graph for the total grid import energy for the node for the various value of c_PV. The graph is observed to be almost consistent for c_PV 0.0 till 0.07 euro/kWh. The reason for this behaviour is that the value of c_PV at 0.0 and 0.03 euro/kWh the value is much lower than the minimum value of c_e_buy. The algorithm can utilize generated PV power to support the load demand and EV charging demand (if any) and sell the remaining energy at c_e_sell. The grid involvement is decreased and is seen in situations when there is no or less PV generation.

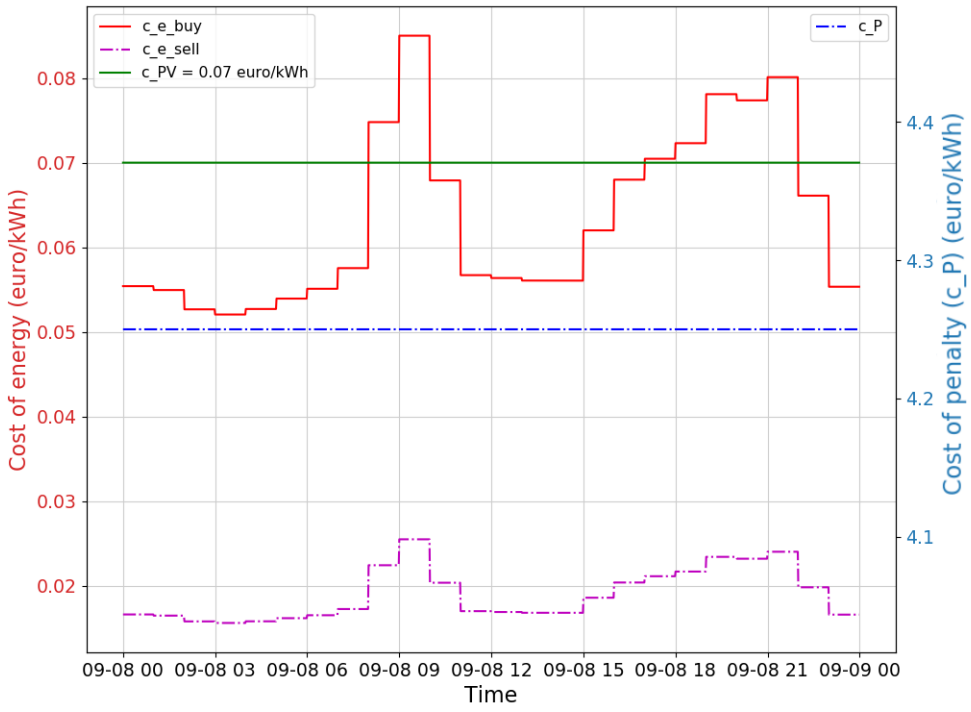

Figure 4.12: Cost vs time for c_PV = 0.07 euro/kWh date: 08/09/2018

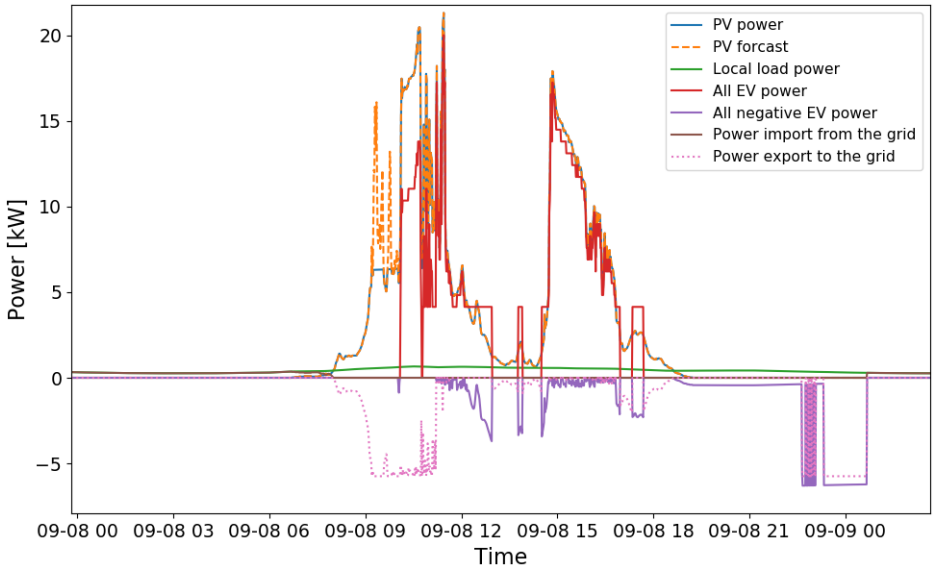

Figure 4.13: Node power profile for c_PV = 0.07 euro/kWh date: 08/09/2018

The aberration occurs at c_PV 0.07 euro/kWh when the grid import power is the same as the lower value of c_PV. The figure 4.13 shows the node plot for date: 08/09/2018 for c_PV at 0.07 euro/kWh. The aberration for 0.07 euro/kWh c_PV can be explained with the help of cost vs time plot in figure 4.12 and node power

profile 4.13. It can be seen in figure 4.12 that the value of c_PV for date 08/09/2018 (green plot line) is higher than c_e_buy (red plot lines) between 09:00 -11:00 and then again from 17:00 to 22:00. The first EV that arrives at charger 1 on 08/09/2018 is at 10:00 as seen from the table 4.1. Before the arrival of the first EV, the PV power utilized is the same as forecast power because of the limitation of the algorithm so it will not be accounted for in this analysis. The controller then determines the optimization horizon based on arrival and departure time and start the optimization process. During the parking time of the EV, the cost of buying energy from the grid is higher than the c_PV value. The algorithm realizes this and charges the EV using the PV power. The PV forecast power (dotted orange plot line) is sufficient enough to charge the EV and meet the local load demand until 12:00. After which the existing EV at other charger performs V2G operation to support PV in charging other EV and reduce the grid involvement. The situation repeats from 15:00 when the EV performs V2G to aid the PV and the lower c_PV value as compared to c_e_buy makes PV as the main power source. It can also be noted that using PV to supply the demand at c_PV can also be beneficial as PV can export power to the grid and generate revenue which is not the case when the grid is involved.

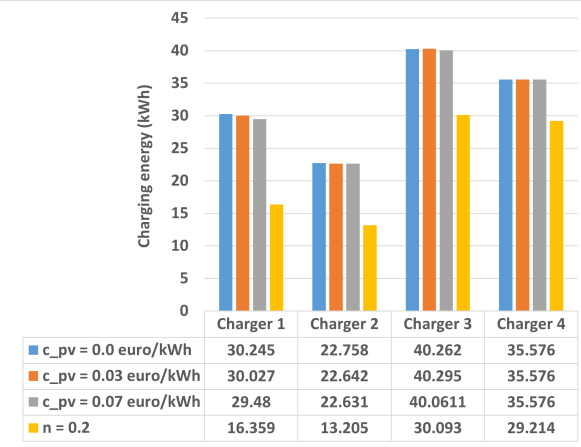

	Charger 1	Charger 2	Charger 3	Charger 4
c_pv = 0.0 euro/kWh	30.245	22.758	40.262	35.576
c_pv = 0.03 euro/kWh	30.027	22.642	40.295	35.576
c_pv = 0.07 euro/kWh	29.48	22.631	40.0611	35.576
n = 0.2	16.359	13.205	30.093	29.214

Figure 4.14: Charging energy of the EV for vaious c_PV

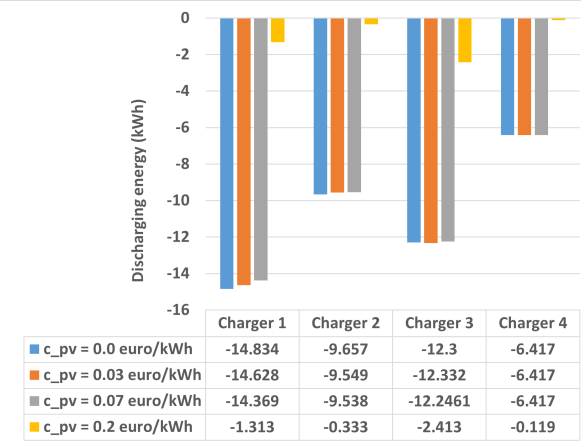

	Charger 1	Charger 2	Charger 3	Charger 4
c_pv = 0.0 euro/kWh	-14.834	-9.657	-12.3	-6.417
c_pv = 0.03 euro/kWh	-14.628	-9.549	-12.332	-6.417
c_pv = 0.07 euro/kWh	-14.369	-9.538	-12.2461	-6.417
c_pv = 0.2 euro/kWh	-1.313	-0.333	-2.413	-0.119

Figure 4.15: Discharging energy of the EV for vaious c_PV

As changing the c_PV can change the behaviour of the PV and grid import it is necessary to analyse how the change in c_PV affects the charging and V2G energy. Figure 4.14 and figure 4.15 shows charging energy and discharging energy for all the charger and the duration of optimization for different values of c_PV. The bar graph represents the charger and color represents the change in the value of c_PV. It can be observed that EVs arriving at charger 1-3 shows a decrease in charging energy and discharging energy as c_PV increases. The change in the behaviour is pretty intuitive as increasing the cost of PV generation will increase the overall cost for charging therefore the EV charging energy is reduced. As the EV is charged at 0.0 euro/kWh using PV, the EV participates in V2G to support PV and reduce grid involvement as explained in the above analysis. At c_PV 0.2 euro/kWh, the grid acts as the main source. As the grid is involved in charging the EVs, the algorithm only uses the grid to charge the EVs to their requested energy. EVs only perform V2G only when supporting the grid in charging other EVs and gets charged back when the cost is lower. Charger 4 is seen to have almost a similar value for c_PV 0.0 -0.07 euro/kWh but decreased at c_PV 0.2 euro/kWh. It is because the EVs at charger 4 is scheduled to arrive when the PV generation decreases. The PV charge the EV using the help of the grid. Again, involving the grid increases the overall cost therefore the EVs are charged as per the remaining energy request.

A cost comparison is done along with node energy distribution to see how the energy supply behaviour changes as the c_PV increases. Figure 4.16 shows node energy distribution and figure 4.17 shows total cost of energy distribution for the node vs c_PV. It can be seen from the figure that, as the c_PV value increases the PV is less prioritized as the main source and only supply energy when the value of c_PV is less than c_e_buy or before and after the optimization horizon. As the PV energy decreases the grid comes into the picture to supply the load demand which also restricts the frequency of charging and discharging of EV. For c_PV 0.07 and 0.2 euro/kWh a large cost of PV generation is seen because the node experience PV power during the period before and after the optimization horizon. It has also been observed that c_pv=0.07 has the highest PV cost, even higher than c_pv=0.2 it is because its involvement in charging the EV when the cost of buying energy from the grid is higher than 0.07 euro/kWh.

After looking at the charging and discharging energy of the EVs it is necessary to check if the EVs are

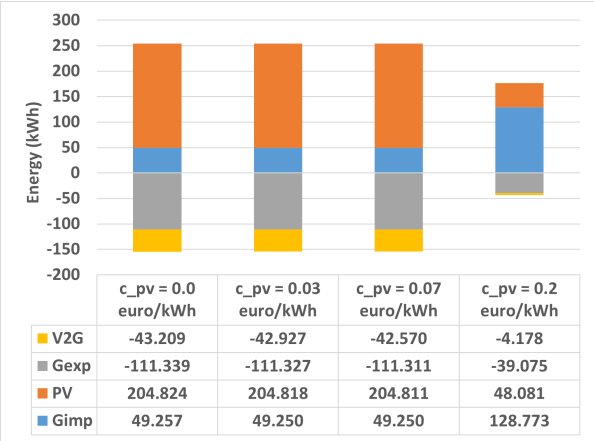

	c_pv = 0.0 euro/kWh	c_pv = 0.03 euro/kWh	c_pv = 0.07 euro/kWh	c_pv = 0.2 euro/kWh
V2G	-43.209	-42.927	-42.570	-4.178
Gexp	-111.339	-111.327	-111.311	-39.075
PV	204.824	204.818	204.811	48.081
Gimp	49.257	49.250	49.250	128.773

Figure 4.16: Energy distribution for various values of c_PV

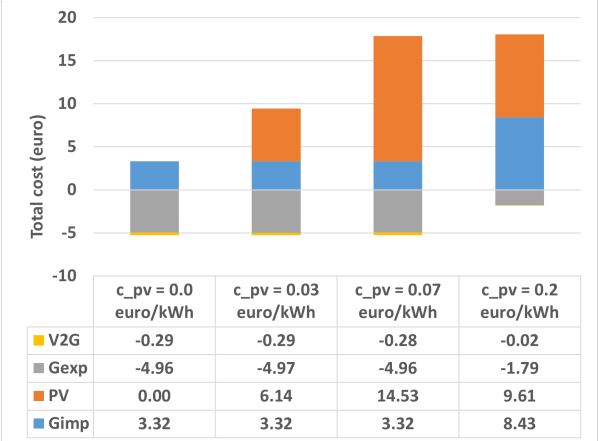

	c_pv = 0.0 euro/kWh	c_pv = 0.03 euro/kWh	c_pv = 0.07 euro/kWh	c_pv = 0.2 euro/kWh
V2G	-0.29	-0.29	-0.28	-0.02
Gexp	-4.96	-4.97	-4.96	-1.79
PV	0.00	6.14	14.53	9.61
Gimp	3.32	3.32	3.32	8.43

Figure 4.17: Cost distribution for various values of c_PV

charged to their requested energy at the end of their parking to avoid penalty. Table 4.5 shows the d_gap value at the departure time of the EV. D_gap refer to the remaining energy that EV needs to be charged to in order to fulfil the energy request. It is calculated by subtracting the energy request with energy at the departure time and arrival battery energy. It can be seen that the d_gap value for various values of c_PV is 0 kWh which implies that the energy request of the EVs is fulfilled at the end of their parking, therefore, will incur no penalty. It can also be said that the cost of PV generation does not affect the d_gap value.

	t_arr(DD-MM-YY hh:mm)	t_dep(DD-MM-YY hh:mm)	d_gap for c_PV = 0.0 euro/kWh	d_gap for c_PV = 0.03 euro/kWh	d_gap for c_PV = 0.07 euro/kWh	d_gap for c_PV = 0.2 euro/kWh
Charger 1	**07-09-18 08:28**	**07-09-18 10:48**	**0**	**0**	**0**	**0**
Charger 4	**07-09-18 10:19**	**07-09-18 10:24**	**0**	**0**	**0**	**0**
Charger 3	**07-09-18 11:52**	**07-09-18 12:07**	**0**	**0**	**0**	**0**
Charger 4	**07-09-18 17:28**	**07-09-18 18:56**	**0**	**0**	**0**	**0**
Charger 1	**08-09-18 10:00**	**08-09-18 17:51**	**0**	**0**	**0**	**0**
Charger 3	**08-09-18 11:13**	**09-09-18 00:41**	**0**	**0**	**0**	**0**
Charger 4	**08-09-18 11:38**	**08-09-18 13:00**	**0**	**0**	**0**	**0**
Charger 2	**08-09-18 16:20**	**08-09-18 19:59**	**0**	**0**	**0**	**0**
Charger 1	**09-09-18 08:20**	**09-09-18 14:43**	**0**	**0**	**0**	**0**
Charger 4	**09-09-18 13:02**	**09-09-18 22:38**	**0**	**0**	**0**	**0**
Charger 3	**09-09-18 14:51**	**09-09-18 17:49**	**0**	**0**	**0**	**0**
Charger 2	**09-09-18 17:19**	**09-09-18 19:06**	**0**	**0**	**0**	**0**
Charger 1	**10-09-18 09:10**	**10-09-18 10:02**	**0**	**0**	**0**	**0**
Charger 2	**10-09-18 10:17**	**10-09-18 15:40**	**0**	**0**	**0**	**0**
Charger 3	**10-09-18 14:21**	**10-09-18 16:49**	**0**	**0**	**0**	**0**
Charger 1	**10-09-18 16:54**	**10-09-18 17:38**	**0**	**0**	**0**	**0**
Charger 4	**10-09-18 18:37**	**10-09-18 20:38**	**0**	**0**	**0**	**0**

Table 4.5: d_gap at departure for various value of c_PV

Concluding the analysis, it can be said that the PV cost plays a crucial role in determining other power parameters. Given the optimization does not have control over the PV generation after or before the optimization horizon the higher cost of PV generation can have a very large cost of the energy value of the node. The cost of PV generation has significant effect on the grid involvement and V2G application of the EV. It is observed that lower c_PV value provides flexibility to the optimizer in utilizing the PV power as much as possible. The remaining or excess power can be exported to the grid which will compensate for any grid energy import cost.

4.3. Analysis for grid import limitation

As mentioned in the earlier section that this thesis prioritizes in the use of renewable energy (solar energy) in providing the demand for local load and EV charging. Due to the uncertainty in the PV generation, because of the unpredictable weather and as not using any energy storage, dependability of the system is affected. To tackle this situation, grid support is added to the node which comes into picture when the PV fails to supply the demand. However, an imbalance can be caused in the grid due to an increase or decrease in the frequency, or due to faults which would make the grid incapable of supplying the agreed power demand. In a situation like this, the grid performs load shedding operation where the electricity supply to some areas is temporarily decreased or deprived to prevent widespread power cuts. It is important to analyse how the algorithm will behave if the grid import power is reduced from full capacity (100%) to the 10%. Table 4.1 shows the EV parameter data for the duration arriving at each charger. The EV arrival at a charger is shown by the first column. During a day, multiple EV can arrive at the charger; for example on 07/09/2018 two EV arrive and connect to charger 4. Therefore, repeated value of charger number shows multiple EV charging events. The table also consists of arrival time, battery size, parking duration, departure time and energy request.

4.3.1. Methodology

The grid import limitation analysis is being performed to observe the change in behaviour of the algorithm by restricting the grid import power. In order to perform this analysis, several steps are being taken into account which are as follows:

1. A set of parameters are kept constant which might affect the outcome of the optimization process. The parameters which are kept constant during the whole analysis are described below:
    - Cost of selling energy or c_e_sell value is taken as 0.7*c_e_buy
    - All the assumptions mentioned in section 3.1 hold in this analysis as well.
2. After the parameters are defined, the maximum grid import power which is 17.25 kW (refer to assumptions) is varied from 100% of the value to 10%.
3. A decrease in the grid import power will imply that the grid is performing load shedding operation to prevent widespread power cut.
4. An analysis is then performed for the range of values, separately, to see PV and EV behaviour.
5. Finally, various plot to show the behaviour change is plotted and the observation is explained.

4.3.2. Analysis

To analyse the results clearly, one of the day from the duration is selected which is 10-09-2018 whose EV input data can be seen from Table 4.1. The EV input data provide an idea of how the EV are arriving, leaving and what are the energy demands during the day and using that data one can predict how EVs will be scheduled to charge when the PV is prominent as grid import power decreases. Figure 4.18 shows the node power profile for the grid import power at 10% for the duration.

It can be seen from the figure 4.18 when the grid is at 10% capacity (maximum import power is 1.75 kW), PV power is used to supply the load demand and charge the EV. Grid involvement is observed when the PV generation is 0 kWh or insufficient to meet local load demand. EVs are scheduled to charge when PV generation is sufficient and performs V2G to aid PV in supplying any energy demand. It can be seen that the grid export power is at the maximum limit for most of the time, that is because when the EV isn't charging and have sufficient energy to perform V2G it aids the PV to export the energy at the maximum limit (5.75 kW) to maximize the profit. EVs also perform V2G operation to charge the EVs that come during the off-peak

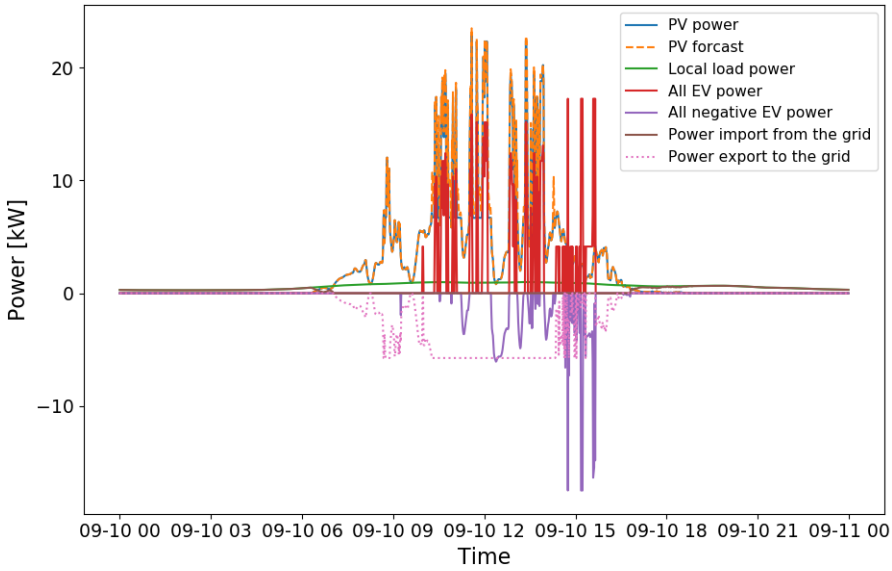

Figure 4.18: Node power profile for grid import limitation at 10%

PV generation hours. Changing the grid import power hardly affects the total PV power extracted, however, it largely affects the schedule of charging, discharging and recharging of the EVs which in turn changes the behaviour of the PV power profile a little.

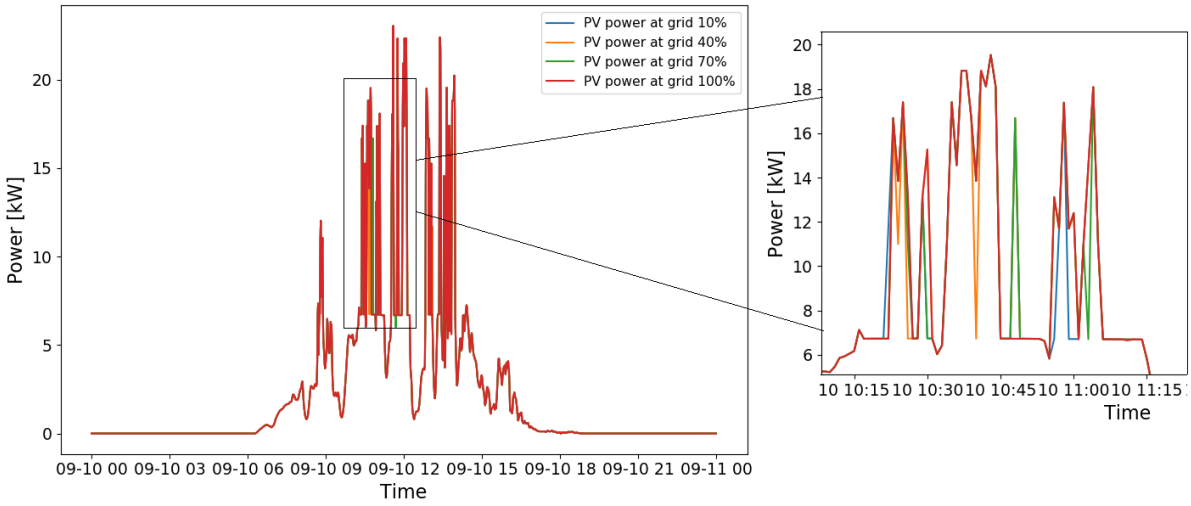

Figure 4.19: PV power for different grid import power

Figure 4.19 shows the PV power profile for the day and the range of values of grid import power. It can be seen from the figure that the plot for PV power is the same for most of the time. However, a change in the value of PV power is observed from 10:15 to 11:15 among the plot which is in the parking time of the EV at charger 2 as seen from Table 4.1. The reason for this behaviour can be explained using the SOC plot of EV at the charger 2 for various grid import power percentage value. Figure 4.20 shows the SOC for EV at charger 2 for various value of grid import power % during the duration of parking.

Figure 4.20 shows two highlights, namely HT1 and HT2, the difference in the behaviour of SOC when the grid import power changes. It can be seen from HT1 in the figure that the EV is charged to SOC greater than the requested SOC. The reason for this behaviour is that the EV arrives duration when the PV generation is high. PV charges the EV to a value higher than the requested SOC to use it as backup support when the generation is insufficient. As highlighted by HT1, it can be observed that the EV is charged at different charging rates. The possible reason for this behaviour is related to minimizing the overall cost. As grid import % increases, the algorithm has to involve the grid in the case when PV generation is insufficient to supply any

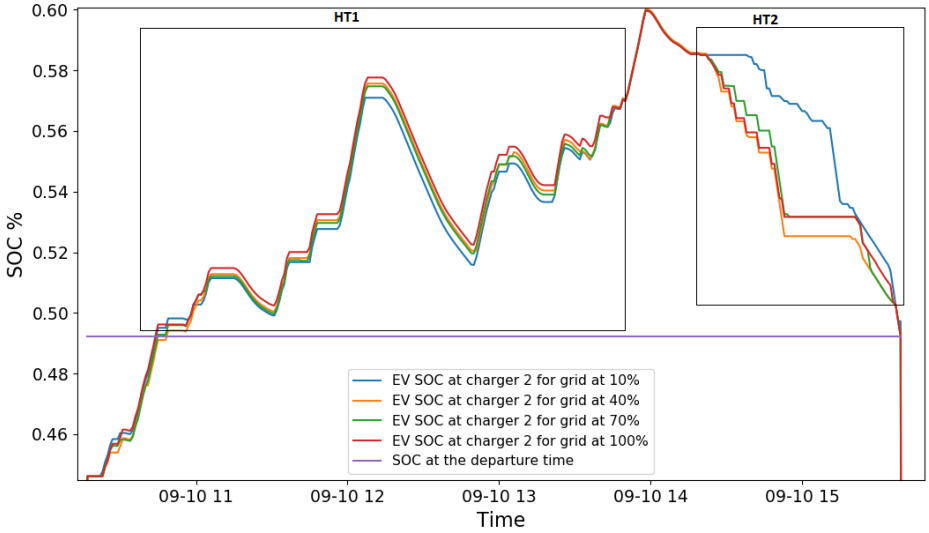

Figure 4.20: SOC for various grid import power for EV at charger 2

energy demand. A higher grid import power will enable the grid to supply the energy demand of the user, when PV is unable to, which would increase the overall cost of charging. Therefore, to minimize the cost the algorithm schedules the EVs to be charged much quicker to utilize the high PV generation as much as possible. The second highlight, HT2, in the figure 4.20 shows the difference in the rate of change of SOC for various grid %. The difference occurs after the arrival of EV at charger 3. EV at charger 3 arrives at 14:20 with an energy demand of 5 kWh and parking duration of 148 minutes. The data can also be seen in table 4.1.

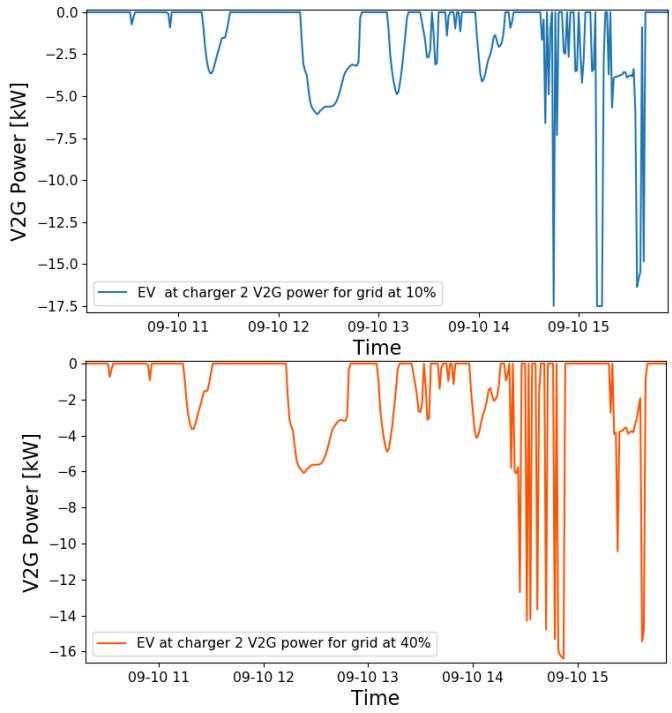

Figure 4.21: V2G power vs time for grid at 10% and 40%

The EV at charger 2, during the arrival of EV at charger 3, is at 58.5% of SOC. At the end of the departure, 15:39, the EV at charger 2 is expected to have a SOC of 49.21%. The energy capacity of the battery for EV at charger 2 is 50 kWh which means that EV can provide 4.645 kWh of energy through V2G. Given the PV

generation and amount of V2G energy that can be provided by the battery it can be assumed that the EV at charger 2 can supply the energy demand. However, in the HT2 in figure 4.20 it can be seen at grid import % above 40% the SOC follows almost the same rate of change which is not the case for SOC for the grid at 10%. The reason for the change in behaviour can also be seen in figure 4.21 which shows V2G energy vs time for grid at 10% [blue plot lines] and 40% [orange plot lines]. It can be seen that the EV at grid 10% are scheduled to discharge in fewer cycles as compared to that at grid 40%. The possible reason can be that as the grid import power increases the optimizer realizes it can recharge the EV using grid import energy when EV SOC falls below the requested SOC and the departure time is close. Doing so will allow the CSO to avoid any possible penalty for not meeting the energy request of the EV.

	SOC_arr	**SOC_requested**	**SOC_dep of EVs at 10% gimp**	**SOC_dep of EVs at 40% gimp**	**SOC_dep of EVs at 70% gimp**	**SOC_dep of EVs at 100% gimp**
Charger 1	**0.4896**	**0.4916**	**0.4916**	**0.4916**	**0.4916**	**0.4916**
Charger 2	**0.4461**	**0.4921**	**0.4972**	**0.4924**	**0.4924**	**0.4924**
Charger 3	**0.3683**	**0.4183**	**0.4183**	**0.4183**	**0.4183**	**0.4183**
Charger 1	**0.4646**	**0.4726**	**0.4646**	**0.4727**	**0.4726**	**0.4726**
Charger 4	**0.4090**	**0.5180**	**0.4090**	**0.5180**	**0.5180**	**0.5180**

Table 4.6: SOC of EV for various vales of gimp %

As the grid import power decreases, the PV becomes the main source and tries to supply the demand of the local load as well as charge the EVs to the requested energy demand to prevent any possible penalty for not fulfilling the EV demand. However, PV power works during the day and without a storage system, it can't provide when there is no or insufficient generation. So, it is necessary to check how the EV charging is affected when the PV generation is not sufficient, is there a possible penalty, or how the grid import power varies as the grid import power increases. Table 4.6 shows the SOC at the departure time for EVs that arrive at the charger on 10-09-2018 for different values of grid import %. At grid import power at 10% the grid and PV are unable to supply power to EVs arriving at off-peak hours. It is because of which second EV arriving at charger 1 and first EV at charger 4 during off-peak hours depart with SOC less than requested. It can also be observed that the optimizer ensures that at higher values of the grid import power, the SOC of the EVs are equal to the requested SOC irrespective of their arrival time, it is because at higher grid import power the grid can supply the power when PV or V2G are not sufficient enough to supply the demand. Moreover, the SOC value is the same from 40% to 100%. It can be implied that, for the duration of the simulation, the grid import power equal to or greater than 40% the EVs will be charged to their requested SOC. The input energy from the grid and the PV will be sufficient enough to supply the energy demand.

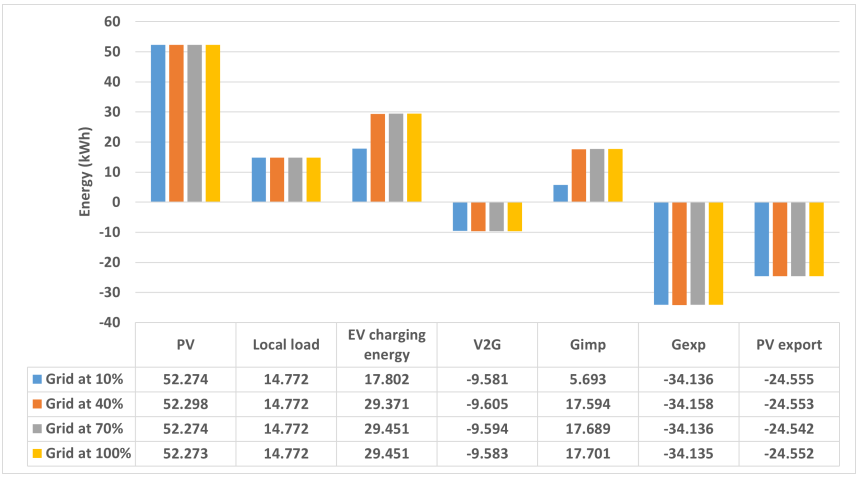

	PV	Local load	EV charging energy	V2G	Gimp	Gexp	PV export
Grid at 10%	52.274	14.772	17.802	-9.581	5.693	-34.136	-24.555
Grid at 40%	52.298	14.772	29.371	-9.605	17.594	-34.158	-24.553
Grid at 70%	52.274	14.772	29.451	-9.594	17.689	-34.136	-24.542
Grid at 100%	52.273	14.772	29.451	-9.583	17.701	-34.135	-24.552

Figure 4.22: Node energy distribution for various value of grid %

Figure 4.22 shows the energy distribution of the node for the duration of optimization. Increasing the grid import power to 40% will allow the grid to support the system by providing 7 kW of power. Earlier analyses

showed that the grid import power along with PV is sufficient enough to charge the EV and supply the local load. In the plot, it can be seen that an increase in EV charging energy is seen when grid import power increase from 10% to 40%. The algorithm tries to charge the EV as much as possible with the help of the PV and grid. The PV provide additional support to the grid as seen by the slight increase PV generation from 52.682 kW to 52.706 kW. It is because, at limited maximum grid import power, not charging the EV will incur a penalty. The value of PV generation again slightly decreases from 52.706 to 52.683 kW for a value greater than 40%. The reason for this is the grid import power has increased from 7 kW to 12.25 kW. An increased grid import power made the grid capable to supply any energy demand when the PV generation is insufficient or 0 kWh. A decrease in the V2G energy is seen as the grid import % increases. The reason for that is at higher grid import power the EV will not have to participate in V2G as the grid can supply the energy demand when necessary. It is to be noted that as the duration is for the analysis is selected as one of the day because of which the difference is very negligible. However, the difference can be higher for longer duration of the simulation.

	Requested energy	**Remaining energy 10%**	**Remaining energy 40%**	**Remaining energy 70%**	**Remaining energy 100%**
Charger 1	**24.58144418**	**0**	**0**	**0**	**0**
Charger 2	**24.60584262**	**0**	**0**	**0**	**0**
Charger 3	**41.83345019**	**0**	**0**	**0**	**0**
Charger 1	**23.63470105**	**0.4**	**0**	**0**	**0**
Charger 4	**51.80965996**	**10.9**	**0**	**0**	**0**

Table 4.7: Remaining energy request of EV for various vales of gimp %

Previous analysis shows how grid import power affects the charging of EV and how lowering the grid import power can have a penalty for not charging the EV involved. Figure 4.23 shows the penalty cost for various value of grid import power. To calculate the penalty cost, the remaining energy at the end of the departure is calculated. The energy at the end of departure is calculated using equation 3.4 in section 3.1.3. After calculating the remaining energy, shown in table 4.7, the value is multiplied by $50 * max(costofbuyingenergy)$. The maximum cost of buying energy for the date 10/09/2018 is 0.08362 euro/kWh. The value of battery capacity is taken from table 4.1. Putting a restriction on the algorithm by using a large penalty cost will ensure the EV demands are met (if the supply is sufficient). It can be seen from figure 4.23 that after 40%, the penalty is 0 euro. This implies that all the EVs are charged to their requested energy and hence involve 0 euro penalty. However, for grid import power at 10% as the EV at charger 1 and 4 is not charged to their requested energy as seen from table 4.7, therefore a penalty will be given to the EV user from the CSO. The value of the penalty for EV at charger for various value of grid import % can be determined from figure 4.23.

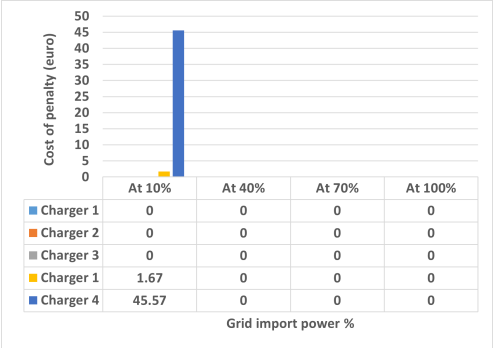

Figure 4.23: Cost of penalty for various value of grid %

In this analysis, when the grid import power % was changed from 10% to 100% a difference in the behaviour of PV, EV charging schedules and V2G changes are observed. It can be said that lowering the grid import power can have EVs not charged to their requested energy, therefore, will include high penalty which is a loss for the CSO. To decrease the possibilities of any penalty an energy storage system can be used at the node. A storage system will provide backup support when grid capacity is low and PV and V2G from EV cannot meet the energy demand. However, an storage system will increase the infrastructure and logistics

cost. To decrease the loss for the CSO, it can be recommended that an agreement must be made beforehand with the user which will allow the CSO to pay less or almost no penalty for not charging the EV when the grid capacity is reduced to 10% when the grid is incapable to aid the PV in meeting the energy demand of EV and local load.

4.4. Analysis for cost of selling energy (c_e_sell)

One of the parameters that can affect the behaviour of the algorithm is the cost of selling electricity or c_e_sell as mentioned in equation 3.1. This value represents the cost of all the energy that is being exported to the grid either via PV or EV through V2G. The sensitivity analysis of this parameter is done to observe the change in the behaviour of the optimization process by changing the value of c_e_sell from 0 euro/kWh to 95% of c_e_buy. The values selected are 0,35,70,95 % of c_e_buy. The value of c_e_sell as 0 euro/kWh represents there will not be any income involving selling the energy to the grid. The value of 35% - 95% is selected based on variation in the energy market [60]. Market dynamics ensure that the value of c_e_sell can't be equal to or greater than c_e_buy [15], therefore the maximum value of c_e_sell is taken as 95% of c_e_buy. Changing the value of c_e_sell can affect parameter such as grid power import and export, charging power, V2G power, PV power, the total cost of energy and finally the time when EVs are scheduled to charge. Figure 4.24 below shows a cost comparison which is useful for understanding the analysis.

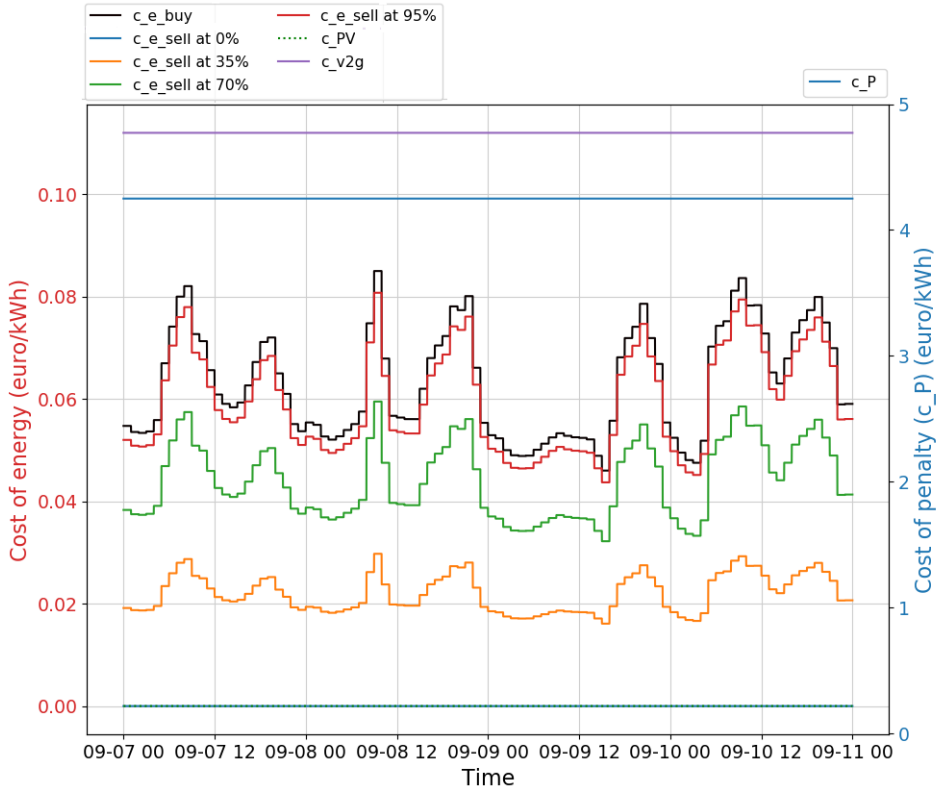

Figure 4.24: Cost vs time for various value of c_e_sell

4.4.1. Methodology

The cost of selling energy analysis is being performed to observe the change in behaviour of the algorithm by changing the value of c_e_sell. In order to perform this analysis, several steps are being taken into account which are as follows:

1. A set of parameters are kept constant which might affect the outcome of the optimization process. The parameters which are kept constant during the whole analysis are described below:
    - All the assumptions mentioned in section 3.1 hold in this analysis as well.

2. After the parameter is kept constant, the value of c_e_sell which is equal to n*c_e_buy, where n is the percentage value, is changed from 0.0 to 0.95.
3. At every increase in the value of n, the node power profile is checked and the values are recorded.
4. A comparative study between the cost of selling energy (c_e_sell) and parameters such as grid power import and export, charging and V2G energy and so on is done to analyse the change in the behaviour due to change in c_e_sell.
5. Finally, various plot to show the behaviour change is plotted and the observation is explained.

4.4.2. Analysis

As mentioned earlier, the cost of selling can change the behaviour of how PV power is utilized? The cost of selling is varied from 0.0*c_e_buy to 0.95*c_e_buy and the overall node power plot is plotted. The plot is then zoom in to one day to analyse more clearly. Figure 4.25 and 4.26 shows the power profile for date 07-09-2018 (start date) for the two extremes of the cost of selling the energy. From figure 4.24 it can be seen that the cost of PV generation (c_PV = 0.0 euro/kWh) lies below the c_e_buy which is the cost of buying energy from the grid, and the PV power is prioritized as the main power source to supply the demand and the grid comes into picture when the PV generation is less than the demand. It is to be noted that because of the limitation of the algorithm an assumption is made that the PV power measured is the same as the forecast power in case of the period before and after the optimization horizon which is estimated by considering the arrival and departure time of the EV (a detailed explanation is explained in section 3.4.2).

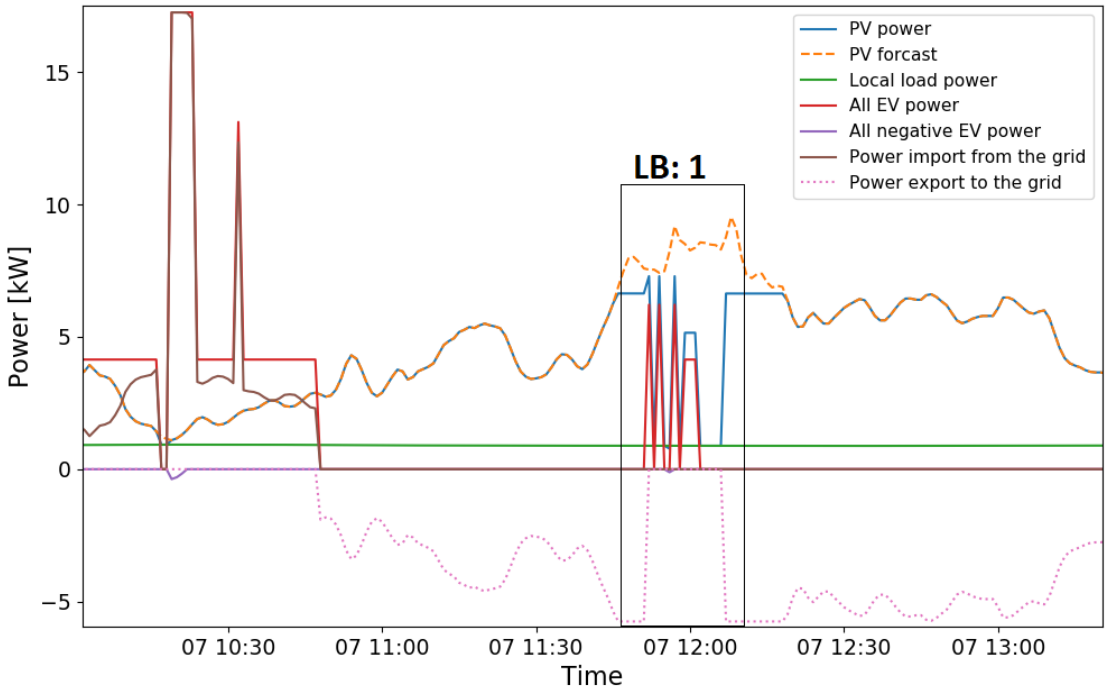

Figure 4.25: Node power profile for date: 07/09/2018 at c_e_sell = 0.0*c_e_buy

Apart from the assumption, it can be observed from the figure 4.25 that at c_e_sell equal to 0.0*c_e_buy the PV tries to only generate power sufficient enough to meet the supply of local load and EV charging. When there are no EV charging scheduled during the interval and the profit obtained by selling the power to the grid is zero, the discontinuity in the export power profile around noon is observed (LB: 1 in figure 4.25). The case is not the same when the cost of selling increases to 95% of the cost of buying. The PV power in that case provides the demand as well as generate profit by selling the remaining power to the grid (LB: 2 in 4.26).

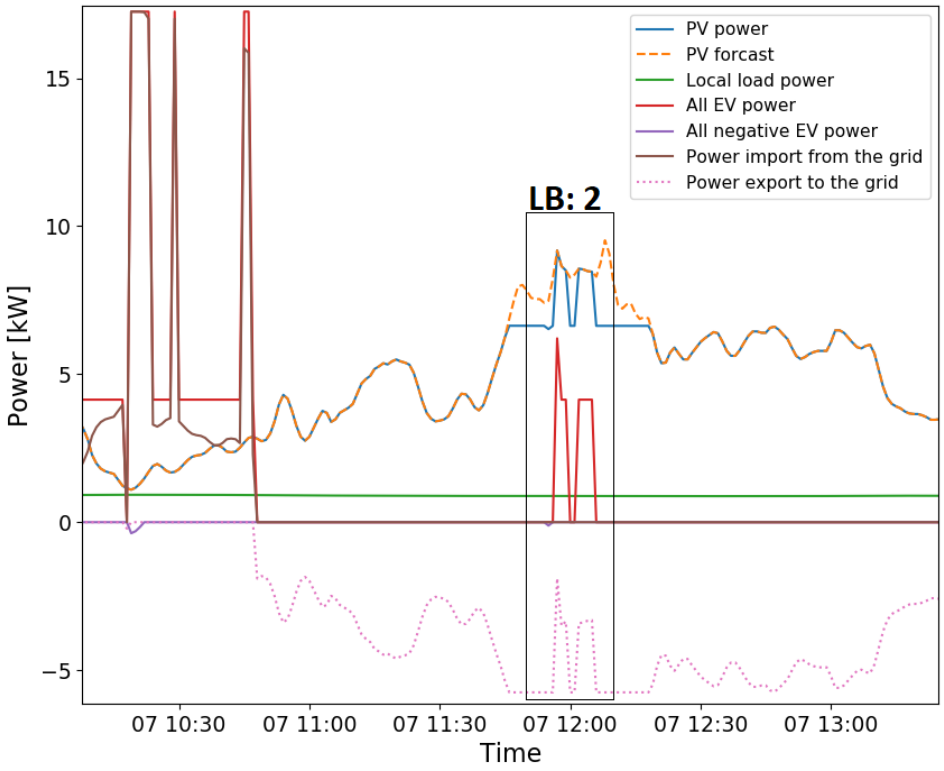

Figure 4.26: Node power profile for date: 07/09/2018 at c_e_sell = 0.95*c_e_buy

After analysing the power profile for the date 07-09-2018, it can be implied that increasing the value of c_e_sell directly affects the PV involvement in supplying the load demand. Change in PV generation can affect the charging and discharge cycle for the EVs as the optimizer will try to utilize the PV power as much as possible and send the remaining energy to the grid to generate more profit. For a clear analysis of charging and discharging of the EV, first point to notice is how the EVs arrive and depart at the chargers during the whole duration which is shown in Table 4.1.

Figure 4.28 shows the node power profile for the date: 08/09/2018 for c_e_sell at 0.0*c_e_buy. It can be seen from the figure that the algorithm behaves the same way as during the date: 07/09/2018 where the PV power is curtailed to supply only the energy demand. A distinguishable behaviour is seen when the EV arrive during the duration of 'LB: 3' in figure 4.28. It can be seen that the EV at one of the charger discharge to supply the EV demand of another EV. The reason for involving EV in charging another EV instead of the grid can be explained with the help of figure 4.27 where the cost of buying energy from the grid is plotted against time. It can be seen during the duration of 'LB: 3' from 16:45 - 18:15 the cost of buying is increasing and involving the grid to charge the EV will involve higher cost of energy. To prevent that, EV perform V2G to charge EV at other chargers and support the PV.

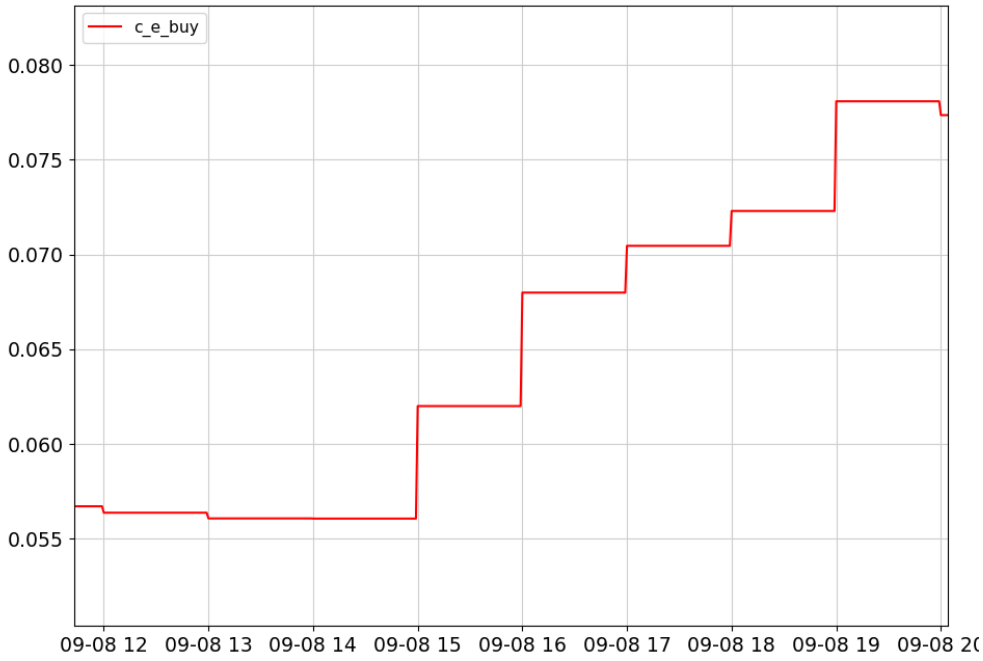

Figure 4.27: c_e_buy for date: 08/09/2018

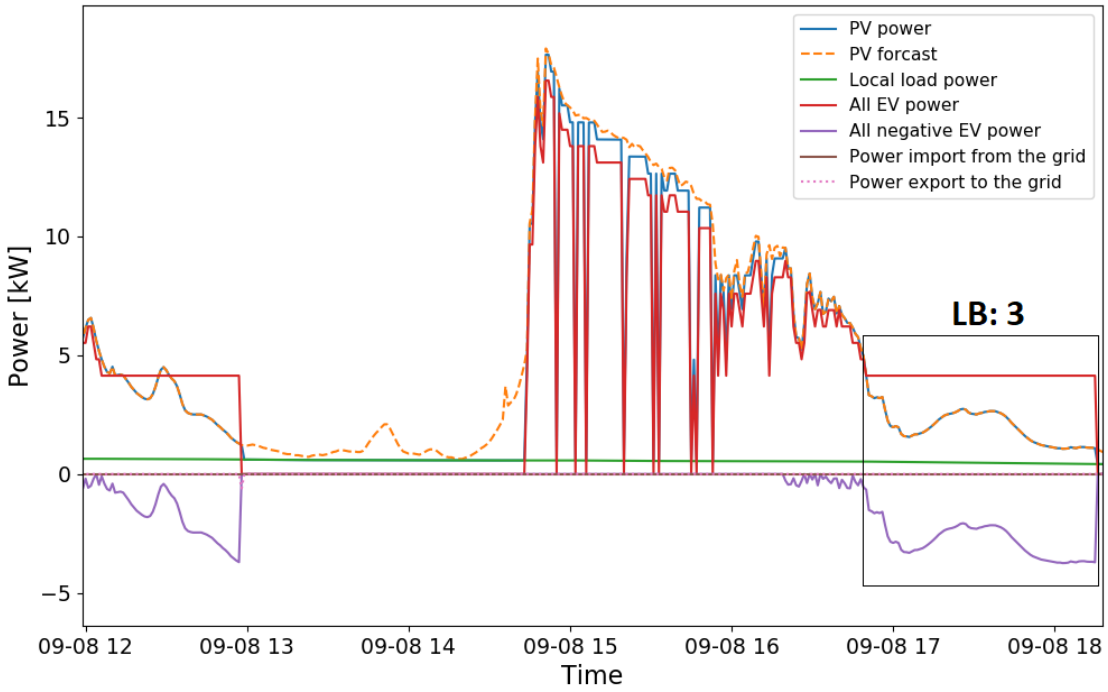

Figure 4.28: Node power profile for date: 08/09/2018 at c_e_sell = 0.0*c_e_buy

Figure 4.29 shows the node power profile for the date: 08/09/2018 for c_e_sell at 0.95*c_e_buy. Two distinguishable feature can be observed in the figure as compared to figure 4.28. The first difference is labelled as 'LB: 4'. During the interval of 'LB: 4' the grid is seen being involved in charging the EV which is not the case when c_e_sell = 0.0*c_e_buy. The change in the behaviour of the algorithm is seen as it increases the involvement of grid at c_e_sell = 0.95*c_e_buy is because during the interval the c_e_buy value is decreasing significantly. As the cost of selling energy is now almost equal to cost of buying energy, any grid involvement cost can be compensated by the profit from PV power export or V2G which is seen in 'LB: 5'. During the in-

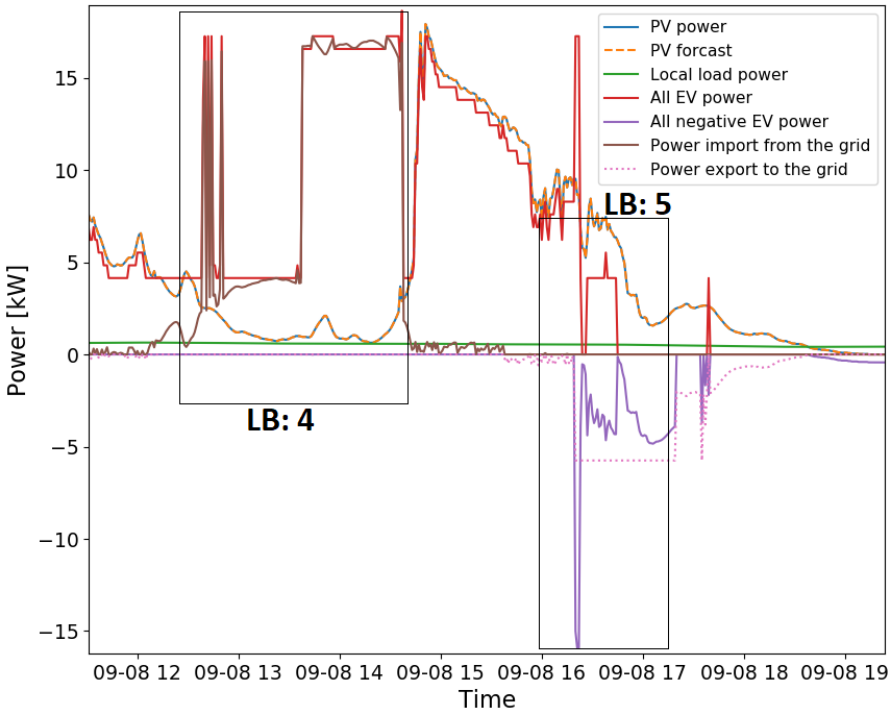

Figure 4.29: Node power profile for date: 08/09/2018 at c_e_sell = 0.95*c_e_buy

terval of 'LB: 5' the EV not only support the PV in charging other EV but also help in maximizing the export power which was not the case during 'LB: 3'.

Changing the c_e_sell value can affect the charging and discharging cycle of the EV. It is necessary to check if the EVs are charged to their requested energy at the end of their parking to avoid penalty. First, a comparison is done for charging energy and discharge energy of the EV for different value of c_e_sell. Figure 4.30 shows the charging energy and figure 4.31 shows the discharging energy of the EVs for the duration of the simulation for various value of c_e_sell. From the figures the following observation can be made; an increase in the charging energy and discharging energy is seen for EVs at the chargers as the value of c_e_sell increases. The reason for this behaviour is that as the value of n increases, the value of c_e_sell becomes much larger as compared to the value of c_PV which allows PV to become the main source in supplying the demand and generate larger profit by exporting power to the grid. An increase in the PV generation and more involvement of the grid increases the flexibility of the EVs to participate more in the V2G services. EVs participating in V2G gets recharged using the PV power at no cost. Moreover, if there is grid import to support the EV an increase in overall cost of energy for the node. The overall cost can be reduced by PV export energy profit.

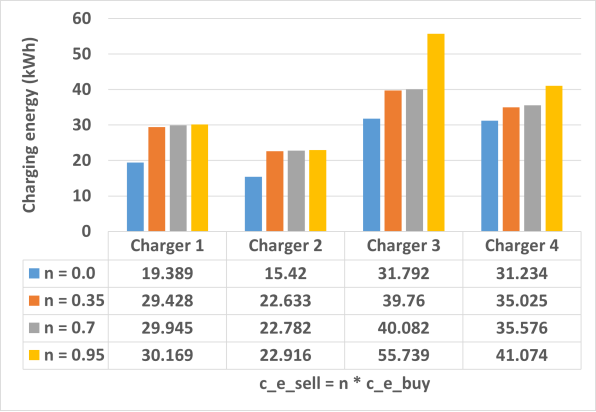

	Charger 1	Charger 2	Charger 3	Charger 4
n = 0.0	19.389	15.42	31.792	31.234
n = 0.35	29.428	22.633	39.76	35.025
n = 0.7	29.945	22.782	40.082	35.576
n = 0.95	30.169	22.916	55.739	41.074

Figure 4.30: Charging energy of the EV

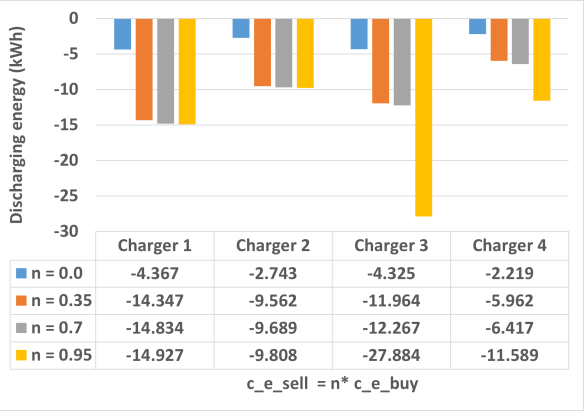

	Charger 1	Charger 2	Charger 3	Charger 4
n = 0.0	-4.367	-2.743	-4.325	-2.219
n = 0.35	-14.347	-9.562	-11.964	-5.962
n = 0.7	-14.834	-9.689	-12.267	-6.417
n = 0.95	-14.927	-9.808	-27.884	-11.589

Figure 4.31: Discharging energy of the EV

	t_arr(DD-MM-YY hh:mm)	t_dep(DD-MM-YY hh:mm)	d_gap for c_e_sell = 0*c_e_buy	d_gap for c_e_sell = 0.35*c_e_buy	d_gap for c_e_sell = 0.7*c_e_buy	d_gap for c_e_sell = 0.95*c_e_buy
Charger 1	**07-09-18 08:28**	**07-09-18 10:48**	**0**	**0**	**0**	**0**
Charger 4	**07-09-18 10:19**	**07-09-18 10:24**	**0**	**0**	**0**	**0**
Charger 3	**07-09-18 11:52**	**07-09-18 12:07**	**0**	**0**	**0**	**0**
Charger 4	**07-09-18 17:28**	**07-09-18 18:56**	**0**	**0**	**0**	**0**
Charger 1	**08-09-18 10:00**	**08-09-18 17:51**	**0**	**0**	**0**	**0**
Charger 3	**08-09-18 11:13**	**09-09-18 00:41**	**0**	**0**	**0**	**0**
Charger 4	**08-09-18 11:38**	**08-09-18 13:00**	**0**	**0**	**0**	**0**
Charger 2	**08-09-18 16:20**	**08-09-18 19:59**	**0**	**0**	**0**	**0**
Charger 1	**09-09-18 08:20**	**09-09-18 14:43**	**0**	**0**	**0**	**0**
Charger 4	**09-09-18 13:02**	**09-09-18 22:38**	**0**	**0**	**0**	**0**
Charger 3	**09-09-18 14:51**	**09-09-18 17:49**	**0**	**0**	**0**	**0**
Charger 2	**09-09-18 17:19**	**09-09-18 19:06**	**0**	**0**	**0**	**0**
Charger 1	**10-09-18 09:10**	**10-09-18 10:02**	**0**	**0**	**0**	**0**
Charger 2	**10-09-18 10:17**	**10-09-18 15:40**	**0**	**0**	**0**	**0**
Charger 3	**10-09-18 14:21**	**10-09-18 16:49**	**0**	**0**	**0**	**0**
Charger 1	**10-09-18 16:54**	**10-09-18 17:38**	**0**	**0**	**0**	**0**
Charger 4	**10-09-18 18:37**	**10-09-18 20:38**	**0**	**0**	**0**	**0**

Table 4.8: d_gap at departure for various value of c_e_sell

After looking at the charging and discharging energy of the EVs it is necessary to check if the EVs are charged to their requested energy at the end of their parking to avoid penalty. Table 4.8 shows the d_gap value at the departure time of the EV. D_gap refer to the remaining energy that EV needs to be charged to in order to fulfil the energy request. It is calculated by subtracting the energy request with energy at the departure time and arrival battery energy. It can be seen that the d_gap value for various values of c_e_sell is 0 kWh which implies that the energy request of the EVs is fulfilled at the end of their parking, therefore, will incur no penalty. It can also be said that the change in the value of c_e_sell does not affect the d_gap value.

Finally, a cost comparison is done along with node energy distribution for the different values of n to see how the energy distribution behaviour changes as the cost of selling increases to 95% of buying cost. Figure 4.32, 4.33 shows node energy distribution and cost of energy vs n (c_e_sell = n*c_e_buy), it can be seen from the figure that, as the cost of selling gets close to the buying cost the profit obtained by selling power to the grid increases which was expected as optimizer will now allow the excess power to be exported to the grid to reduce the overall cost of energy. It is also seen that as the selling cost increases the V2G services also increases thereby the loss of battery degradation also increases due to the increase in the cycle of charging and discharging. Increased charging and discharging cycle might involve possibility when the EV leaves the charging station without its energy requirement fulfilled. To avoid that, the grid also increases its import power to support PV in charging the EV or supplying the local load demand.

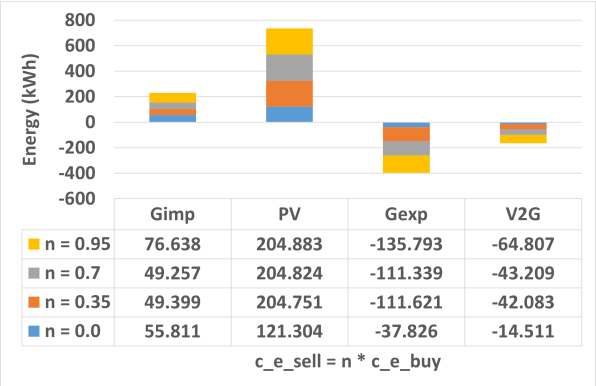

Figure 4.32: Energy distribution for various values of c_e_sell

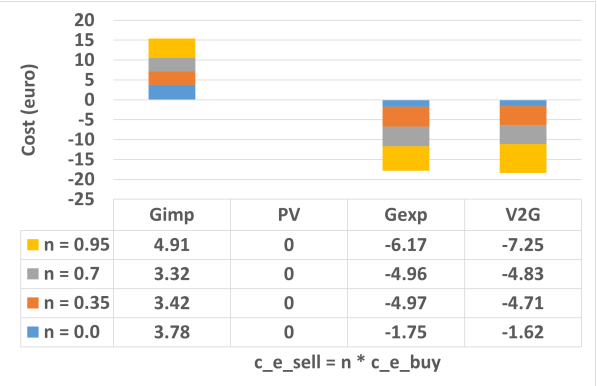

Figure 4.33: Cost distribution for various values of c_e_sell

To summarize everything that have been observed so far, it is safe to say that as the algorithm is more oriented towards providing benefit to the node as increasing the cost of selling the energy have its repercussions on the grid and the CSO. It's been determined that increasing the cost of selling energy increases the grid dependency because algorithm increase in the amount of export power to the grid is , thereby making a generous profit for the node. It is to be advised to the CSO that an agreement regarding the percentage of the cost of selling with the node owner must be done beforehand to provide benefit to both user and CSO. The selection of the value should be in such a way that the PV can generate sufficient profit by exporting power, V2G losses are minimum, there is no possible penalty and finally the grid has less involvement which would decrease the overall cost.

4.5. Summary

After the development of the mathematical model and algorithm in chapter 3, in this chapter, several case studies were performed for sensitivity parameters that affect the behaviour of the algorithm. The parameters selected for the case studies were cost of penalty for unfinished charging, cost of PV generation, grid import power limitation and cost of selling energy to the grid. In the cost of penalty case study, it was observed how crucial this parameter was in fulfilling the request of EV user energy demand. At 0.0 euro/kWh cost of penalty, the EVs were seen to leave the charger without their request fulfilled, therefore to avoid that an increased cost of penalty value was used. For the cost of PV generation case study, it was observed how changing the cost of PV generation has a significant effect on the grid involvement and V2G. Another case study was performed for grid import power limitation which was done to observe how the algorithm behaves when the grid performs load shedding operation due to faults. It was observed that the algorithm benefits the node and EV user at lower grid import power and by not fulfilling the demand, therefore, making CSO vulnerable to possible penalties. To avoid that it was suggested that an agreement must be made beforehand with the user which will allow the CSO to pay less or almost no penalty for not charging the EV when the grid capacity is reduced. Finally, the cost of selling energy to the grid case study was performed and it was observed that the algorithm again provide benefit to the node by increasing the amount of export power to the grid is, and using the grid in charging the EVs. It was advised that the CSO must have an earlier agreement on the percentage of the cost of selling with the node owner to provide benefit to both user and CSO. After the case study was performed, the algorithm was observed not having major control over the V2G application of the EVs. Therefore, a proposal was made for a more effective battery degradation model which will control the V2G application of EVs. The new battery degradation model selection and implementation are mentioned in chapter 5.

5

Battery degradation model

In section 3.2.3, a simplified version of the battery degradation is used which calculate the cost of battery degradation by $\sum_{j=1}^{J} \Delta T \sum_{t=1}^{T} p_{n,j,t}^{e-} * C_{n,j}^{Bat(V2G)}$ where $p_{n,j,t}^{e-}$ is the discharging power from electric vehicles and $C_{n,j}^{Bat(V2G)}$ is the degradation cost in euro/kWh. The value of $C_{n,j}^{Bat(V2G)}$ is calculated as shown in section 3.2.3 is 0.112 euro/kWh. The simplified model equation can be also inferred as the cost of selling energy from the battery and does not model the actual degradation of the battery. In section 2.3.1, the literature of battery degradation mechanism the two aging mechanism of battery degradation was discussed. The battery aging mechanism discussed are Calendar aging and cyclic aging. For this thesis, calendar aging is out of scope, and the focus will be on capacity loss due to cyclic aging and stress factor influencing cyclic aging. To calculate the capacity loss of the EV due to frequent charging and discharging when the EV participated in V2G application, one of the important stress factor that affects the cyclic aging: C-rate is taken into consideration. The section deals with the formulation of capacity loss due to the C-rate stress factor, the modelling of the total capacity loss, implementation and comparison of the algorithm with the simplified model with the new model. Finally, a comparison of a smart charging algorithm with uncontrolled charging is done and results are analysed.

5.1. C-rate stress factor

C-rate is defined as the rate at which a battery is charged or discharged. The manufacturers under nominal condition define the C-rate of a battery based on its nominal capacity. The C-rate is dependent on the capacity of the battery and for a battery capacity of 1Ah, and 1C C-rate it will imply that the battery will be fully charged or discharged in 1 hour if the current is 1A. Similarly, a C-rate of 2C will imply that the battery will charge and discharge completely in half-hour. A larger C-rate will imply a higher current value and as mentioned in the literature a higher current can leads to faster degradation. In this thesis, the battery degradation model comprises the stress factor C-rate which affects cyclic aging. The model for this thesis is derived from the study in [54], where the loss of capacity due to C-rate is modelled by the following equation 5.1.

$$Q_{loss\%} = (a * T^2 + b * T + c) * e^{(d*T+e)*I_{rate}} * Ah \tag{5.1}$$

where;

- a,b,c,d,e are the curve fit parameters
- T is the temperature in K
- I_{rate} is the C-rate
- Ah is the throughput

The value of a,b,c,d,e, is determined in the study [54] is determined as follows:

a	**8.61E-6, 1/Ah-K^2**
b	**-5.13E-3, 1/Ah-K**
c	**7.63E-1, 1/Ah**
d	**-6.7E-3, 1/K-(C-rate)**
e	**2.35, 1/(C-rate)**

Table 5.1: Curve fitting values

Equation 5.1 can be taken as two parts. The first part is the C-rate dependence and the second part is throughput *Ah*. The C-rate dependence is exponential implementing the equation in existing objective function will make it non-linear. Equation 5.1 is remodelled as a linear equation to introduce in the existing MILP algorithm. In this thesis, the simplification of the equation 5.1 is done based on the I_{rate}. The simplification can be done by determining the relationship between Ah and I_{rate}. I_{rate} is calculated from the current as shown in equation 5.2, where I is current in ampere and Q(Ah) is the throughput capacity of the battery. The linearization of the equation 5.1 and development of the degradation model is done with respect to the battery of EV. Suppose for battery energy capacity 50 or 100kWh, at EV battery voltage 375V [68] the Q(Ah) will be 133 or 266 Ah. It has been assumed that the EV arriving at the charger will provide the Q(Ah) of the battery to ensure that the history of aging of the EV battery is taken into account.

$$I_{rate} = \frac{I(A)}{Q(Ah)} \tag{5.2}$$

A relationship between Ah and I_{rate} is determined to simplify the model. The following steps show the relationship between Ah and I_{rate}. It is to be noted that Ah is calculated per timestep Δt which is 1 minute. The Ah in the equation for Δt is taken as dAh and calculated as in equation 5.3

$$dAh = \frac{I * \Delta t}{60} \tag{5.3}$$

$$dAh = \frac{I * \Delta t}{60},$$
$$I = \frac{dAh * 60}{\Delta t},$$

Substituting the value of I in equation 5.2

$$I = \frac{dAh * 60}{\Delta t},$$
$$I_{rate} = \frac{dAh * 60}{\Delta t * Q(Ah)}.$$
$$dAh = \frac{I_{rate} * Q(Ah) * \Delta t}{60}$$

Substituting the value of dAh in equation 5.1

$$Q_{loss\%} = (a * T^2 + b * T + c) * e^{(d*T+e)*I_{rate}} * \frac{I_{rate} * Q(Ah) * \Delta t}{60} \tag{5.4}$$

In equation 5.4 the relationship between I_{rate} and $Q_{loss\%}$ is modelled, and the model is then linearized by using the curve fit tool of the MATLAB. To use the curve fit, first, the value of $Q_{loss\%}$ is determined for a range of values I_{rate}. The range of values is selected based on a maximum I_{rate} for an EV of 133 Ah which is 0.34C [with respect to EV battery] for a maximum power supply of 17.25kW (grid import limitations). The I_{rate} is varied from 0 to 0.5 in very small steps of 0.0001 and the value of $Q_{loss\%}$ is calculated for T = 310K and curve fit is performed. The study in [48] determines that C-rate does not have a direct influence on degradation at temperatures near room temperature. Therefore a temperature value of 310K is selected as it is much higher than the room temperature [48]. Figure 5.1 shows the curve obtained for $Q_{loss\%}$ vs I_{rate} and its linear

relationship can be formulated as equation 5.5 where a = 0.0002938 and b = 7.353e-07 for 133 Ah battery. The linear fit gives an R^2 of 0.9968 and values of a and b, for any other capacity EV say x Ah, the value will change as x/133 * a(133 Ah) and x/133 *b(133 Ah) where x is the capacity of the battery of an EV, a(133 Ah) and b(133 Ah) are curve fit values for 133 Ah EV.

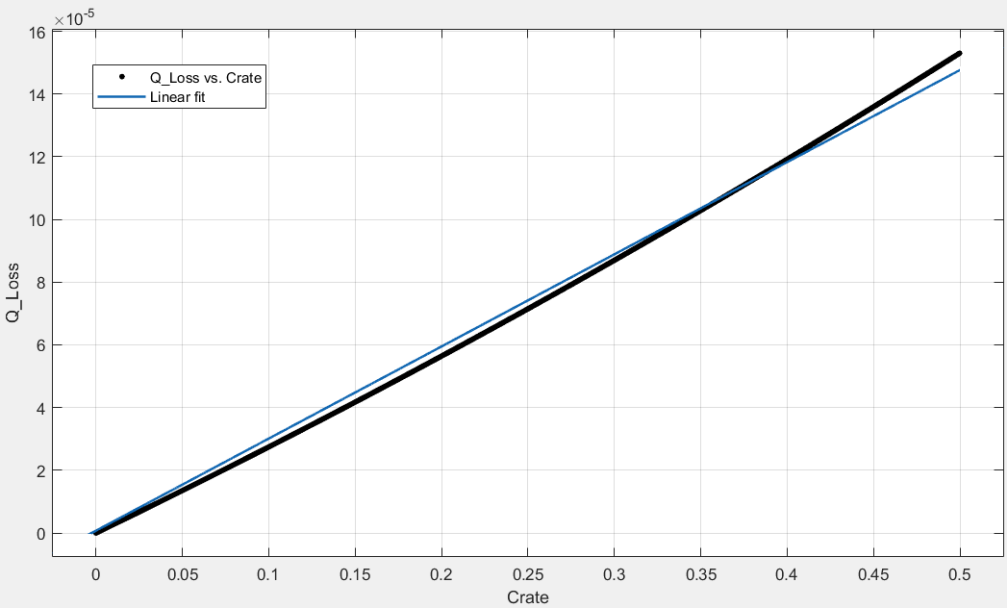

Figure 5.1: $Q_{loss\%}$ vs I_{rate}

$$Q_{loss\%} = a * I_{rate} + b \tag{5.5}$$

Finally, percentage total capacity loss or $Qloss_{total}[\%]$ for the duration of optimization T is given by equation 5.6 where T is the duration of optimization. The equation is formulated assuming that the capacity loss due to other stress factors is not coupled with C-rate model.

$$Qloss_{total}[\%] = \sum_{t=0}^{T} Q_{loss\%} \tag{5.6}$$

For the duration T, to prove that the linearization of equation 5.1 does not have significant variation with the value obtained with 5.6 a EV arriving at charger 4 on 10.09.2018 is selected to calculate the percentage total capacity loss using both equation. The EV data can be obtained from Table 4.1 in chapter 4. The C-rate for the charging or discharging is determined using equation 5.2. The percentage capacity loss for the duration of parking is determined using equation 5.1 and 5.6 and the value obtained is 0.004% and 0.0041% respectively. Therefore, it can be said that the linearization did not lead to a significant error in percentage capacity loss.

The daily degradation percentage [α] is calculated using $\alpha = \frac{100}{(lifetime*365)}$ assuming EV is charged daily. The 100% depicts the End of Life where the capacity drops from 100% to 0% [69] which is not the case in real life when the battery needs to be replaced after 80% capacity loss [48]. The $Qloss_{total}[\%]$ for any EV for that day should be less than or equal to α, which will be used as a constraint for the optimization process. For example, if the lifetime of the battery provided by manufacturers is 10 years, the value of α would be 0.021 expected % change in capacity in a day.

Modified Objective function

The objective function before this model as explained in section 3.2.3, is used to calculate the cost of battery degradation is given by $\sum_{j=1}^{J} \Delta T \sum_{t=1}^{T} p^{e-}_{n,j,t} * C^{Bat(V2G)}_{n,j}$. By implementing the revised battery degradation model, the function to calculate the cost of battery degradation can be changed to equation 5.7 where $Q_{n,j}$ is the

capacity of the battery of EV and the value of $C^{cap}_{n,j}$, cost of battery per capacity, is 175 euro/per Ah battery capacity [68].

$$\sum_{j=1}^{J} Qloss_{total,(n,j)}[\%] * Q_{n,j} * C^{cap}_{n,j} \tag{5.7}$$

The objective function equation 3.1 will change as shown in equation 5.8.

$$Min.C^{opt}_{n} = \sum_{j=1}^{J} (B^{a}_{n,j} + d_{n,j} - B_{n,j,T^{d}_{j}}) * C^{p}_{n,j} + \Delta T \sum_{t=1}^{T} p^{PV}_{n,t} * C^{PV} + \Delta T \sum_{t=1}^{T} p^{g(imp)}_{n,t} * C^{e(buy)}_{t} - p^{g(exp)}_{n,t} * C^{e(sell)}_{t} + \sum_{j=1}^{J} Qloss_{total,(n,j)}[\%] * Q_{n,j} * C^{cap}_{n,j} \tag{5.8}$$

Sub-functions

$$I^{rate}_{n,j,t} = \frac{p^{e+}_{n,j,t} * \eta^{ev}_{n,j}}{V^{bat}_{n,j} * Q^{Ah}_{n,j}} - \frac{p^{e-}_{n,j,t}}{V^{bat}_{n,j} * Q^{Ah}_{n,j} * \eta^{ev}_{n,j}} \tag{5.9}$$

$$Qloss_{n,j,t}[\%] = a_{n,j} * I^{rate}_{n,j,t} + b_{n,j} \tag{5.10}$$

$$Qloss_{total,(n,j)}[\%] = \sum_{t}^{T} Qloss_{n,j,t}[\%] \tag{5.11}$$

Several new parameters are introduced in the optimization problem as decision variables and input parameters. Equation 5.9 - 5.11 shows sub-functions associated with the new battery degradation model. In equation 5.9, $I^{rate}_{n,j,t}$ is the C-rate that is calculated using the charging power $p^{e+}_{n,j,t}$ or discharging power $p^{e-}_{n,j,t}$ to and from the battery divided by $*Q^{Ah}_{n,j}$ the Ah battery capacity and $V^{bat}_{n,j}$ the voltage of the EV battery. The C-rate is calculated with respect to EV, therefore the charging power $p^{e+}_{n,j,t}$ or discharging power $p^{e+}_{n,j,t}$ is multiplied and divided by efficiency $\eta^{ev}_{n,j}$ respectively. Equation 5.10 calculate the $Q_{loss\%}$ where $a_{n,j}$ and $b_{n,j}$ has the same meaning as in equation 5.5. Finally, $Qloss_{total,(n,j)}[\%]$ is calculated as shown in equation 5.11. It is necessary to determine the constraints associated with the parameters to limit the behaviour. The equations below shows the constraints associated with the decision variables.

Constraints

$$0 \leq I^{rate}_{n,j,t} \leq 0.5 \tag{5.12}$$

$$0 \leq Qloss_{n,j,t}[\%] \tag{5.13}$$

$$0 \leq Qloss_{total,(n,j)}[\%] \leq \alpha \tag{5.14}$$

Equation 5.12 is the constraint for C-rate, the maximum value of C-rate is taken as 0.5C. As mentioned earlier, $Qloss_{total,(n,j)}[\%]$ which is the total percentage capacity loss of the battery for a day is less than allowable % change in capacity in a day α which is calculated earlier for 80% capacity reduction and lifetime of 10 years as 0.021%.

5.2. Case studies

After the implementation of the mathematical model and incorporating it in the existing smart charging algorithm, a comparative analysis of the C-rate stress factor aging model and simplified battery degradation is made. This section focus on the detailed analysis of both models and finally, the smart charging algorithm is compared with uncontrolled charging to prove that control and optimized schedule charging of EV along with V2G services and battery degradation model are beneficial as compared to uncontrolled charging.

5.2.1. Comparison of C-rate stress factor degradation model with simplified battery degradation model

In this section, a comparative analysis of the battery degradation model is done. Earlier in chapter 3, a simplified version of the battery degradation had been used, however, it does not model the actual degradation and does not have more control over how EVs perform V2G. In this chapter, a revised model of battery degradation is used which models the cyclic aging of the battery due to the C-rate stress factor. After implementing the mathematical model in the existing MILP smart charging algorithm, the simulation is performed using several assumptions to mimic physical scenarios, which are as follows:

1. The duration of the simulation is 4 days with 1 minute timestep
2. As mentioned earlier during the simplification of the equation 5.1, the temperature used is 310K
3. Cost of EV battery per capacity is taken as 175 euro per Ah battery capacity
4. EV battery voltage is taken as 375V
5. All the assumptions mentioned in section 3.1 holds in this simulation as well

Analysis

The analysis is done for four days from date 07-09-2018 till 10-09-2018. The analysis is done based on the factor that how the behaviour of the algorithm changes using the C-rate battery degradation model as compared to the simplified model. It is hypothesised that the C-rate degradation model will decrease the amount of PV generation as it will charge the EV close to the requested energy to prevent additional degradation. The charging and discharging behaviour of the algorithm will change and it will affect the grid involvement as well. To prove the earlier hypothesis, Figure 5.2 and Figure 5.3 shows the node power profile data for the date 08-09-2018 for simplified battery degradation model and C-rate degradation model.

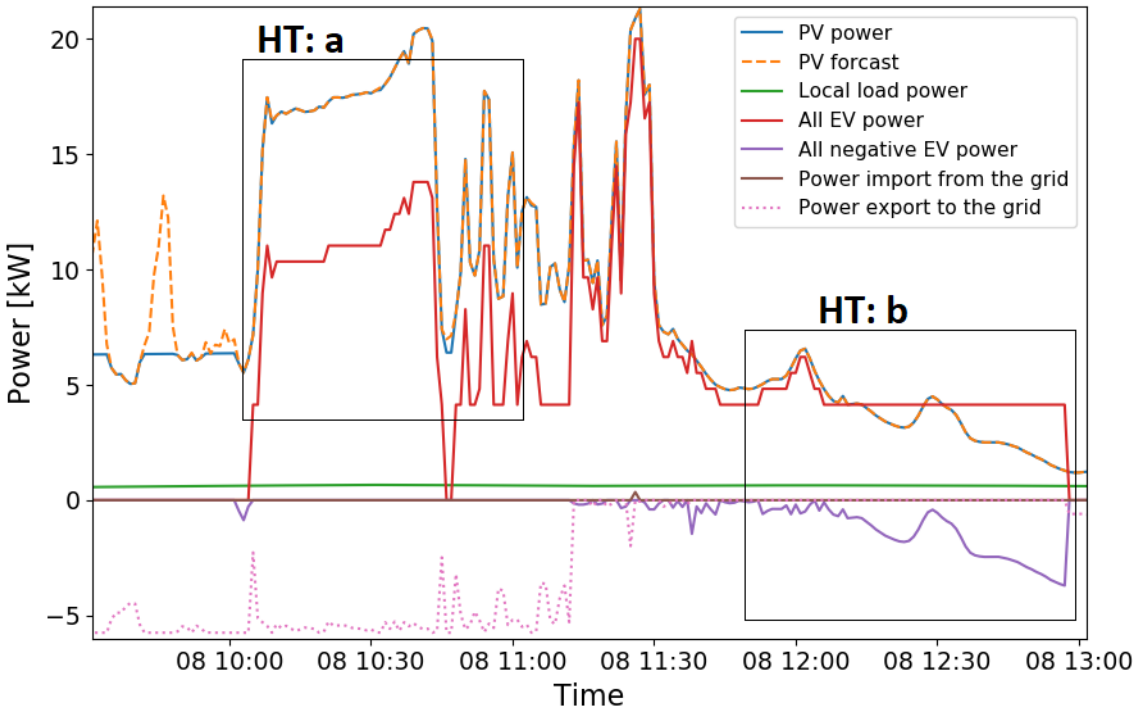

Figure 5.2: Node power profile for 08-09-2018 for simplified battery degradation model

Highlight box, HT: a' and 'HT: c', in Figure 5.2 and Figure 5.3 shows the power profile for EV arriving at charger 1 at 10:00 with an energy request of 5.2kWh (from Table 4.1). In the case of a simplified battery degradation model or at 'HT: a' the PV starts charging the EV and obtain substantial profit by exporting power to the grid. The EV is charged continuously and charged to energy more than requested energy so that it can

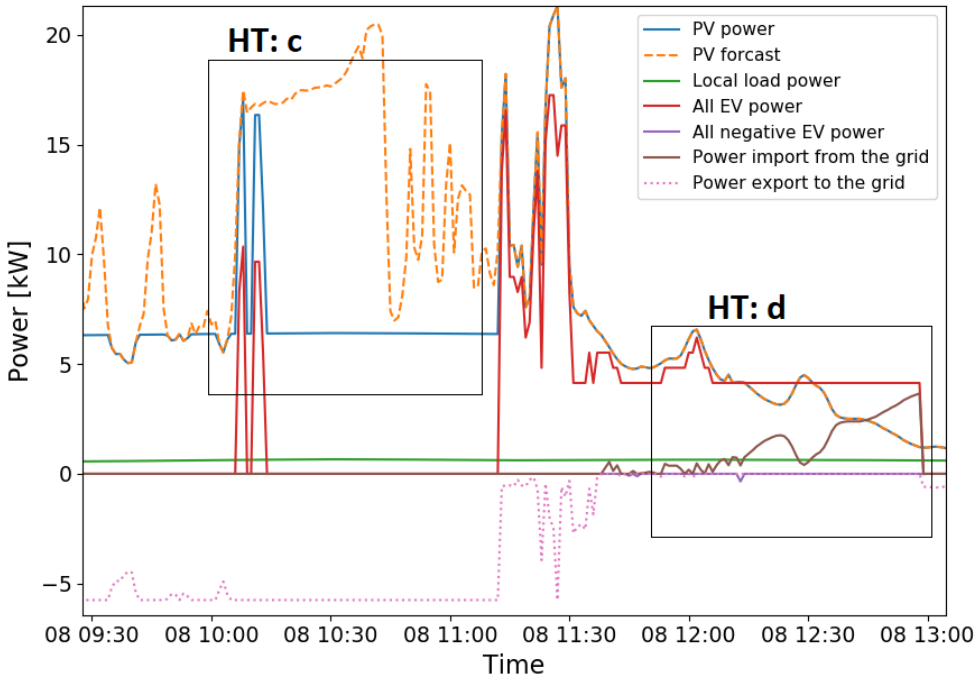

Figure 5.3: Node power profile for 08-09-2018 for C-rate degradation model

be used as a backup source when the PV generation is not sufficient. This is not the case when the algorithm incorporates the C-rate degradation model. The same EV shows a different charging schedule as seen in 'HT: c'. In 'HT: c', the PV power is seen to get curtailed to a value sufficient to charge the EV, supply the local load demand and export power. The EV does not only experience a change in charging schedule but also charged with less power. The reason for a difference in the behaviour is because: first, the C-rate degradation model mentioned earlier in this chapter is dependent on charging or discharging rate or C-rate. The increase in the charging or discharging power will increase the C-rate therefore will increase the % capacity loss. Another reason why the behaviour change is seen during the scheduling of the charging of EV is that with the C-rate degradation model, charging the EV to a higher energy than the requested energy will increase the capacity loss and will incur higher degradation cost. The EV charging more than the requested energy will involve EV to undergo additional charging cycles. As the C-rate model is charging or discharging current rate dependent, for every additional charging the capacity loss will increase. Therefore, it can be said that the C-rate degradation model takes battery degradation into account more seriously and reduce the capacity loss by preventing EV to charge more than requested and with less power.

Implementation of the C-rate degradation model limits the amount of charging energy for the EVs, it can be asked *how the EVs are charging so that its demands are fulfilled?* To answer this, the focus will now be on 'HT: b' and 'HT: d' in Figure 5.2 and Figure 5.3 respectively. As stated earlier, that when a simplified degradation model is implemented, the PV charge the EVs more than the requested energy (only if the PV generation is sufficient) and use V2G application of EVs to supply the demand of other EV or local load when generation is insufficient or to reduce the grid involvement. The aforementioned statement can be verified in 'HT: b' when EV at charger 1 provides V2G power to charge EV at charger 4 which can be seen by (purple plot line) in negative power axis. This is not the case when the C-rate degradation model is implemented. The EVs with the C-rate degradation model, even though have sufficient energy, does not participate in V2G much to support PV in supplying the demand. However, an unfinished charging will lead to the possibility of penalty, to avoid that the grid is involved in supplying the demand as seen in 'HT: d' (brown plot lines).

As the C-rate degradation model changes the charging and V2G cycles and power for the EVs, it is necessary to check if the EVs are charged to their requested energy at the end of their parking to avoid penalty. First, a comparison is done for energy at the departure of the EV with the requested energy is done. Figure 5.4 shows the requested energy and energy at departure for both degradation model for EVs arriving at various chargers during the duration of the simulation. The requested energy indicates the amount of energy the EV must

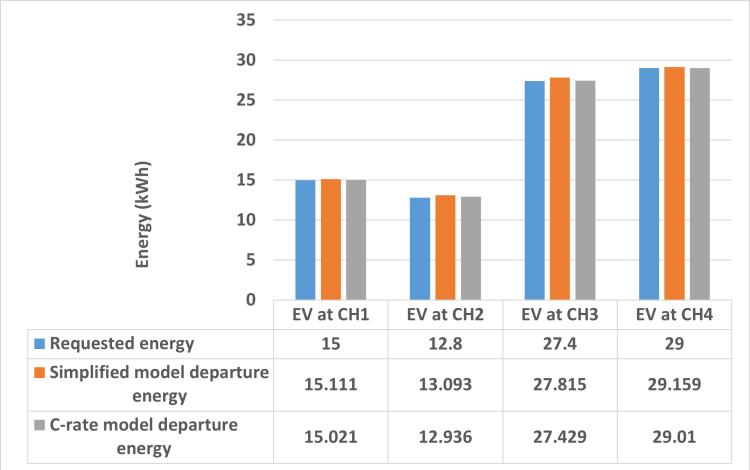

Figure 5.4: Energy comparison for simplified and C-rate battery degradation model

have at the departure. Simplified model and C-rate degradation model departure energy indicate the energy at the departure using both the models. It can be seen when a simplified model is implemented, the EVs at the chargers are charged more than the requested energy which is not the case with the C-rate degradation model. In the C-rate degradation model, the energy at departure is almost similar to the requested energy. The reason is that during the simplified model, as stated earlier, the EVs do not have a strict degradation dependent factor which can limit how much the EV can charge. The PV generation cost is 0.0 euro/kWh, the cost of charging EV using PV is 0.0 euro. EV and PV user can make a profit by exporting the power to the grid or EV can be used as a backup source to prevent an increased cost due to grid involvement. However, with the C-rate degradation model, the algorithm uses the degradation of the EVs as a priority and limit the amount of energy that the EVs can be charged or discharged to. The energy is kept as close as the requested energy to avoid increased degradation. After looking at the departure energy as a whole, Table 5.2 shows individual EV remaining request energy or d_gap value. A zero d_gap indicate that the EV request is fulfilled.

	t_arr(DD-MM-YYYY hh:mm)	**t_dep(DD-MM-YYYY hh:mm)**	**d_gap(dep)**
Charger 1	**07-09-2018 08:28**	**07-09-2018 10:48**	**0**
Charger 4	**07-09-2018 10:19**	**07-09-2018 10:24**	**0**
Charger 3	**07-09-2018 11:52**	**07-09-2018 12:07**	**0**
Charger 4	**07-09-2018 17:28**	**07-09-2018 18:56**	**0**
Charger 1	**08-09-2018 10:00**	**08-09-2018 17:51**	**0**
Charger 3	**08-09-2018 11:13**	**09-09-2018 00:41**	**0**
Charger 4	**08-09-2018 11:38**	**08-09-2018 13:00**	**0**
Charger 2	**08-09-2018 16:20**	**08-09-2018 19:59**	**0**
Charger 1	**09-09-2018 08:20**	**09-09-2018 14:43**	**0**
Charger 4	**09-09-2018 13:02**	**09-09-2018 22:38**	**0**
Charger 3	**09-09-2018 14:51**	**09-09-2018 17:49**	**0**
Charger 2	**09-09-2018 17:19**	**09-09-2018 19:06**	**0**
Charger 1	**10-09-2018 09:10**	**10-09-2018 10:02**	**0**
Charger 2	**10-09-2018 10:17**	**10-09-2018 15:40**	**0**
Charger 3	**10-09-2018 14:21**	**10-09-2018 16:49**	**0**
Charger 1	**10-09-2018 16:54**	**10-09-2018 17:38**	**0**
Charger 4	**10-09-2018 18:37**	**10-09-2018 20:38**	**0**

Table 5.2: d_gap at departure using C-rate degradation model

The decrease in the charging energy is seen for the EVs at the charger as the C-rate degradation model limits the charging rate and energy to avoid increased battery degradation. The question then arises *how or when the EVs can perform V2G?* The answer to this can be provided by first looking at how much the discharge energy has been affected by implementing the C-rate degradation model. Figure 5.5 shows the discharge

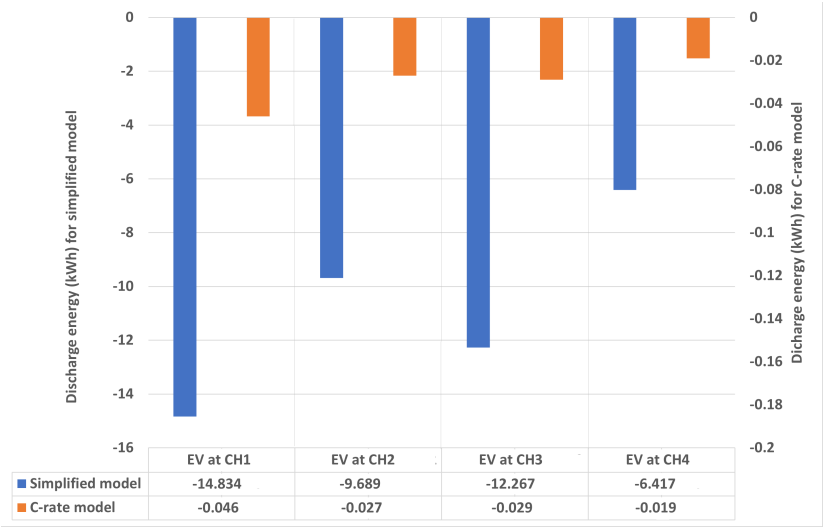

Figure 5.5: Discharge energy for simplified and C-rate degradation model

energy for simplified and C-rate degradation model. It can be seen from the tabulated data in the figures that the discharge energy for the C-rate degradation model has significantly decreased as compared to the simplified model. It can be said that the reason for this is similar to the change in behaviour seen in figure 5.6. It has been stated earlier that with the C-rate degradation model the EVs are charged close to the requested energy to limit the battery degradation. EVs can't perform higher V2G even though it has sufficient energy as it would discharge the battery and avoid penalty the EVs will be subjected to recharging. This will increase the frequency of charging and discharging cycles which would then increase the degradation. The EVs are seen performing V2G only when it can reduce the cost of energy imported from the grid and support PV in supplying the demand. The aforementioned statement can be verified by the following figure 5.6 which shows the power profile of EV at charger 4 on 10-09-2018. In figure 5.6 'HT: e' shows a drop in the grid import power (brown plot lines) and increase in V2G power in the negative power axis (purple plot lines). The reason for this can be explained by an example by looking at the cost of degradation and cost of grid energy import calculated for the value of V2G power. The value obtained after the calculation is 0.02 euro and 0.04 euro respectively.

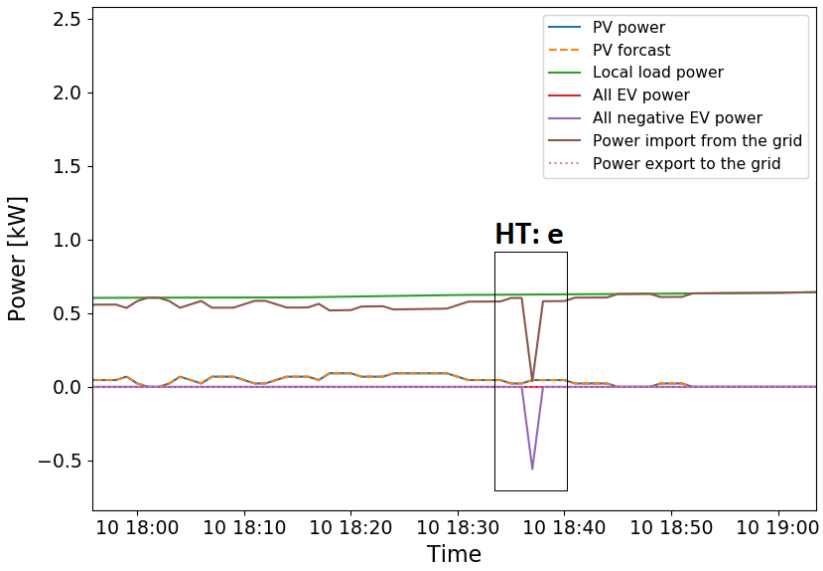

Figure 5.6: Node power profile [section] for EV at charger 4 on 10.09.2018

Finally, a cost comparison is done along with node energy distribution for the degradation models. Figure

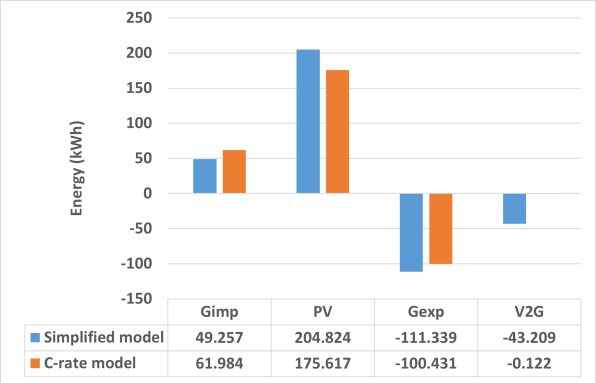

Figure 5.7: Energy comparison for degradation models

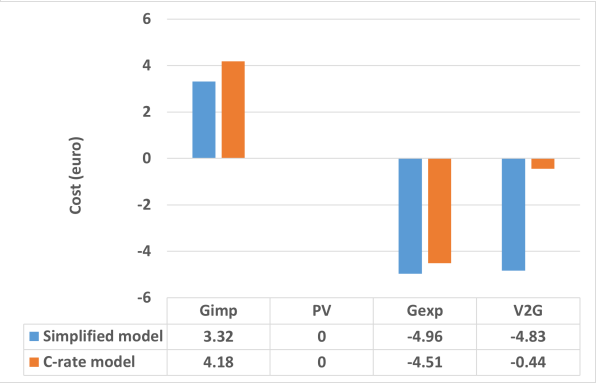

Figure 5.8: Cost comparison for degradation models

5.7 and 5.8 shows node energy comparison and total energy cost comparison for both models. From the earlier analysis, it can be inferred that the decrease in V2G energy will increase the grid import energy as the algorithm will try to reduce the possibility of penalty. This can be done by increasing the grid import to support PV in supplying the local load and EV energy request. From figure 5.7, an increase in the grid import energy or Gimp is seen for the C-rate model. A decrease in the PV energy is seen for the C-rate model, as the EVs are charged close to their requested energy and does not charge to higher energy to serve as a backup source anymore in case PV generation is insufficient which is seen by the decrease in V2G energy for C-rate model.

	t_arr(DD-MM-YY hh:mm)	**t_dep(DD-MM-YY hh:mm)**	**Qloss [%] for simplified model**	**Qloss [%] for C-rate model**
Charger 1	**10-09-2018 09:10**	**10-09-2018 10:02**	**5.99E-05**	**3.63E-05**
Charger 2	**10-09-2018 10:17**	**10-09-2018 15:40**	**7.72E-03**	**8.10E-04**
Charger 3	**10-09-2018 14:21**	**10-09-2018 16:49**	**8.93E-04**	**8.85E-04**
Charger 1	**10-09-2018 16:54**	**10-09-2018 17:38**	**1.43E-04**	**1.43E-04**
Charger 4	**10-09-2018 18:37**	**10-09-2018 20:38**	**1.90E-03**	**1.90E-03**

Table 5.3: Qloss[%] for degradation models

Summarizing everything that has been seen so far, it can be said that implementing the C-rate model has limited the charging and V2G energy of the EV battery. Doing so, the algorithm prevents the EV to degrade much quicker than expected which can also be seen in Table 5.3 which shows capacity loss% for both the models for EVs arriving at the charger on date 10.09.2018. It can be seen using the C-rate model, the capacity loss % has decreased significantly except for EV arriving during off-peak hours (when the PV generation is insufficient). During the off-peak hours, EVs perform V2G to reduce the impact of grid import if the cost of degradation is less than the grid import energy cost. Concluding this analysis, it can be said that a trade-off can be performed for EV users if they decide to generate profits by performing uncontrolled V2G and degrade the battery much quicker or participate in controlled V2G and generate minimal profit and save the battery from faster degradation.

5.2.2. Comparison of smart charging algorithm with uncontrolled charging

In this thesis, a smart charging algorithm is developed to minimize the cost of energy by providing control and optimized schedule charging of EVs along with V2G services and battery degradation model. After sensitivity parameters analysis in chapter 4 and developing a C-rate battery degradation model to limit the V2G services (earlier in this chapter), this section focuses on a comparative analysis between the developed algorithm and uncontrolled charging. The analysis is necessary as it would help in determining how beneficial and effective the developed algorithm is as compared to uncontrolled charging.

Analysis

To perform the analysis, a simulation is done for date 10-09-2018 for both uncontrolled charging and smart charging algorithm. The simulation for both charging scheme is done with the same assumptions as mentioned in section 3.1. Apart from the assumption in section 3.1, it is to be noted that the uncontrolled charging does not have the V2G feature and smart charging algorithm incorporates V2G and the C-rate degradation model. Therefore the main focus of the analysis will be comparing the charging strategy, node energy and cost analysis and the cost of charging the EVs for both smart and uncontrolled charging.

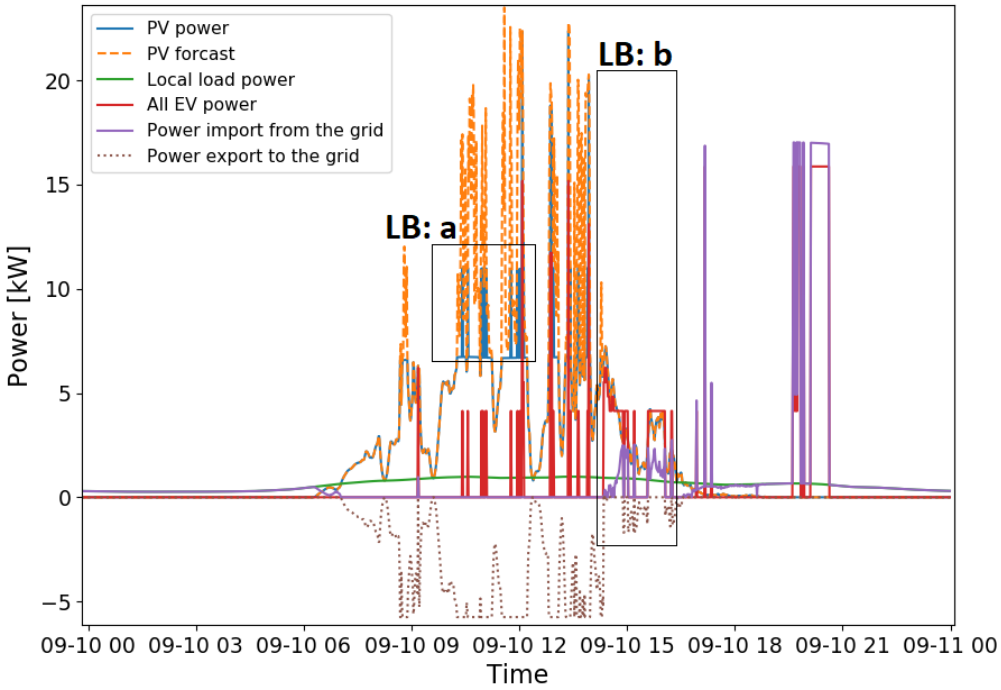

Figure 5.9: Node power profile for smart charging on 10.09.2018

Figure 5.9 and 5.10 shows node power profile for smart charging and uncontrolled charging respectively. The first noticeable difference to observe between the aforementioned figure is the PV power (depicted in blue plot lines). The PV power in Figure 5.9 follows the forecast power before and after the optimization horizon. The PV power is only optimized during the optimization horizon. This can be observed in 'LB: a' where the PV power is curtailed to supply the energy demands and export power at maximum of 5.75kW to the grid. This is not the case during the uncontrolled charging in Figure 5.10. The PV power during uncontrolled charging follows the forecast power or gets curtailed to to max export power, irrespective of the EV charging schedule, and charge the EVs and supply local load demand. When PV is not supporting grid in charging and supplied the local load demand, the remaining power is exported to grid at at maximum of 5.75kW.

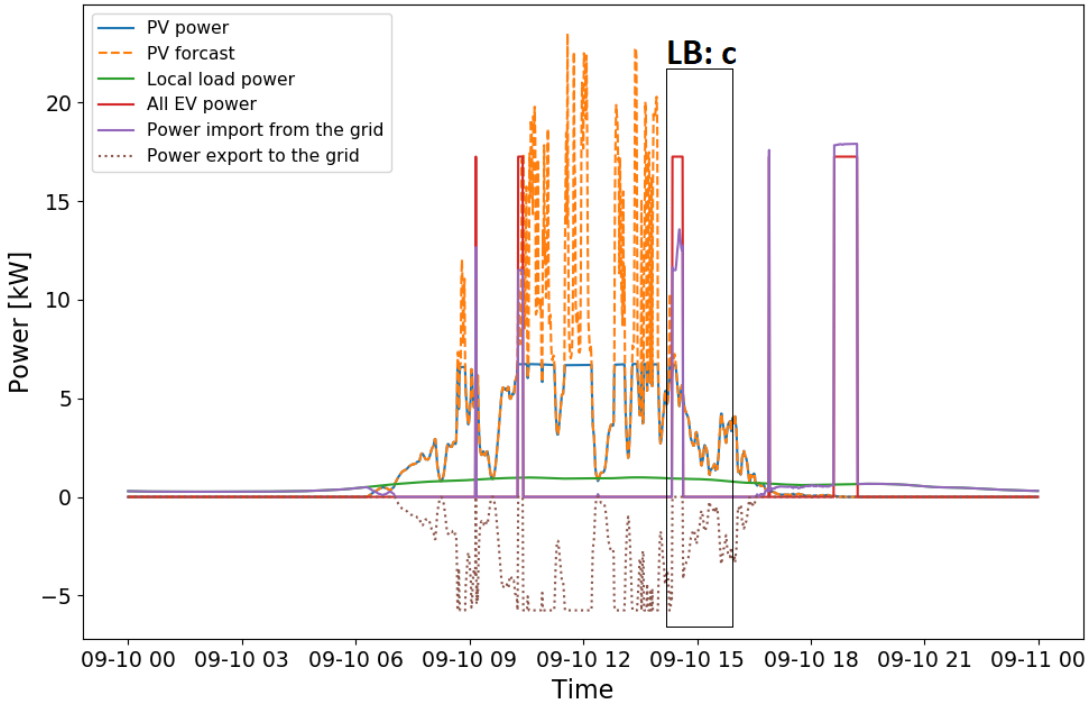

Figure 5.10: Node power profile for uncontrolled charging on 10.09.2018

Another difference that can be observed is for the EV charging schedule. The EV charging power in both the figures is depicted by red plot lines. In Figure 5.9, the EVs are charged in intervals and at less power as compared to Figure 5.10 where the EVs are charged at maximum power of 17.25kW. The reason for the difference is that using uncontrolled charging strategy starts charging the EV as soon as it connect to the charger. The smart charging algorithm schedules the charging of EVs in such a way that it minimizes the cost of energy and reduce the grid involvement by prioritizing PV. The statement of less grid involvement can be observed in 'LB: b' and 'LB: c' in both figures. In Figure 5.9 ['LB: b'], the grid is only involved when the PV generation is insufficient to adhere to energy demands. The charging of EVs with smart charging is scheduled in such a way that it uses grid import power at when the cost of buying energy is comparative lower. However, in Figure 5.10 ['LB: c'], as the EVs are charged immediately after they are connected to the charger without any concern for the cost of energy. When PV power is not be sufficient to deliver power at 17.25kW, the grid is involved to support PV in charging the EVs.

	t_arr(DD-MM-YYYY hh:mm)	**t_dep(DD-MM-YYYY hh:mm)**	**Cost with Uncontrolled charging [euro]**	**Cost with Smart charging [euro]**
Charger 1	**10-09-2018 09:10**	**10-09-2018 10:02**	**0.017**	**0.000**
Charger 2	**10-09-2018 10:17**	**10-09-2018 15:40**	**0.073**	**0.000**
Charger 3	**10-09-2018 14:21**	**10-09-2018 16:49**	**0.210**	**0.090**
Charger 1	**10-09-2018 16:54**	**10-09-2018 17:38**	**0.021**	**0.025**
Charger 4	**10-09-2018 18:37**	**10-09-2018 20:38**	**0.833**	**0.851**

Table 5.4: Cost of charging EV comparison for smart and uncontrolled charging

As mentioned earlier in this section, the EVs with smart charging and C-rate degradation model charges the EV to requested energy demand and so does the uncontrolled charging. Therefore, after analysing the charging schedule of EV and impact of both the algorithms on PV and the grid, the focus now will be on the

cost of charging for EV. From Table 4.1, it can be seen that there are 5 EVs arriving at the chargers on date 10.09.2018. It has been explained earlier repetition of charger number for the same day in the table depicts that the charger can have multiple EVs arriving to it. Table 5.4 shows comparison for the cost of charging EV with uncontrolled charging method and smart charging algorithm. It can be observed from the table that EV arriving on charger 1,2,3 earlier during the day experiences either 0.0 euro or comparatively lower cost of energy using smart charging which is not the case with uncontrolled charging. The reason for this is with smart charging the charging is prioritized using PV and it provides energy at 0.0 euro/kWh. The EV charging are scheduled to utilize the PV generation and only uses the grid when the PV power is insufficient. Due to the involvement of grid in charging EV at charger 3, the EV user has to pay 0.09 euros for charging the EV.

It can also be observed that the EV arriving at charger 1 at 16:54 and at charger 4 at 18:37 experience higher cost with smart charging than with uncontrolled charging. The reason for this is can be explained using figure 5.6 where it has been observed that EV participates in V2G to reduce the overall cost of energy for the node when the PV generation is insufficient. Performing the V2G decreases the energy of the battery and to avoid penalty the algorithm charges the EV for the reduced energy too because of which the EV user experiences higher cost of energy.

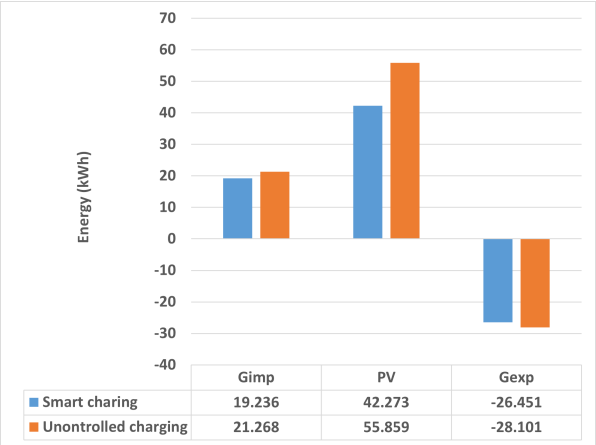

Figure 5.11: Energy comparison for charging strategies

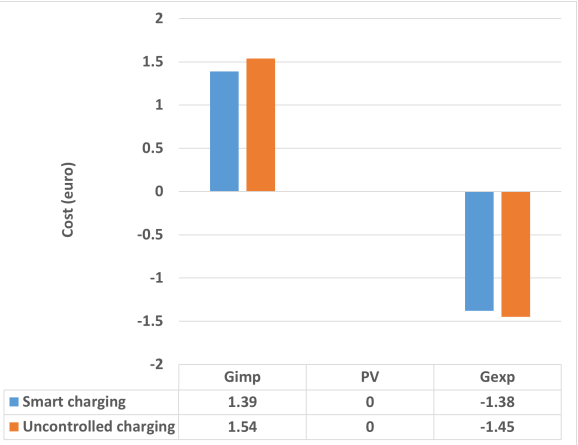

Figure 5.12: Cost comparison for charging strategies

Finally, a node energy distribution and cost comparison is done for both charging strategies. Figure 5.11 and 5.12 shows node energy distribution and cost distribution for both charging strategies. The following points can be observed from figures:

- The grid import energy or Gimp is seen to be higher for uncontrolled charging than smart charging. It is because in smart charging the algorithm schedules the charging of EV to prioritize PV use and reduce the grid involvement.
- The PV energy for uncontrolled charging strategies is higher than smart charging as the PV power in smart charging is optimized during the parking time of EV whereas in uncontrolled charging the PV power is limited to maximum export power and local load demand when not charging the EVs.
- As the PV power is not curtailed and prioritized in uncontrolled charging, PV can export higher energy as compared to when the smart charging strategy is used.

As cost is proportional to the energy utilized, figure 5.12 shows the same trend as figure 5.11. It is to be noted that the cost of using PV energy is 0.0 euro/kWh which explains the 0.0 euro for PV.

5.3. Summary

In chapter 4, it was identified that the simplified model did not have much control over the V2G application which might lead to faster degradation of the batteries. To avoid that, a more effective model is proposed for battery degradation to control capacity loss due to cyclic aging considering the C-rate stress factor. The new degradation model was derived from the work of [54] and was linearized to be adapted to the existing MILP algorithm. After the model was developed, the model was implemented and a comparative study was done

to observe the effectiveness of the model as compared to the simplified model. The newly developed C-rate model was found to be much effective in controlling V2G and charging power, frequency and EV batteries were less susceptible to faster degradation. Finally, a comparative study was done between a smart charging algorithm with a newly developed model and uncontrolled charging. The smart charging algorithm was found to be prioritizing more renewable utilization, less EV charging cost and relatively less grid involvement.

6

Conclusions & Recommendations

During this thesis, a smart charging algorithm was developed which utilizes the V2G application of the EVs. The V2G application of the EVs provided various services like as a backup source to support PV, financial benefits for node and EV user and so on. Participating in V2G leads to increased frequency of charging and discharging cycle, therefore a battery degradation model is included in the algorithm to prevent faster degradation. After the development phase, the algorithm was verified and conclusions were drawn about the sanity of the algorithm which is explained in section 6.1. Section 6.2 provides recommendation for future work.

6.1. Conclusions

In the previous chapters, the smart charging with V2G application considering the effect of battery degradation was developed. Various case studies were analyzed which provide an answer to the research questions mentioned in chapter 1.

1. **How to formulate an optimal and cost-effective smart charging algorithm for EVs charging when EVs can participate in V2G?**

   After a thorough literature study, it was determined most of the smart charging algorithm either does not include battery degradation or focus on one aspect of V2G. Therefore, in this thesis (based on the project of *OSCD*[65]) to develop an optimal and effective smart charging algorithm a mathematical model was developed in chapter 3. The model is a cost minimization objective function and formulated as a MILP problem. The model is developed to minimize the cost of energy for the EV user and prioritizes the PV in supplying the local load and EV demand. Prioritizing the PV as the main source to supply the demand reduces the impact of EV charging on the grid and is only involved when the PV generation is insufficient. The mathematical model also includes a bidirectional feature of EV to perform V2G application because of which it has been observed when EV has sufficient energy and can participate in V2G will help PV in supplying the energy demand, reduce grid involvement and provide financial benefits. The EV supporting the PV using V2G will imply discharging the battery and will reduce the involvement of the grid but at the expense of faster battery degradation which was analysed in the case study in chapter 5. Further explanation is given when answering the following question.

   (a) **How do the mathematical model and developed algorithm mimic the physical world?**

   The mathematical model and developed algorithm can be divided into four parts. The first equation deals with the cost of unfinished charging of EVs. EVs arriving at the charger request an energy demand that the battery should be charged to before the departure. To ensure that, the cost of penalty for unfinished EVs charging is used. The cost of the penalty is kept at 50*maximum cost of buying energy for the day. The second part is the cost of PV generation. This thesis, as mentioned earlier, prioritizes PV use and ensure that the cost of PV generation is kept at 0.0 euro/kWh assuming that all the cost leading to cost of PV is paid-off. The PV can also export any extra power back to the grid at a maximum of 5.75kW to obtain profit for a generation. The higher PV utilization is seen during the case studies in chapter 4 and 5 when the grid is only involved in

extreme cases like when PV generation cost is very high, or the cost of selling energy to the grid is very close to the cost of buying energy from the grid, or when the cost of penalty for unfinished charging isn't substantial. The third part of the model deals with the cost of buying energy or selling energy from and to the grid. The grid imports power only when PV is unable to supply the energy demand and EV can not support it with V2G. The grid also receives power sold to it from the PV or EV at a maximum of 5.75 kW. The fourth part of the model deals with the cost of battery degradation due to V2G and is explained in further questions.

(b) **How is the battery degradation is taken into consideration?**

The fourth part of the model deals with the loss in the form of the cost of battery degradation that the user has to bear if the user decides to participate in V2G activity. The cost of battery degradation, that the users has to bear, is given by $C_{n,j}^{Bat(V2G)}$. The battery degradation model used in chapter 3 is a simplified version which can also be interpreted as the cost of selling energy from the battery. The cost of battery degradation per kWh of discharge energy when the simplified battery degradation model is taken as 0.112 euro/kWh. This simplified model allows EV to participate in V2G to help PV in supplying the energy demand and exporting power at 5.75kW. This model, however, does not model the actual aging of the battery and does not have strict control over when and how much the EV should discharge. The model effectiveness is only limited by the cost of 0.112 euro/kWh, the constraint for discharged power and the cost of penalty for unfinished charging. This model is used for the initial phases of the study to understand how the bidirectional feature of the algorithm works and parameters that can affect the behaviour of the algorithm. A more effective model is developed in chapter 5 and the conclusion of the model developed is discussed to answer the research question 2.

(c) **What are the factors or parameters that affect the behaviour of the algorithm?**

After the mathematical model is formulated and the algorithm is developed, various parameters are selected that can affect the behaviour of the algorithm. Chapter 4 deals with the case studies on how those parameters affect the algorithm. The parameters taken into consideration are the cost of penalty for unfinished charging, cost of PV generation, grid import power limitation and cost of selling energy to the grid.

Starting with the cost of penalty for unfinished charging, it has been observed that the cost of penalty plays an important role in determining the EV charging or discharging schedule. It was observed that the value of the cost of penalty is 50*maximum cost of buying energy, the algorithm will charge all the EVs to their requested energy demand, and EV users will be satisfied as they can depart with their demand fulfilled.

During the second case study about the cost of PV generation, it was also observed that it plays an important role in determining other power parameters like EV charging power, grid import power and so on. The cost of PV generation has a significant effect on the grid involvement and V2G application of the EV. It is important to realize that fixing the value of the cost of PV generation below the minimum cost of selling to the grid will provide flexibility to the optimizer in utilizing the PV power as much as possible.

For the grid import power limitation case study, it can be said that lowering the grid import power can have EVs not charged to their requested energy, therefore, will include a high penalty which is a loss for the CSO. To decrease the loss for the CSO, it can be recommended that an agreement must be made beforehand with the user which will allow the CSO to pay less or almost no penalty for not charging the EV when the grid capacity is reduced

Finally, during the cost of selling energy to the grid study, it was observed that the algorithm is more oriented towards providing benefit to the node as increasing the cost of selling the energy have its repercussions on the grid and the CSO. Increasing the cost of selling energy increases the grid dependency because the algorithm increases the amount of export power to the grid is, thereby making a generous profit for the node. It is to be advised to the CSO that an agreement regarding the percentage of the cost of selling with the node owner must be done beforehand to provide benefit to both user and CSO.

2. **How do V2G services of the smart charging algorithm be used to prevent faster battery degradation? How is the degradation model developed and how effective it is as compared to a simplified model?**

   During the literature, it was observed that the battery degradation that happens due to cyclic aging is because of the stress factor like SOC, temperature and C_rate. The C_rate stress factor is selected to develop the degradation model for the algorithm. The model was derived from the work in [54] and was linearized to adapt to the existing MILP algorithm. The linearization was done by determining the relation between C-rate and throughput. The linear mathematical equation developed was observed to have an accuracy of 0.99% and was incorporated to the algorithm. The developed algorithm is compared with the simplified model and it was observed that the newly developed degradation model or C-rate model prevents the EV to degrade much quicker than with the simplified model. It can be seen using the C-rate model, the capacity loss % has decreased significantly except for EV arriving during off-peak hours (when the PV generation is insufficient). During the off-peak hours, EVs perform V2G to reduce the impact of grid import if the cost of degradation is less than the grid import energy cost. It can be said that a trade-off can be performed for EV users if they decide to generate profits by performing uncontrolled V2G and degrade the battery much quicker or participate in controlled V2G and generate minimal profit and save the battery from faster degradation.

3. **How effective and optimal the developed smart charging algorithm is as compared to uncontrolled charging?**

   Finally, the developed smart charging algorithm is compared to uncontrolled charging and it was observed that the cost of charging EV with smart charging algorithm is either 0.0 euro or significantly lower as compared to uncontrolled charging. This is not the case when the EV arrives at off-peak hours during when the EVs are observed to help reduce the overall cost for the node on the expense of the higher cost of charging as compared to uncontrolled charging. The grid involvement is observed to be much lower in the case of smart charging than uncontrolled charging and PV power is observed to be prioritized in smart charging unlike the case in uncontrolled charging. As cost is proportional to the energy utilized, the overall cost for the node is observed for smart charging is lower than with uncontrolled charging.

6.2. Recommendations for future work

During this thesis, a smart charging algorithm with V2G function is developed considering the effects of battery degradation due to V2G. In section 3.1 various assumptions were taken into account and the mathematical model and algorithm were developed for a node. The ongoing research on developing smart charging algorithm is vast and new applications can be added to improve the existing algorithm. Various recommendations can be advised for the advancement of the field and opening way for future research which are as follows:

1. Scalable: The mathematical model and algorithm developed was done with the perspective of one node with 4 chargers. The limitation was assumed to check the behaviour of the algorithm more critically. However, the algorithm is designed in such a way that more node can be added to the algorithm. This creates an opportunity for inter-node power transfer to reduce the grid involvement even further.

2. Expanding the application for V2G: In chapter 2, during the literature study of V2G it was found that V2G services can be used for multiple ancillary services like peak shaving, frequency regulation, spinning reserve and so on. The algorithm developed in this thesis has V2G working as a backup power source to help the PV in reducing grid involvement and reduce the overall cost of energy. The flexibility of the optimization problem and algorithm provides an opportunity to add other V2G applications to improve the system.

3. A complete battery degradation model: V2G services of EVs can have an adverse effect on battery degradation as it involves frequent charging and discharging cycles. The degradation model in this thesis used was based on cyclic aging using the C-rate stress factor and was derived from an empirical model. Using an empirical model will provide an overview insight of how the system or model will behave and does not necessarily always provide similar results as an experimented model. The limitation provides an opportunity to expand the battery degradation model introducing other stress factor and calendar aging to understand the practical capacity fading of EV batteries.

Bibliography

[1] Deloitte Insights, *"Electric vehicles,"*.Available: https://www2.deloitte.com/uk/en/insights/focus/future-of-mobility/electric-vehicle-trends-2030.html. [Accessed: 31-Jan-2021].

[2] Cheng, K.W.E.. (2009). *Recent development on electric vehicles.* 2009 3rd International Conference on Power Electronics Systems and Applications, PESA 2009. 1 - 5.

[3] M. Guarnieri, *"Looking back to electric cars"*, 2012 Third IEEE HISTory of ELectro-technology CONference (HISTELCON), Pavia, 2012, pp. 1-6, doi: 10.1109/HISTELCON.2012.6487583.

[4] *"Future of Electric Vehicles & New EV Technology"*, [Online 05-Sep-2020.].Available:https://www.arrow.com/en/research-and-events/articles/the-history-and-future-of-electric-vehicles.[Accessed:11-Jan-2021].

[5] Sevindik and O. Aysenur, World Energy Outlook, Ankara: International Energy Agency, pp. 1, 2013.

[6] Battery Electric Vehicle, July 2017, [online] Available: https://en.wikipedia.org/wiki/Battery_electric_vehicle.

[7] *Global EV Outlook 2017*, France, pp. 5, 2017.

[8] *Energy Technology Perspectives 2012*, August 2017, [online] Available: http://www.iea.org/publications/freepublications/publication/technology-roadmap-electric-and-plug-in\-hybrid-electric-vehiclesfoldout.html.

[9] S. Deilami, A. S. Masoum, P. S. Moses, and M. A. S. Masoum, *"Real-time coordination of plug-in electric vehicle charging in smart grids to minimize power losses and improve voltage pro_le,"* IEEE Transactions on Smart Grid, vol. 2, no. 3, pp. 456467, 2011.

[10] Al-Alawi BM, Bradley TH. *"Review of hybrid, plug-in hybrid, and electric vehicle market modeling studies"*. Renewable Sustainable Energy Rev 2013; 21:190–203.

[11] H. A. J. I. Zakaria, M. O. U. N. I. R. Hamid, E. L. M. A. R. J. A. N. I. Abdellatif, and A. M. A. R. I. R. Imane, *"Recent Advancements and Developments for Electric Vehicle Technology,"* 978-1-7281-0827-8, 2019.

[12] S. Enyedi, *"Electric cars — Challenges and trends,"* 2018 IEEE International Conference on Automation, Quality and Testing, Robotics (AQTR), Cluj-Napoca, 2018, pp. 1-8, doi: 10.1109/AQTR.2018.8402776.

[13] M. Yilmaz and P. T. Krein, *"Review of Battery Charger Topologies, Charging Power Levels, and Infrastructure for Plug-In Electric and Hybrid Vehicles,"* IEEE Trans. Power Electron., vol. 28, no. 5, pp. 2151–2169, May 2013.

[14] SAE Standard J1772, *"SAE Electric Vehicle and Plug-in Hybrid Electric Vehicle Conductive Charge Coupler,"* pp. 1–93, 2010

[15] Chandra Mouli, G. R. (2018). *"Charging electric vehicles from solar energy: Power converter, charging algorithm and system design"* DOI: 10.4233/uuid:dec62be4-d7cb-4345-a8ae-65152c78b80f

[16] W. Kempton, V. Udo, K. Huber, K. Komara, and S. Letendre, *"A test of vehicle-to-grid (V2G) for energy storage and frequency regulation in the PJM system,"* pp. 1–32, 2008

[17] W. Kempton and J. Tomić, *"Vehicle-to-grid power implementation: From stabilizing the grid to supporting large-scale renewable energy,"* J. Power Sources, vol. 144, no. 1, pp. 35280–294, 2005

[18] D.P. Birnie, *"Solar-to-vehicle (S2V) systems for powering commuters of the future"*, J Power Sources, 186 (2009), pp. 539-542, 10.1016/j.jpowsour.2008.09.118

[19] M. Muratori, *"Impact of uncoordinated plug-in electric vehicle charging on residential power demand,"* Nature Energy, January 2018

[20] Kawamura N, Muta M. *"Development of solar charging system for plug-in hybrid electric vehicles and electric vehicles"*. In: 2012 Int conf renew energy res appl, IEEE; 2012. p. 1–5.

[21] K. Uddin et al., *"The viability of vehicle-to-grid operations from a battery technology and policy perspective,"* Energy Policy, vol. 113, pp. 342-347, February 2018

[22] G.R. Chandra Mouli, P. Bauer, M. Zeman, *"System design for a solar powered electric vehicle charging station for workplaces"*, Applied Energy, Volume 168, 2016, Pages 434-443, ISSN 0306-2619, https://doi.org/10.1016/j.apenergy.2016.01.110.

[23] Mesentean S, Feucht W, Kula H-G, Frank H. *"Smart charging of electric scooters for home to work and home to education transports from grid connected photovoltaic-systems"*. In: 2010 IEEE int energy conf, IEEE; 2010. p. 73–8.

[24] Cutler SA, Schmalberger B, Rivers C. *"An intelligent solar ecosystem with electric vehicles"*. In: 2012 IEEE int electr veh conf, IEEE; 2012. p. 1–7

[25] M. van der Kam, W. van Sark. *"Smart charging of electric vehicles with photovoltaic power and vehicle-to-grid technology in a microgrid; a case study Appl Energy"*, 152 (2015), pp. 20-30, 10.1016/j.apenergy.2015.04.092

[26] Y.-M. Wi, J.-U. Lee, and S.-K. Joo, *"Electric vehicle charging method for smart homes/buildings with a photovoltaic system,"* IEEE Trans. Consum. Electron., vol. 59, no. 2, pp. 323–328, May 2013

[27] D. van der Meer, G. R. Chandra Mouli, G. Morales-Espana, L. Ramirez Elizondo, and P. Bauer, *"Energy Management System with PV Power Forecast to Optimally Charge EVs at the Workplace,"* IEEE Trans. Ind. Informatics, vol. 14, no. 1, pp. 311–320, 2018.

[28] P. Sanchez-Martin, S. Lumbreras, and A. Alberdi-Alen, *"Stochastic Programming Applied to EV Charging Points for Energy and Reserve Service Markets,"* IEEE Trans. Power Syst., vol. 31, no. 1, pp. 198–205, Jan. 2016

[29] Nathaniel S. Pearre, Hajo Ribberink, *"Review of research on V2X technologies, strategies, and operations, Renewable and Sustainable Energy Reviews"*, Volume 105, 2019, Pages 61-70, ISSN 1364-0321, https://doi.org/10.1016/j.rser.2019.01.047.

[30] Tuttle DP, Fares RL, Baldick R, Webber ME. *"Plug-In Vehicle to Home (V2H) duration and power output capability."* In: Proceedings of IEEE transportation electrification conference and expo (ITEC); 2013. pp. 1–7.

[31] Hinkle C, Millner A, Ross W. *"Bi-directional power architectures for electric vehicles"*; 2011. pp. 1–6.

[32] Mullan J., Harries D., Bräunl T., Whitely S. *"The technical economic and commercial viability of the vehicle-to-grid concept"*. Energy Policy. 2012; 48:394–406.

[33] C.D. Parker, *"Encyclopaedia of Electrochemical Power Sources"*, 2009

[34] Mahmoud Ghofrani, Eric Detert, Negar Niromand Hosseini, Amirsaman Arabali, Nicholas Myers and Phasith Ngin (October 5th 2016). *"V2G Services for Renewable Integration, Modeling and Simulation for Electric Vehicle Applications, Mohamed Amine Fakhfakh, IntechOpen"*, DOI: 10.5772/64433. Available from:https://www.intechopen.com/books/modeling-and-simulation-for-electric-vehicle-applications/v2g-services-for-renewable-integration

[35] Díaz-González F., Sumper A., Gomis-Bellmunt O., Villafáfila R. *"A review of energy storage technologies for wind power applications"*. Renewable and Sustainable Energy Reviews. 2012; 16(4):2154–2171.

[36] Zhang M., Chen J. *"The energy management and optimized operation of electric vehicles based on microgrid."* IEEE Transactions on Power Delivery. 2014; 29:1427–1435.

[37] Aunedi M., Strbac G. *" Efficient system integration of wind generation through smart charging of electric vehicles".* In: Proceedings of 8th International Conference and Exhibition on Ecological Vehicles and Renewable Energies (EVER); 2013. pp. 1–12.

[38] Verzijlbergh R.A., de Vries L.J., Lukszo Z. *"Renewable energy sources and responsive demand. Do we need congestion management in the distribution grid?"* IEEE Transactions on Power Systems. 2014; 29 (5):2119–2128.

[39] Goonewardena M., Le L.B. *"Charging of electric vehicles utilizing random wind: A stochastic optimization approach".* In: IEEE Globecom Workshops (GC Wkshps); 2012. pp. 1520–1525.

[40] Hu W., Su C., Chen Z., Bak-Jensen B. *"Optimal operation of plug-in electric vehicles in power systems with high wind power penetrations".* IEEE Transactions on Sustainable Energy. 2013; 4:577–585.

[41] Aunedi M., Strbac G. *" Efficient system integration of wind generation through smart charging of electric vehicles".* In: Proceedings of 8th International Conference and Exhibition on Ecological Vehicles and Renewable Energies (EVER); 2013. pp. 1–12.

[42] Schuller A., Hoeffer J. *"Assessing the impact of EV mobility patterns on renewable energy oriented charging strategies".* Energy Procedia. 2014; 46:32–39.

[43] Gottwalt S., Schuller A., Flath C., Schmeck H., Weinhardt C. *"Assessing load flexibility in smart grids: Electric vehicles for renewable energy integration".* In: IEEE Power and Energy Society General Meeting (PES); 2013. pp. 1–5.

[44] Mets K., De Turck F., Develder C. *"Distributed smart charging of electric vehicles for balancing wind energy".* In: Proceedings of IEEE 3rd International Conference on Smart Grid Communications (SmartGridComm); 2012. pp. 133–138.

[45] Andrew W. Thompson, *"Economic implications of lithium ion battery degradation for Vehicle-to-Grid (V2X) services"*, Journal of Power Sources, Volume 396, 2018, Pages 691-709, ISSN 0378-7753, `https://doi.org/10.1016/j.jpowsour.2018.06.053.`

[46] L. Lu, X. Han, J. Li, J. Hua, M. Ouyang *"A review on the key issues for lithium-ion battery management in electric vehicles"*, J. Power Sources, 226 (2013), pp. 272-288, 10.1016/j.jpowsour.2012.10.060

[47] S.J. An, J. Li, C. Daniel, D. Mohanty, S. Nagpure, D.L. Wood *"The State of Understanding of the Lithium-ion-battery Graphite Solid Electrolyte Interphase (SEI) and its Relationship to Formation Cycling"*, Carbon N. Y, vol. 105 (2016), pp. 52-76

[48] L. Lam and P. Bauer, *"Practical Capacity Fading Model for Li-Ion Battery Cells in Electric Vehicles "*, in IEEE Transactions on Power Electronics, vol. 28, no. 12, pp. 5910-5918, Dec. 2013, 10.1109/TPEL.2012.2235083.

[49] K. Smith, G. Kim, T. Markel, A. Pesaran *"Design of electric drive vehicle batteries for long life and low cost"* IEEE 2010 Work. Accel. Stress Test. Reliab., Denver, Colorado (2010), pp. 1-29 NREL/PR-5400-48933

[50] K. Uddin, S. Perera, W. Widanage, L. Somerville, J. Marco *"Characterising lithium-ion battery degradation through the identification and tracking of electrochemical battery model parameters Batteries"*, 2 (2016), p. 13, doi: 10.3390/batteries2020013

[51] E. Prada, D. Di Domenico, Y. Creff, J. Bernard, V. Sauvant-moynot, F. Huet *"A simplified electrochemical and thermal aging model of LiFePO4 -graphite Li-ion Batteries: power and capacity fade simulations"* J. Electrochem. Soc., 160 (2013), pp. A616-A628, doi: 10.1149/2.053304jes

[52] K. Uddin, T. Jackson, W.D. Widanage, G. Chouchelamane, P.A. Jennings, J. Marco *"On the possibility of extending the lifetime of lithium-ion batteries through optimal V2G facilitated by an integrated vehicle and smart-grid system"* Inside Energy, 133 (2017), pp. 710-722, doi: 10.1016/j.energy.2017.04.116

[53] M. Ben-Marzouk, A. Chaumond, E. Redondo-Iglesias, M. Montaru, S. Pelissier *"Experimental protocols and first results of calendar and/or cycling aging study of lithium-ion batteries"* - the MOBICUS project 29th World Electr. Veh. Symp. Exhib. (EVS 29), Montreal, Canada (2016), pp. 388-397

[54] Wang, John & Purewal, Justin & Liu, Ping & Hicks-Garner, Jocelyn & Soukazian, Souren & Sherman, Elena & Sorenson, Adam & Vu, Luan & Tataria, Harshad & Verbrugge, Mark. (2014). *"Degradation of lithium ion batteries employing graphite negatives and nickel-cobalt-manganese oxide + spinel manganese oxide positives: Part 1, aging mechanisms and life estimation"*. Journal of Power Sources. 269. 10.1016/j.jpowsour.2014.07.030.

[55] Suri, Girish & Onori, Simona. (2016). *"A control-oriented cycle-life model for hybrid electric vehicle lithium-ion batteries"*. Energy. 96. 644-653. 10.1016/j.energy.2015.11.075.

[56] Johannes Schmalstieg, Stefan Käbitz, Madeleine Ecker, Dirk Uwe Sauer, *"A holistic aging model for Li(NiMnCo)O2 based 18650 lithium-ion batteries"*, Journal of Power Sources, Volume 257, 2014, Pages 325-334, ISSN 0378-7753, https://doi.org/10.1016/j.jpowsour.2014.02.012.

[57] A. Hoke, A. Brissette, K. Smith, A. Pratt and D. Maksimovic, *"Accounting for Lithium-Ion Battery Degradation in Electric Vehicle Charging Optimization,"* in IEEE Journal of Emerging and Selected Topics in Power Electronics, vol. 2, no. 3, pp. 691-700, Sept. 2014, doi: 10.1109/JESTPE.2014.2315961.

[58] John Wang, Ping Liu, Jocelyn Hicks-Garner, Elena Sherman, Souren Soukiazian, Mark Verbrugge, Harshad Tataria, James Musser, Peter Finamore, *"Cycle-life model for graphite-LiFePO4 cells"*, Journal of Power Sources, Volume 196, Issue 8, 2011, Pages 3942-3948, ISSN 0378-7753, https://doi.org/10.1016/j.jpowsour.2010.11.134.

[59] Martin Petit, Eric Prada, Valérie Sauvant-Moynot, *"Development of an empirical aging model for Li-ion batteries and application to assess the impact of Vehicle-to-Grid strategies on battery lifetime"*, Applied Energy, Volume 172, 2016, Pages 398-407, ISSN 0306-2619, https://doi.org/10.1016/j.apenergy.2016.03.119.

[60] "NEDU - NEDU", NEDU, 2021. [Online]. Available: https://www.nedu.nl/. [Accessed: 11- May- 2021].

[61] Platform.elaad.io, 2021. [Online]. Available: https://platform.elaad.io/download-data/filedownload.php?file=elaadnl_open_ev_datasets.xlsxcode=open. [Accessed: 11- May- 2021].

[62] Solaren-power.com, 2021. [Online]. Available: https://solaren-power.com/pdf/manuals/TABUCHI-INVERTER-M250-25kW-Three-phase-Inverter.pdf. [Accessed: 11- May- 2021].

[63] T. R. Ricciardi, K. Petrou, J. F. Franco and L. F. Ochoa, "Defining Customer Export Limits in PV-Rich Low Voltage Networks," in IEEE Transactions on Power Systems, vol. 34, no. 1, pp. 87-97, Jan. 2019, doi: 10.1109/TPWRS.2018.2853740.

[64] Widén, Joakim & Munkhammar, Joakim. (2013). Evaluating the benefits of a solar home energy management system: impacts on photovoltaic power production value and grid interaction.

[65] "OCSD", 2021. [Online]. Available: https://www.tudelft.nl/ewi/over-de-faculteit/afdelingen/electrical-sustainable-energy/dc-systems-energy-conversion-storage/research/orchestrating-smart-charging-in-mass-deployment-oscd-project. [Accessed: 11- May- 2021].

[66] C. Zhou, K. Qian, M. Allan and W. Zhou, "Modeling of the Cost of EV Battery Wear Due to V2G Application in Power Systems," in IEEE Transactions on Energy Conversion, vol. 26, no. 4, pp. 1041-1050, Dec. 2011, doi: 10.1109/TEC.2011.2159977.

[67] "LCOE_Renewable_Energy_Technologies", 2021. [Online]. Available: https://www.ise.fraunhofer.de/content/dam/ise/en/documents/publications/studies/EN2018_Fraunhofer-ISE_LCOE_Renewable_Energy_Technologies.pdf. [Accessed: 11- May- 2021].

[68] `https://www.tesla.com/en_eu`

[69] Y. Wang, Z. Zhou, A. Botterud, K. Zhang and Q. Ding, "Stochastic coordinated operation of wind and battery energy storage system considering battery degradation," in Journal of Modern Power Systems and Clean Energy, vol. 4, no. 4, pp. 581-592, October 2016, doi: 10.1007/s40565-016-0238-z.